

RIJKSUNIVERSITEIT GRONINGEN

BSC. ASTRONOMY

---

# Environmental Dependence of AGN and Star-Formation Activity

---

*Author:*  
Marenthe HOPMA

*Supervisor:*  
John MCKEAN

July 12, 2016

## Abstract

In this project data from the Very Large Array (VLA) archive is taken which was made in 2006 while observing Cl1604 at  $z = 0.9$ , the largest supercluster at such high redshift. We start in the introduction with a brief history of Active Galactic Nuclei (AGN) detections and an explanation on what they are and how they can be detected and then move on to the supercluster we will study. We then take a look at what interferometers are, how they work and describe how the VLA works. We then explain how the data was reduced before we state our results. With this data we found a total of 100 sources within a 15 arcminute radius from our pointing center at R.A. 16:04:13.191, Decl. 43:13:50.8 and with a flux of  $S > 6\sigma$ . From different literature we found the R.A. and Decl. of the 10 confirmed clusters within Cl1604 and proceeded to find the number densities. Of only 4 clusters we found a significant increase in number density with respect to the average overall density. When comparing the sources we found to two similar surveys of the same area (the NVSS and FIRST) and at the same wavelength (1.4 GHz) we are able to match 5 and 14 sources respectively. When comparing to an X-Ray survey of Kocevski et al. (2009) we can match 18 sources to their X-Ray counterparts, of which 15 can be matched to their optical counterparts. We confirm 7 AGN, 2 of which lie close to one of the clusters within Cl1604, but none within 1 Mpc of the center of one of the clusters, confirming the theory that AGN are usually found at the outer edges of clusters, rather than in the middle.

# Contents

<b>1</b>	<b>Introduction</b>	<b>2</b>
1.1	AGN . . . . .	2
1.2	Cl1604 . . . . .	2
<b>2</b>	<b>Interferometer</b>	<b>4</b>
2.1	Basics of the interferometer . . . . .	4
2.2	Visualization . . . . .	6
2.3	The VLA . . . . .	7
<b>3</b>	<b>Data reduction</b>	<b>7</b>
3.1	Observations . . . . .	7
3.2	Pre-calibration . . . . .	9
3.3	Calibration . . . . .	11
3.4	Imaging . . . . .	12
<b>4</b>	<b>Results</b>	<b>14</b>
4.1	Object detection . . . . .	14
4.2	Number counts . . . . .	15
4.3	Comparing with other surveys . . . . .	19
<b>5</b>	<b>Discussion</b>	<b>22</b>
<b>6</b>	<b>Conclusions</b>	<b>27</b>
	<b>Appendices</b>	<b>30</b>
<b>A</b>	<b>Images</b>	<b>30</b>
<b>B</b>	<b>MS details of dataset A</b>	<b>43</b>
<b>C</b>	<b>The code for dataset A</b>	<b>45</b>

# 1 Introduction

## 1.1 AGN

The general assumed theory of an AGN is a super massive black hole in the center of the galaxy which is fed by the accretion of gas. A simple model can be seen in Figure 1

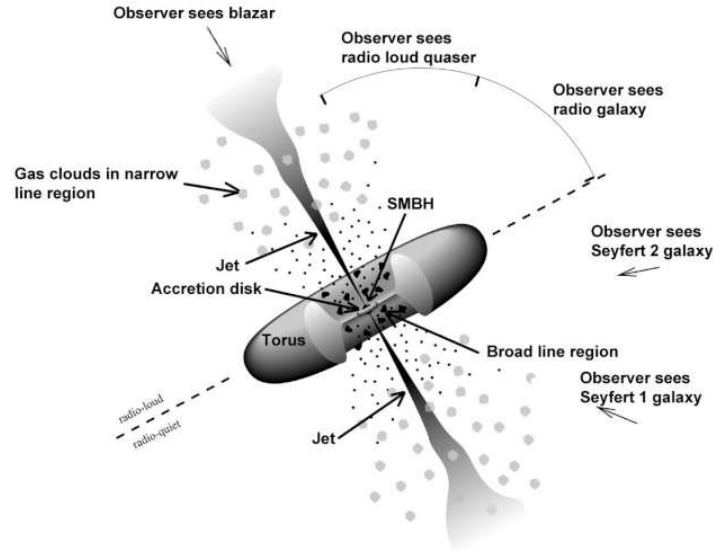


**Figure 1:** Model of Active Galactic Nuclei (AGN). The small object in the middle is usually a black hole with a mass of  $10^6 - 10^9 M_{\odot}$ . The energy of the AGN comes from the gravitational potential of the infalling surrounding material in the accretion disk. Somewhat further away is an opaque torus of accreting material. Two thin jets are ejected in the polar directions. (Image by NASA)

Optical spectral lines from the accretion disk of the AGN are dominated by H, He, C, N, O, Mg and Ne, which is similar to HII regions. The extreme broadening of these spectral lines is due to the rapid rotation of the disk. In typical spectra two distinct line profiles can be identified: The broad-line region (BLR) corresponding to velocities of  $\approx 10,000$  km/s, which is proposed to come from the accretion disk, and the narrow-line region (NLR) corresponding to velocities of several hundreds km/s, which should come from a more extended region high above the disk. The circum nuclear disk was first observed by Miyoshi et al. (1995) in NGC 4258 and contained  $H_2O$  masers, which are quite rare for AGN. The bright core emits synchrotron radiation over the whole spectrum, but only about 10% are radio-loud.

We thus find that the spectra of many quasars extend over 11 decades of the electromagnetic spectrum. The relative strength of the source depends on the orientation of the AGN and the direction of the jet (a head on jet can cause an increased intensity due to Doppler boosting). AGN have a common anomaly in the blue part of the spectrum called the 'blue bump', which may be caused by the accretion disk.

Star-forming galaxies can also be identified by synchrotron radiation. At 1.4 GHz this dominates at least one order of magnitude over free-free emission (Condon, 1992). The synchrotron spectrum is known to evolve over time due to the energy loss by the radiating electrons. Therefore, by studying the synchrotron spectrum an estimate can be made of how long an object has been radiating. Star formation takes place in molecular clouds. The process causes a strong emission of CO in the millimeter part of the spectrum, causing this to be a good indicator of star formation galaxies.

## 1.2 Cl1604

In this bachelor project we will look at VLA observations of the Cl1604 supercluster at  $z = 0.9$ , which is the largest supercluster mapped at high redshift.

Initially Cl1604 was identified as two separate clusters Cl1604+4301 and Cl1604+4321 by Gunn et al. (1986). A study by Lubin et al. (2000) found four distinct red galaxy density peaks in an area of

10.4'  $\times$  18.2'. In 2004 Gal & Lubin spectroscopically confirmed 230 cluster members which they used to find that all four density peaks formed one connected supercluster. In 2005, Gal et al. wanted to find the boundaries of the supercluster. They measured a largest projected separation of approximately 9.6  $h_{70}^{-1}$  Mpc with an apparent depth of approximately 93  $h_{70}^{-1}$  Mpc. With some more studies of Postman et al. (1998, 2001) and Gal et al. (2008), four more large overdensities were added, coming to a total of 8 cluster areas within the supercluster Cl1604.

In 2008, Gal et al. used a new, improved photometric calibration and modification process on the data from Lubin et al. (2000) and Gal et al. (2005) with a combination of two original pointings with the Carnegie Observatories Spectroscopic Multislit and Imaging Camera (COSMIC) and two pointings with the Large Format Camera (LFC). The objects they found were cross referenced with new data of the Sloan Digital Sky Survey (SDSS). An improved catalog was made by selecting objects based on photometric errors. This was done by comparing both LFC pointings with each other and both COSMIC pointings, and making a hybrid map with both results. Together with the additional spectroscopy from Gal et al. (2005) modifications to the density mapping algorithms could be made. With these new density maps a total of ten clusters were found. The details of these clusters were listed in table 1 of their paper, which can be seen here in Table 1. The density maps are shown in Figure 2, a Figure from Gal et al. (2008), where the overdensities are marked.

**Table 1:** TABLE FROM GAL ET AL. (2008)  
Cl 1604 Cluster Coordinates, Redshifts, and Velocity Dispersions

ID	Name	R.A. (J2000.0) (deg)	Decl. (J2000.0) (deg)	Within 0.5 $h_{70}^{-1}$ Mpc		Within 1.0 $h_{70}^{-1}$ Mpc		Within 1.5 $h_{70}^{-1}$ Mpc				
				N	$Z_{mean}$	$\sigma(N_{agree})$	N	$Z_{mean}$	$\sigma(N_{agree})$	N	$Z_{mean}$	$\sigma(N_{agree})$
A	Cl 1604+4304	241.08946	43.07613	21	0.89838	$532 \pm 127(2)$	32	0.89861	$619 \pm 96(3)$	36	0.89832	$682 \pm 109(3)$
B	Cl 1604+4314	241.09890	43.23550	20	0.86574	$756 \pm 83(3)$	32	0.86531	$811 \pm 76(3)$	47	0.86569	$767 \pm 76(3)$
C	Cl 1604+4316	241.03162	43.26313	8	0.93451	$439 \pm 256(1)$	18	0.93511	$313 \pm 41(3)$	...	...	...
D	Cl 1604+4321	241.13865	43.35343	28	0.92351	$559 \pm 171(2)$	53	0.92280	$112 \pm 112(2)$	69	0.92340	$668 \pm 103(3)$
E	Cl 1604+4314B	241.02815	43.23343	...	...	...	...	...	...	...	...	...
F	Cl 1604+4322	241.21314	43.37091	7	0.93659	$142 \pm 297(1)$	9	0.93608	$173 \pm 220(1)$	13	0.93532	$435 \pm 129(2)$
G	Cl 1604+4324	240.93754	43.40520	6	0.89932	...	13	0.90075	$409 \pm 101(3)$	21	0.90210	$477 \pm 152(3)$
H	Cl 1604+4322	240.89648	43.37309	6	0.85292	...	10	0.85226	$302 \pm 64(3)$	11	0.85243	$312 \pm 57(3)$
I	Cl 1604+4323	240.79691	43.39176	5	0.90230	...	7	0.90238	$359 \pm 140(3)$	7	0.90238	$359 \pm 140(3)$
J	Cl 1604+4331	240.91905	43.51648	...	...	...	...	...	...	...	...	...

- <sup>a</sup> Overlaps cluster B at this radius.  
<sup>b</sup> No dispersions measured as it overlaps clusters B and C.  
<sup>c</sup> Insufficient redshifts to compute dispersions.  
<sup>d</sup> No spectroscopic coverage.

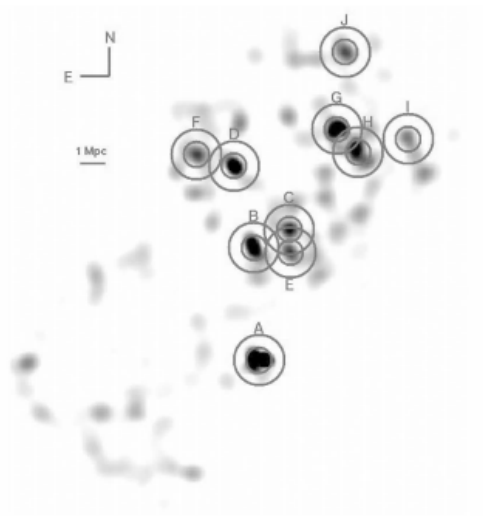


**Figure 2:** Adaptive kernel density map of color-selected galaxies in the Cl 1604 region. Detected cluster and group candidates are marked with circles of 0.5 and 1.0  $h_{70}^{-1}$  radius and labeled with an identifying letter. Figure by Gal et al. (2008).

This supercluster provides an ideal environment for the study of AGN and star-formation galaxies (SFG). In recent debates the position of AGN is questioned. More and more studies seem to agree that AGN occur primarily in the vicinity of clusters (Henry & Briel 1991; Cappi et al. 2001; Pentericci et al. 2002; Molnar et al. 2002, Johnson et al. 2003; D’Elia et al. 2004; Ruderman & Ebeling 2005; Cappelluti et al. 2005; Hudaverdi et al. 2006; Branchesi et al. 2007), where the preferred position seems to be on the outskirts of clusters (Johnson et al. 2003; Ruderman & Ebeling 2005). It appears that this AGN overdensity grows with higher redshift (Cappelluti et al. 2005).

Recent studies also show that the AGN density is higher in clusters than optical studies suggest (Gilmour et al. 2007; Martini et al. 2002, 2006) and note that AGN are most likely to be found in areas of moderate density.

Several studies have also shown a segregation between red early-type galaxies and blue starforming galaxies on the color-magnitude (CM) diagram. In a study by Kocevski et al. (2009) such a CM diagram was made of CL1604, and a significant amount of the AGN ( $\pm 80\%$ ) were found in the sparsely populated transition space between the red and blue sequence. They found that this was because "the AGNs detected were largely hosted by luminous ( $M_V < -21.1$ ), spheroidal and/or bulge dominated galaxies which are bluer than similar galaxies on the system’s red sequence" (Kocevski et al. 2009). The blue cores of these galaxies were interpreted as the remnants of recent star formation. They give two possible explanations for this feature: either AGN are a trigger for galaxies to transform from star-forming systems in the blue cloud to passively evolving galaxies on the red sequence (making blue galaxies 'redder'), or somewhat more alternatively, episodic star formation and AGN activity in galaxies on the red sequence are triggered by galaxy interactions (making red galaxies 'bluer')

It is our intention to look at data taken from the Very Large Array (VLA) archive of the supercluster CL1604 and analyse what we find. In Section 2 we start with describing what an interferometer is and how it works. In Section 3 we describe the observations done by the VLA, how we analyzed them and how we made a wide-field image. In Section 4 we present our results. We make comparisons with other similar radio wavelength surveys of the same area, and also with X-ray observations. We try to determine the nature of some special sources and their properties. Finally, in Section 5 we summarize our conclusions. We assume a standard cosmology with  $H_0 = 70 \text{ km s}^{-1} \text{ Mpc}^{-1}$ ,  $\Omega_m = 0.3$  and  $\Omega_\Lambda = 0.7$ .

## 2 Interferometer

### 2.1 Basics of the interferometer

For this bachelor project radio emission from the cluster CL1604 was studied using the radio telescopes of the VLA. A radio telescope consists of two basic elements: the antenna and the receiver.

The antenna transforms electromagnetic radiation into a voltage that can be detected by the receiver. The response of the antenna to the incoming electromagnetic waves is dependent on the direction it is pointing in (see Figure 3). The large central lobe is called the primary beam. When the antenna is pointing directly at the target source so that the waves are intercepted at the top of the primary beam, the full flux density of the source is measured. However, if the pointing of the antenna is slightly off the measured flux density falls off rapidly. The point of the primary beam where only half of flux density of the target source is measured is called the full-width half-maximum (FWHM).

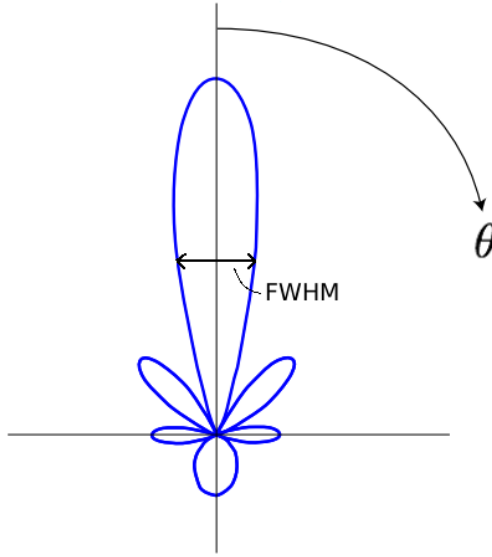


**Figure 3:** The power pattern: the response of an antenna, as seen from the optical axis, to the incoming electromagnetic waves of the target source.

The resolution,  $\theta$  of a radio telescope can be found using:

$$\theta \approx \frac{\lambda}{D} \cdot \alpha , \quad (1)$$

where  $D$  is the diameter of the dish of the telescope,  $\lambda$  the wavelength and  $\alpha$  is a constant that is defined by the aperture illumination. For the telescopes of the VLA  $D = 25$  m, which gives a resolution of  $\approx 29$  arcminutes at a frequency of 1.4 GHz. At this frequency (which is what we used for our research) we have  $\lambda = \frac{c}{\nu} \approx 0.2$  m. We use  $\alpha \approx 1.22$ , which is standard for radio telescopes. For observing smaller sources this dishsize is not enough and bigger dishes are expensive to build. Thus the solution is to combine two or more dishes to form an interferometer. The signals of the dishes can be correlated to effectively increase the diameter, which is now called the baseline  $B$ . We then get a resolution of:

$$\theta \approx \frac{\lambda}{B} \cdot \alpha . \quad (2)$$

To explain how this correlation works we consider a two-element interferometer like in Figure 4. This interferometer consists of two identical antennas, both directed at the same object and thus both receiving the same electromagnetic waves. However, the path to antenna 1 is longer by  $b \cdot \cos \theta = \vec{b} \cdot \hat{s} = \tau_g c$ . Here  $\vec{b}$  is the baseline length and  $\hat{s}$  the unit vector in the direction of the source. We can then define the geometric delay as,

$$t_g = \frac{\vec{b} \cdot \hat{s}}{c} . \quad (3)$$

The voltages received by the two antennas is then slightly different, such that antenna 1 gives  $V_1 = V \cos \omega(t - \tau_g)$ , and antenna 2 gives  $V_2 = V \cos \omega t$ . These signals are multiplied and time averaged by the correlator to give an output response  $R$ ,

$$R = \langle V_1 V_2 \rangle \quad (4)$$

where  $R_c = \left(\frac{V^2}{2}\right) \cos(\omega\tau_g)$  is the real part and  $R_s = \left(\frac{V^2}{2}\right) \sin(\omega\tau_g)$  the imaginary part of  $R$ . This output voltage varies sinusoidally with the delay change. This delay change occurs when the source moves across the sky, changing the response of the interferometer. The sinusoids are called fringes. By changing our baseline length we can change the distance between adjacent negative and positive fringes. With smaller fringes (bigger baseline) smaller objects can be observed. However, objects that appear larger than the adjacent positive and negative fringes cancel out, meaning that they become invisible to that particular baseline.

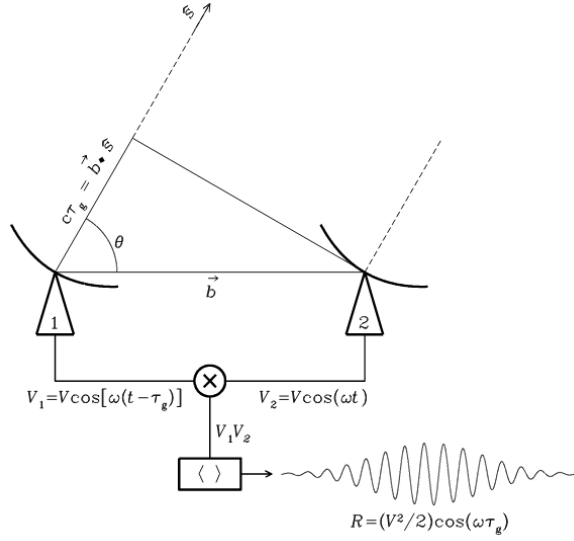


**Figure 4:** Two element interferometer (Figure by Condon J.J. and Ransom R.S., 2015).

To observe objects with different angular sizes, different baselines are needed. The VLA has a total of 27 antennas, resulting in  $\frac{N(N-1)}{2} = 351$  different baselines, each able to observe objects of different sizes.

There are two important factors that can limit the field of view of an interferometer: bandwidth and time smearing. Bandwidth smearing is caused during correlation. The delay  $\tau_g$  can only be corrected for in one particular direction, the delay center. This means that a slight error is added to all sources that are not located exactly at the delay center. The further these sources are away from the center or the bigger the angular offset  $\Delta\theta$ , the bigger this error gets, causing them to appear elongated in the direction of the delay center.

Bandwidth smearing can be solved for by either splitting the bandwidth into many small channels ( $\Delta\nu$ ) to satisfy the equation:

$$\Delta\theta\Delta\nu \ll \theta_s\nu \quad (5)$$

where  $\theta_s = \lambda/B$  and  $\nu$  the observing frequency, or by adding a phase offset to each visibility during correlation.

Time smearing is caused by averaging the integration time  $\Delta t$  of the visibilities. This averaging is done to minimize the rms noise:

$$\sigma_{S\nu} = \frac{SEFD}{\sqrt{\Delta\nu\Delta t}} \quad (6)$$

where  $SEFD = 2k_b T_{SYS}/A_e$ ,  $k_b = 1.38 \times 10^{-23} \text{ m}^2 \text{ kg s}^{-2} \text{ K}^{-1}$  is the Boltzmann constant,  $T_{SYS}$  is the system temperature and  $A_e$  the effective area of the dish. Equation 6 shows that the noise gets smaller when the averaged time is bigger. However, if  $\Delta t$  is large enough for the Earth's rotation to have caused the source to move by more than  $\theta_s = \lambda/b$  in the interferometer frame, the synthesised beam (and thus the sources displayed) will appear tangentially elongated in the uv plane. Time smearing can be restricted by minimizing the integration time according to,

$$\Delta\theta\Delta t \ll \theta_s \cdot 1.37 \times 10^4 \text{ s} . \quad (7)$$

## 2.2 Visualization

The difference between the real and imaginary part of the output response is called the complex visibility:

$$V = R_c - iR_s = Ae^{-i\phi} \quad (8)$$

with amplitude  $A = (R_c^2 + R_s^2)^{1/2}$  and phase  $\phi = \tan^{-1}(R_s/R_c)$ . The response of a two element interferometer to an extended source with brightness distribution  $I_\nu(\hat{s})$  can then be written as,

$$V_\nu = \int I_\nu(\hat{s}) \exp(-i2\pi \vec{b} \cdot \hat{s}/\lambda) d\Omega \quad (9)$$

where  $d\Omega$  is the solid angle. Since each baseline gives a different output voltage, we can see that each visibility is an independent measurement of the sky on some angular scale. All the visibilities together are the response of the interferometer, which is the inverse Fourier transform of the sky brightness distribution. This response to the position in the sky is then written as,

$$V_\nu(u, v, w) = \int \int \frac{I_\nu(l, m)}{(1 - l^2 - m^2)^{1/2}} \cdot \exp[-i2\pi(ul + vm + wn)] dl dm dn \quad (10)$$

where  $u, v, w$  are the Fourier coordinates and  $l, m, n$  are the coordinates in the sky plane. This response is represented in a  $uv$  plane, of which an example can be seen in Figure 7. The difference between Figures 7a and 7d is the time of the observation; the more time is spent, the more the  $uv$  plane is sampled due to the rotation of the Earth.

To get an image from the  $uv$  plane, we must perform a Fourier transform on the data. The Fourier transform gives a point spread function (PSF) based on the  $uv$ -coverage of the data. In Figure 5 we plotted the PSF of all the observed sources for dataset A, which is the first out of four datasets. The better this PSF is sampled (more  $uv$ -coverage), the less sidelobes we see, where an infinite  $uv$ -coverage shows only the circle in the middle. This means that the sidelobes are not real data, but rather artifacts, added by the interferometer.

The dirty image is thus a convolution of the true image with the dirty beam (the PSF). To get rid of the sidelobes and see what is underneath we apply the CLEAN algorithm. Using the CLEAN algorithm, we start with finding the strongest source(s) in the map. Then a portion of the dirty beam at this position is subtracted (usually about 1 - 5%) from the image. This response is then saved in a CLEAN map. Having cleaned this residual, a new dirty map is made, now showing new sources that were earlier obscured by the strong sidelobes. The process is now repeated until no new sources appear and only noise is left in the dirty map. This may take a few thousand iterations. A final map is then made by taking all of the CLEAN components (the sources we observed) and convolving these with the CLEAN beam and then adding back in the residual noise from the dirty image.

## 2.3 The VLA

Our data was taken with the Very Large Array (VLA), which is an interferometer consisting of 27 antennas. All antennas have a dish with a diameter of 25 meter and its largest baseline depends on the configuration of the antennas. Four configurations are generally used: A, with a maximum baseline of 36 km, B with 10 km, C with 3,6 km and D with 1 km. For our observations, configuration B was used (see Figure 6). The VLA has a frequency coverage of 74 to 50,000 MHz. The VLA is located on the Plains of San Agustin, in New Mexico, USA, at an elevation of 2124 meters.

# 3 Data reduction

## 3.1 Observations

For our research of the supercluster Cl1604+432 we used data taken from the VLA archive from 2006. A total of 4 observations were carried out, on the 6th, 10th and 13th of July, and the 4th September, which we name A, B, C and D, respectively. Table 2 lists details of the four different observations. Sources 1331+305 and 0137+331 are the flux-calibrators used at the beginning and end of the observation, respectively. The total observation time includes the time on these calibrators, and the phase calibrator 1635+381. The observation started with a pointing at the first flux-calibrator, then at the phase-calibrator

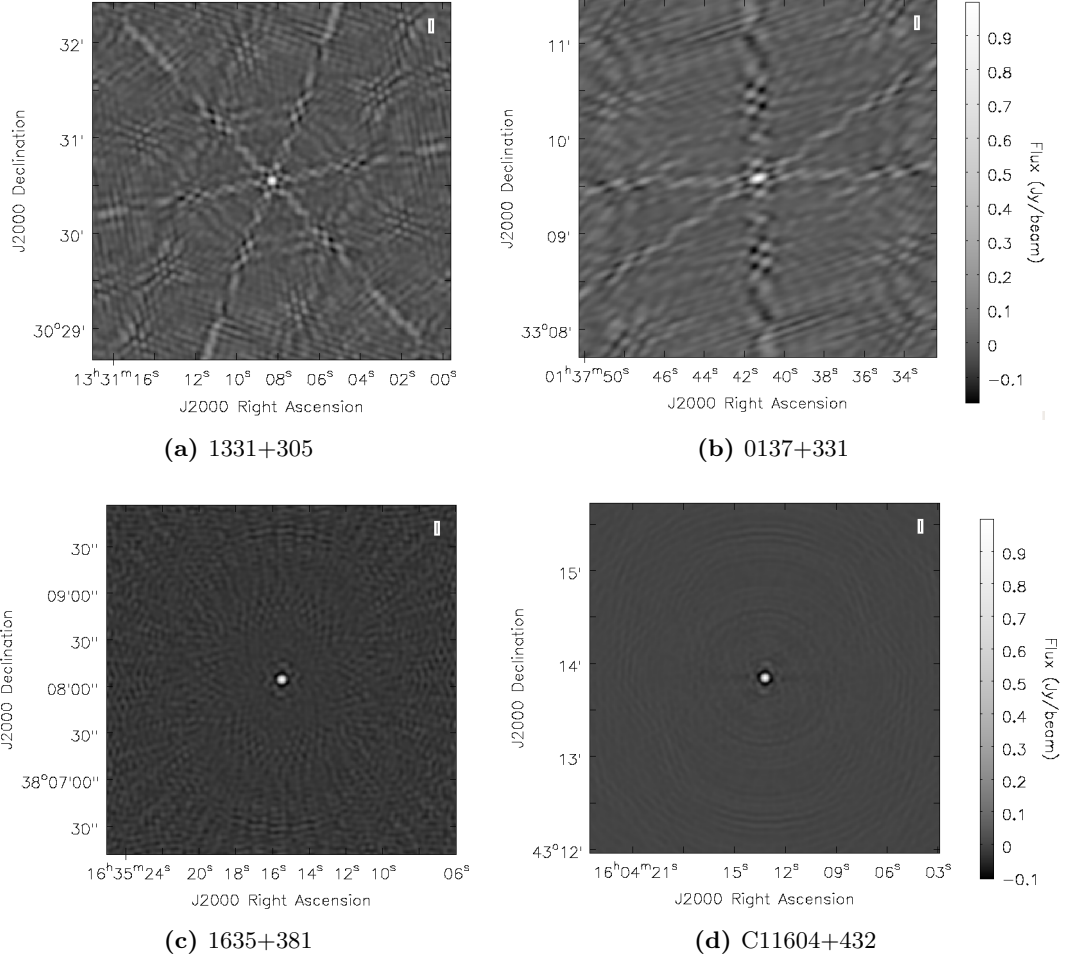


**Figure 5:** PSF of all four observed sources. Figures 5a and 5b show the largest sidelobes. These are the flux calibrators and are also the least sampled. Figure 5c shows less sidelobes due to the longer sampling time and Figure 5d shows the least sidelobes. This clearly shows that the more the uv-plane is sampled, the less sidelobes we get. These sidelobes are thus clearly a result of the interferometer and do not represent real data.

and alternating between the target source and the phase-calibrator, and ended with the phase-calibrator and the last flux-calibrator. Alternations between the target source and the phase-calibrator lasted on average 50 minutes with 4 minutes used on the phase calibrator.

Observations were carried out with the L-band continuum frequencies at 1.36 and 1.44 GHz. For each frequency 7 usable channels of 3.125 MHz with 2 polarizations were used, giving a total bandwidth of 43.75 MHz. The imaging area of the primary beam is a circle with diameter of roughly 29 arcminutes. We can fill this in for Equation 5 to check for bandwidth smearing,

$$\Delta\nu \ll \frac{\theta_s}{\theta_{FWHM}} \nu = \frac{\lambda}{D \cdot 0.5^\circ} * 1.4 \cdot 10^3 \text{ MHz}$$

$$3.125 \text{ MHz} \ll 24 \text{ MHz} \quad (11)$$

which shows us that bandwidth smearing is being solved for.

A visibility integration time of  $t = 3.33 \text{ s}$  was used for all four observations. If we fill this in for Equation 7 we find that,

$$t_{in} \ll \frac{\theta_s}{\theta_{FWHM}} \cdot 1.37 \times 10^4 \text{ s} = \frac{\lambda}{D \cdot 0.5^\circ} \cdot 1.37 \times 10^4 \text{ s}$$

$$3.33 \text{ s} \ll 234.84 \text{ s} \quad (12)$$

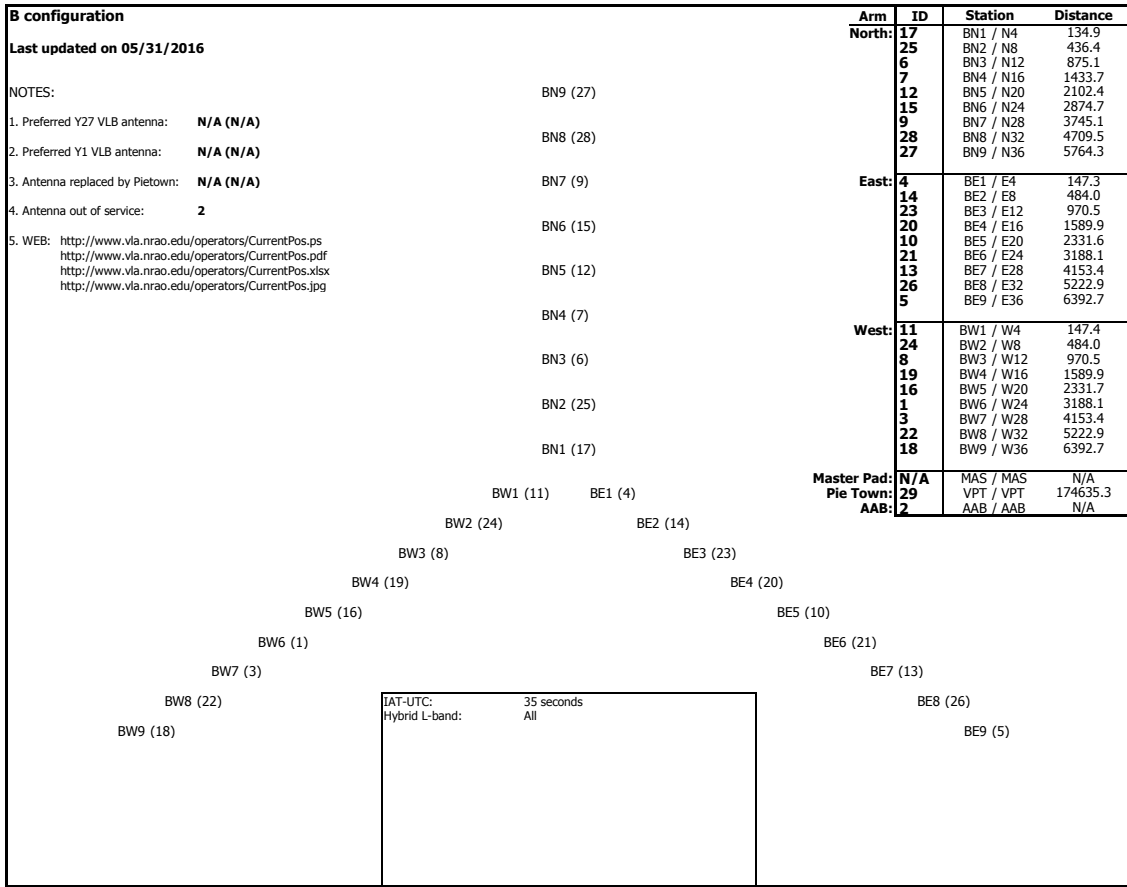


**Figure 6:** B configuration of the VLA. The largest baseline in this configuration is about 10 kilometers.

which shows that the condition is satisfied. For analysis of these observations CASA version 4.6.1 was used.

### 3.2 Pre-calibration

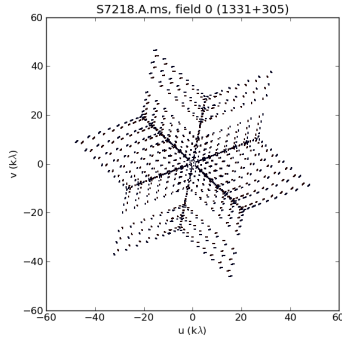
All observations in the archive were split into two files, one going from the start of the observation to midnight, and the second going from midnight to the end of the observation. The first step in CASA was therefore to combine the files. We then applied the command 'listobs', which makes a file of all the Measurement Set (MS) contents (time of observations, names of the antennas and their positions etc), as can be seen in Appendix B. We also plotted the UV samples of all the fields (calibrators and source), to get an idea of the sampling (see Figure 7).

For our observations CASA assumes a standard position of the VLA antennas. An offset of one or more of these antennas can cause problems with calibrations by adding an unknown extra delay, so it is necessary to correct for this. Using the VLA archive we can find a list of antenna offsets with their exact corrected coordinates for every date. With the command 'gencal' using the calibration mode 'antpos', we can correct this in CASA. Also using 'gencal', we corrected for the elevation gain using the calibration mode 'gceff'. Gain is the ratio of input power and output power due to the beam. The CASA command 'gaincurve' can correct for differences in elevation between large antennas.

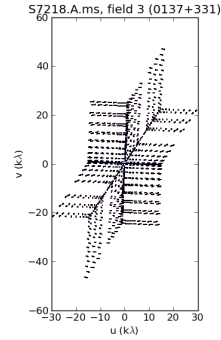
After performing these corrections, we started flagging bad data. From the command 'listobs' the different VLA and EVLA antennas can be identified. The EVLA antennas are equipped with new receivers, which causes problems in the correlator; the signals from the EVLA and VLA antennas cannot

**Table 2:** Details of the four different observations

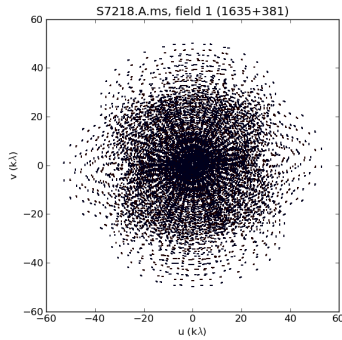
Tag	Date	Total obs. time (ks)	Time (s) on 1331+305	Time (s) on 0137+331	VLA antennas used	Average frequency (GHz)
A	06-07-2006	32.2	460	423.3	22	1.4
B	10-07-2006	32.1	400	427	22	1.4
C	13-07-2006	32.2	460	426.6	22	1.4
D	04-09-2006	28.6	520	416.6	21	1.4



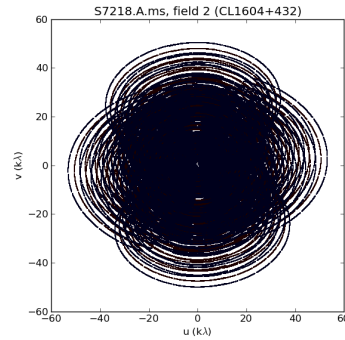
(a) 1331+305



(b) 0137+331



(c) 1635+381



(d) C11604+432

**Figure 7:** UV sampling of the Fourier planes for the observations of 2006 July 7. In figures 7a and 7b we see respectively the flux calibrators 1331+305 at the beginning of the observation, and 0137+331 at the end of the observation. Figure 7c shows the sampling of the point source 1635+381, which was observed multiple times during the observation of the source cluster, which is why it shows more sampling points. Finally figure 7d shows the sampling of our target source C11604+432.

be combined. For the first of the observations there are 5 EVLA antennas, whereas for the rest there are 4. Since at least 4 antennas are needed for calibration, the EVLA antennas are removed and for our purposes remain unused. With not all antennas begin in use at all observations, we are left with 22 VLA antennas for the first 3 observations, and 21 for the fourth.

The remaining baselines were then checked for inconsistencies. This is done by plotting per baseline the amplitude vs time and the phase vs time using the command 'plotms' for the calibrators. The baselines that seemed faulty were removed.

Lastly the extreme outliers needed to be removed. In the CASA log window these outliers can be checked for consistencies (antenna, baseline, time of observation, spw, correlation) and points that give regular faults were then deleted manually.

### 3.3 Calibration

When all the pre-calibrations are done, calibration of the data starts. During calibration we look at our calibrator sources only (sources 1331+305, 0137+331 and 1635+381, to be called fields 0, 1 and 3 respectively), and compare these to the models we have for these sources. We consider our data and the models as tables, and call them  $V_{ij}^{DATA}$  and  $V_{ij}^{MODEL}$ , respectively. When comparing the data to the model quite a few differences become clear, which can have numerous causes. The goal of calibration is to equalize these two tables, which is done by multiplying  $V_{ij}^{DATA}$  with a correction table  $J_{ij}$ :

$$V_{ij}^{DATA} J_{ij} = V_{ij}^{MODEL} \quad (13)$$

This correction table  $J_{ij}$  is a combination of different tables, all to be made during different calibration processes described below. Every process described creates its own part of the correction table, which are in the end all combined to form  $J_{ij}$ .

Before any other calibration is started, the Flux Density Scale (FDS) is set for fields 0 and 3, using the command 'setjy' that CASA provides. This command creates the Fourier transform of a calibrator model when provided, so that the data can be corrected to the proper flux density. The models needed for our observations were all provided by CASA, since these well studied objects have complicated structures.

Before doing the delay corrections, a time average of the phase over all the channels needs to be corrected for. Not all the channels are used for this time average, since the phases for the first and last channels can lay quite far apart. From a total of 7 channels, only numbers 2 to 4 where therefore chosen to make this solution. This was all done using the command 'gaincal' in CASA.

With this time average phase, we can now draw a phase vs. time diagram (see Figure 8). Using this average the delays can be solved for.

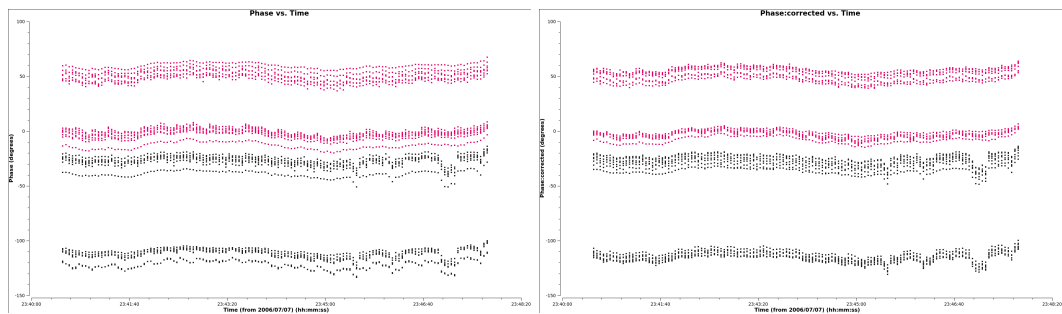


**Figure 8:** Plots of phase vs time before (left) and after (right) applying 'gaincal'. The plots of phase vs time for the middle channels (numbers 2, 3 and 4) have been averaged).

The bandpass can then be determined. This is necessary due to frequency-dependent effects between the transmission and the reception of the signal and effects within the receiver, which cause gain variations. These effects should not change over time, so a special gain type is created to handle these: 'B'. This gaintype 'B' solves for the complex gain in each given channel. This is done using the command 'bandpass'.

The tables created in all the previous calibrations can be used as input for the phase and amplitude calibration. Using the command 'gaincal', with as input the antenna positions, the gaincurve, the delays and the bandpass corrections, the amplitude and phase gain as function of time for each antenna are calculated. As a final measure the flux of the phase calibrator is then compared to the flux of the flux calibrator, and corrected accordingly using the command 'fluxscale'. The final results of the calibration process can be seen in Figures 24 and 25.

Having the calibration completed, the correction tables made in the process need to be added together. For every step we created a correction table  $A_{ij}$ ,  $B_{ij}$ , etc, which are multiplied according to equation 14:

$$A_{ij} \cdot B_{ij} \cdot \dots = J_{ij} \quad (14)$$

This is done by applying the command 'applycal' to all the calibrator sources with as input all the correction tables created in the processes described above. With this done we can apply  $J_{ij}$  to our target source using again 'applycal'. This creates a corrected table for our source. Using this corrected table we

do some final flagging, before we can start imaging. The final result of the amplitude vs time diagram of our target source can be seen in Figure 9.

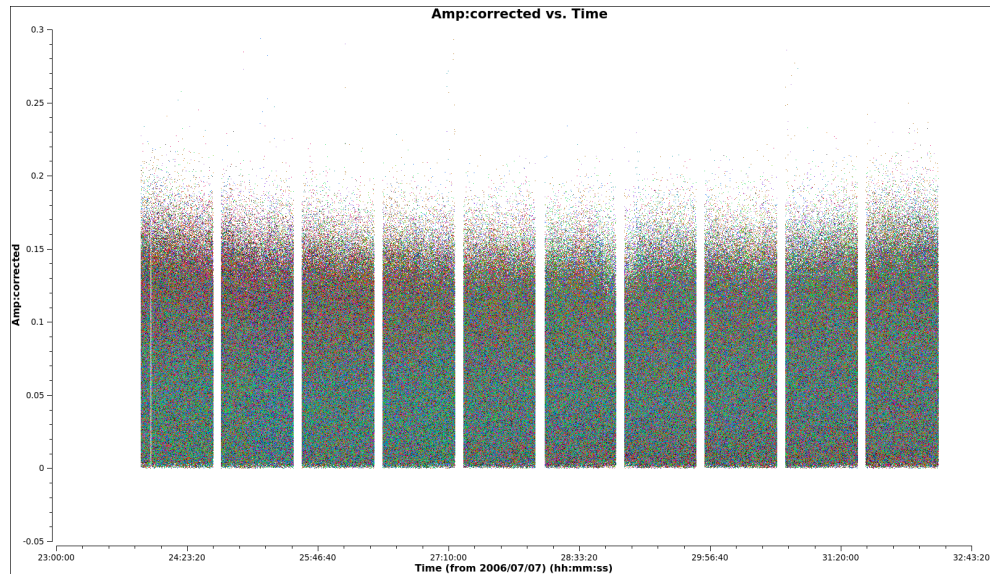


**Figure 9:** The final result of the calibration process presented as the amplitude vs time diagram of the target source (field 2).

### 3.4 Imaging

After calibration the corrected data is separated from the original data. With this corrected data a first raw Fourier transform is performed on the recorded visibilities to create a point spread function (PSF) of the observation (the dirty beam) and our first 'dirty image' (see figure 26a).

In this first image, two bright sources are all that can be seen. These sources and their sidelobes overshadow all other sources in the image. The sidelobes are formed by performing the Fourier transform on our data while creating the dirty image. The way this dirty image comes about is described in section 2.2. We can see in Figure 10 that the sidelobes of the brightest sources can overshadow the fainter sources. By using the command 'clean' from CASA as described in Section 2.2, we can identify these bright sources and reduce the sidelobes around them.

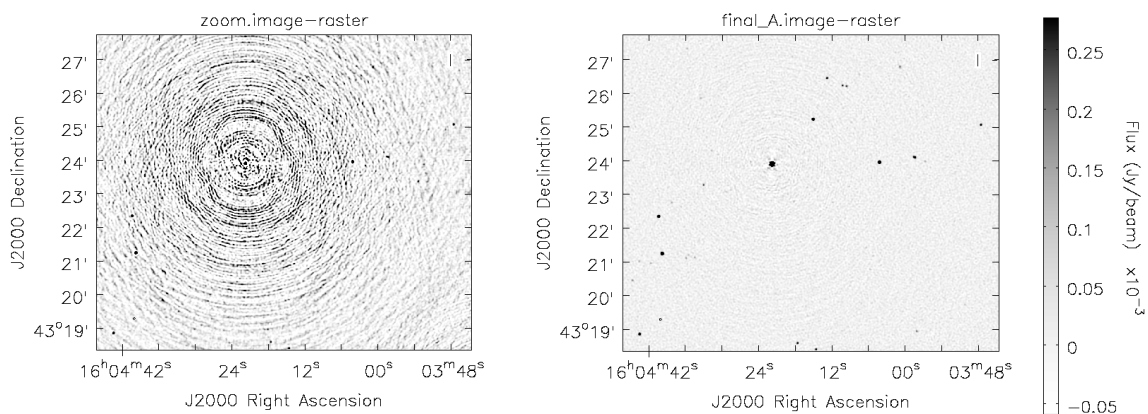


**Figure 10:** Zoomed in image on brightest source at R.A. (J2000)  $16^h04^m21^s$ , decl. (J2000)  $43^{\circ}23'52''$ . *Left:* The source is clearly visible in the middle, with the sidelobes in black around it. The white patches represent the minima of the sinusoidal function. *Right:* The same area on the sky after the complete process of cleaning. Without the heavy sidelobes around the bright sources a lot more fainter sources have become visible. The source also appears bigger on the map which is also a consequence of the cleaning process.

If the region in which you want to clean is left unspecified, the entire map is being 'cleaned'. However, by running the 'clean' command interactively, which opens up the CASA viewer, boxes can be set around regions where it is needed. In the case of image 26a, these boxes have been put around the brightest pixels of the two bright sources. These boxes form the 'deconvolution region' (or mask). Now the command 'clean' can be run. We set a threshold, which is at least thrice the background noise (so  $66\mu\text{Jy}$ ) so as not to clean too far, set the gain to 0.01 (so as to not clean too much per iteration) and choose a number of iterations. When running 'clean' the dirty beam is subtracted from the map, showing all underlying sources. Therefore, for the first run the number of iterations does not have to be higher than 100 to show something new (see figure 26b). These new sources can then be boxed up and the number of iterations can be made larger, since it now takes a little more cleaning to show new sources. This process is repeated until no new sources appear (see figure 27b for the final result).

For short observations, this might be enough. However, we are dealing with a longer observation done over multiple time slots. Every time the antennas are pointed back on the target source after briefly going to the phase calibrator, the target source has moved ever so slightly on the sky. Due to this movement during the observation and because all these short observations of 45 minutes are added together, the sources on our sky-map may appear in places that are slightly off from where they should be, or in extreme cases, they may appear twice due to phase errors. To correct this, we need to perform a process that is called 'self-calibration', before we can continue cleaning. Self-calibration, as opposed to calibration, uses the data, and not a set of calibration sources, for the calibration.

This self-calibration process is initiated by transforming our sky-map back to a revised set of visibilities, using a Fourier transform. In CASA this can be done using the command 'ft'. This ft command adds a source model to the measurement set. We then apply the command 'gaincal' to correct for the phase using the newly made model. Within gaincal, we can choose to solve over a period of time. This means that the period of time we choose is the period over which the observation gets averaged. The bigger this averaging period is, the less noisy our data gets. But a larger averaging time also means we do not account for small time variations of the plane. We therefore start with periods of 20 minutes. We also combine both spectral windows for a better signal-to-noise ratio. After 'gaincal' we apply the calibration using 'applycal', thus creating a new CORRECTED data table.

After having done this self-calibration, we can go back to cleaning our newly 'corrected' map, setting boxes if needed. The processes of self-calibrating and cleaning can then be alternated until no new sources appear. After reaching this threshold, we go back to the command 'gaincal' and change our solution interval to periods of 10 minutes. Now we start again with the cleaning/calibration process and keep going until no new sources appear.

During this process, we continue to decrease our solution interval to 5, 3, 2 and lastly 1 minute, until the background noise does not reduce anymore. At that point, which for us appeared to be at 2 minutes, we seemed to have reached the perfect solution interval. At this point, our rms noise was at about  $\sigma = 20\mu\text{Jy}/\text{beam}$ .

Figures 28, 29 and 30 illustrate the results of the self-calibration process. In Figure 28 we can see the phase offset for all antennas before the self-calibration process. The four different input sources (two spectral windows (spws) and two correlations) yield totally different results with respect to each other and with respect to every other antenna. However, we do see that the phases stay more or less constant over time, which is the result we would expect after calibration.

In Figures 29 and 30 we see the phase offset for all antennas after self-calibration; all the outputs have been compared to the reference antenna (VA15) and multiplied to a correction table, as was also done in the calibration process. The diagrams show that all the phases are now not only pretty constant in time, but also around the 0 point. We can, however see that the diagrams of Figure 30 show more accurate results than Figure 29, which has two causes. Firstly, in Figure 29, the results of the calibrated phase offsets have been averaged over periods of 60 s. In Figure 30, this period was 120 s. Additionally to this bigger period, the results for both the spws have been averaged, all leading to more accurate results.

All the calibration and imaging steps described above have been saved in a script file, which can be seen in Appendix C . This script was made using dataset A and was altered to apply to datasets B, C and D where only the flags need to be changed per dataset. Also for each dataset the image with the best solution interval can then be found, since after each self-calibration 'gaincal' a new image is made.

Having created final images for all four datasets, we wanted to create an image for each set with the primary beam correction. The primary beam has its highest sensitivity in the center, with sensitivity gradually falling off as detections more on the outside of the beam are being made. This causes the flux density of the sources that lie on the edges of our sky map to be increasingly underrepresented.

The final images and their primary beam corrections can be seen in Figures 31, 32, 33 and 34.

Having four final images paves the way for making one combined wide field image. This reduces the overall background rms noise and increases the dynamic range. With this reduced background noise, more sources can be seen in the image frame. The result can be seen in Figure 35.

## 4 Results

### 4.1 Object detection

The final image is  $1 \times 1$  degrees with a resolution of  $7200 \times 7200$  pixels. It has an overall rms noise of  $\sigma = 11 \mu\text{Jy}/\text{beam}$  and  $\sigma = 20 \mu\text{Jy}/\text{beam}$  around the brightest objects and a dynamic range of 6200. Object detection was carried out using PyBDSM.

PyBDSM has four basic commands: `process_image`, `show_fit`, `export_image` and `write_catalog`.

The first is `process_image`. This takes a `.fits` image as input and calculates the background rms and mean images. It finds islands of emission, fits Gaussians and groups those into sources. It allows the decomposition of the image into shapelets, calculation of source spectral indices, derivation of source polarization properties and correction for PSF variation across the image. For our purposes we chose the primary beam corrected image of all four combined datasets. Doing this required us to set the option `'blank_limit'` to  $10^{-5}$ . This has to be done because the primary beam corrected image has no information in the corners of the image, which otherwise gives a fault in PyBDSM.

The command `show_fit` can then be performed to show a quick result of the `process_image`. The results of `show_fit` can be seen in Figures 11 and 12.

Next we used the command `export_image` to export the internally derived images to `.fits` or `CASA` files. Then we can use the last command which is `write_catalog`. This writes the fitted Gaussians, sources and shapelets into an ASCII file.

With this method 538 unique sources with detection significances of  $> 3\sigma$  were found. However, we can see in the top middle image of Figure 11 that most of these sources are at the edges of our map. When investigating a little bit more in the edge of the map, we find sources as in Figure 13, where the sidelobes added by the interferometer are still clearly visible and measured as separate sources.

We therefore chose to throw away all sources that were further away than the FWHM. To find the distance of the FWHM to the pointing center we had two options. One is an approximate formula from the National Radio Astronomy Observatory (NRAO),

$$\theta_{FWHM} = \frac{45}{\nu_{\text{GHz}}} \quad (15)$$

At the observed frequency of 1.4 GHz this gives a diameter of  $\approx 32$  arcminutes, so we'd throw away all sources further away than 16 arcminutes from the pointing center.

The other way to measure the distance to the FWHM was to look at the `'flux'` image produced in the cleaning process (see Figure 14a). Here we can see the primary beam intensity and the position on the map. By using pythagoras we can then find the distance to where the primary beam response is half of what it is at the center (the FWHM). We find that the primary beam response is shaped like an ellipse with a major axis of 21 arcminutes and a minor axis of 15 arcminutes. If we take the minor axis of 15 arcminutes we know that the maximum noise is  $2 \times 11 \mu\text{Jy}$ , whereas when we take the major axis of 21 arcminutes the noise is higher than this at some points. We therefore chose to take the 15 arcminute radius as the distance of the FWHM to the pointing center, which is consistent with the equation from the NRAO.

This left us with 171 sources. At the FWHM the noise is twice as high as in the center of the image (so  $\sigma = 2 \times 11 \mu\text{Jy}$ ). For completeness, we therefore chose to eliminate all sources with rms noise lower than  $6 \times 2 \times 11 \mu\text{Jy}$ . We chose  $6\sigma$  to make sure we do not measure any noise as a possible source. This left us with a total of 100 sources with rms noise  $> 132 \mu\text{Jy}$

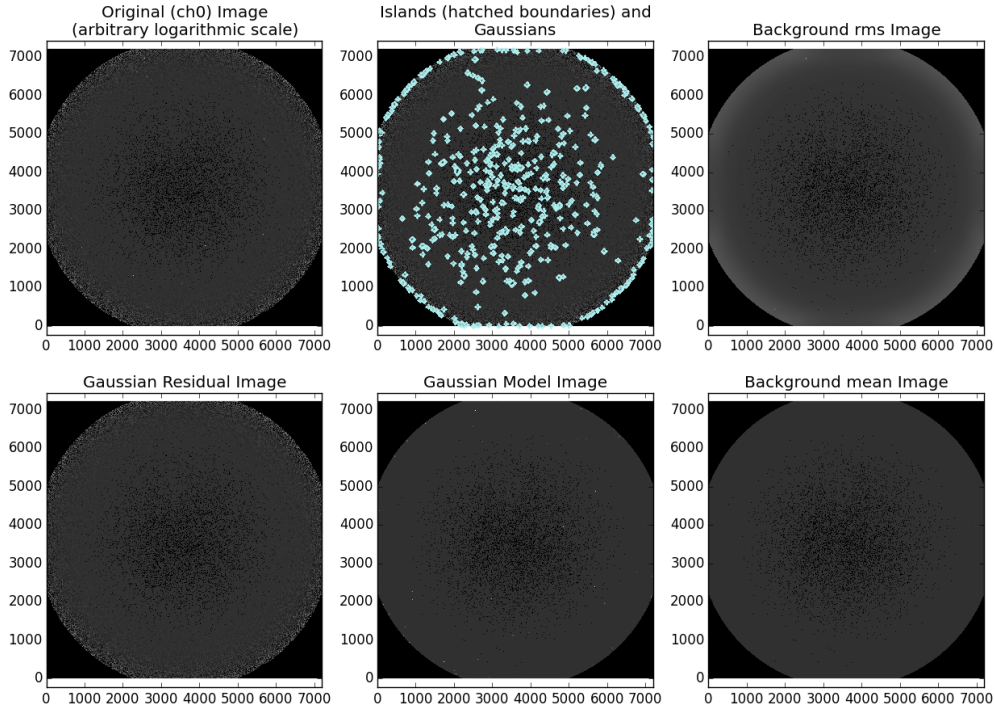


**Figure 11:** Result of 'show\_fit' in PyBDSM. *Upper left:* The original image. The white dots represent the sources. In this image only the brightest sources are visible. *Upper middle:* All islands found by PyBDSM. *Upper right:* Background rms of our image. *Lower left:* Gaussian residual of our image. *Lower middle:* Model made for the image. The model consists of all the boxes we set around the sources we found. *Lower right:* Background mean of our image.

## 4.2 Number counts

To analyze the results it is useful to calculate the number counts. We will start by comparing our number count to a theory. We have used the 'GOODS-N' survey by Morrisson et al. (2010) to this extent. The Great Observatories Origins Deep Survey - North (GOODS-N) is a wide-field radio continuum survey. The new observations described by Morrisson et al. (2010) are based on observations carried out at 1.4 GHz using the VLA in 1996 and 2005. They have used all four configurations (A, B, C and D) for a total of 165 hours adopting the same positions and frequency. For these observations  $7 \times 3.125$  MHz channels were used for both spectral windows, at 1,365 and 1,435 MHz with two polarizations. The integration time of 3.33 s from the 1996 observations were changed to 5 s in 2005 due to experienced difficulties with the correlator. The GOODS-N survey has a resulting map with rms noise of  $\sigma \approx 3.9 \mu\text{Jy}/\text{beam}$  near the center and  $\sigma \approx 8 \mu\text{Jy}/\text{beam}$  at the FWHM at 15 arcminutes from the pointing center at R.A. 12:36:49.4 and decl. +62:12:58.

Since this survey is pointed nowhere near our supercluster, it is merely to give an indication to how many sources we expect to find. In this regard it is much more useful to look at the integrated source counts, rather than at the total source counts. To do this, we start with looking at our primary beam response. In section 2.1 we described the power pattern of the primary beam. At the center, the measured flux intensity is  $1 \times$  the true flux of the object. At the FWHM, this is only  $0.5 \times$  the true flux. In Table 3 we see the measured flux intensity as a function of position and distance from the pointing center. The positions of the FWHM and all points lying in between were found using Figure 14a, which is created during the cleaning process.

In column 2 of Table 3 we give the flux density limit as a function of the minimum rms noise. In section 4.1 we stated that the rms noise in the center is  $\sigma = 0.011$  mJy. At the FWHM this noise is

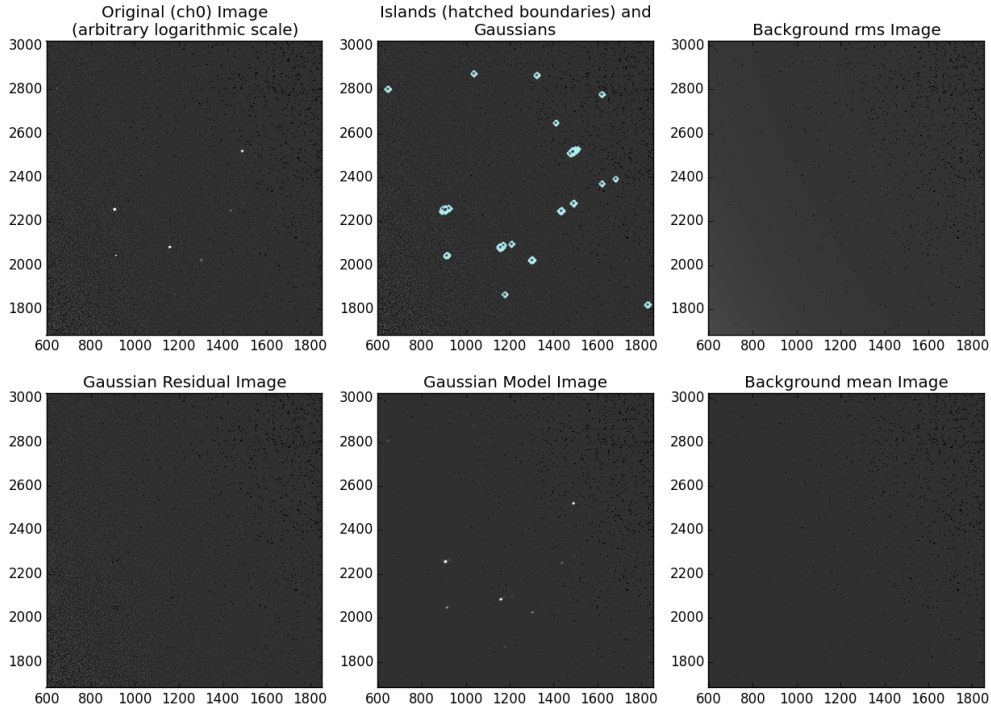


**Figure 12:** Result of 'show\_fit' in PyBDSM. This is the same image as in Figure 11, where we zoomed in on a few sources to see a better comparison between the image, the model and the islands found with PyBDSM.

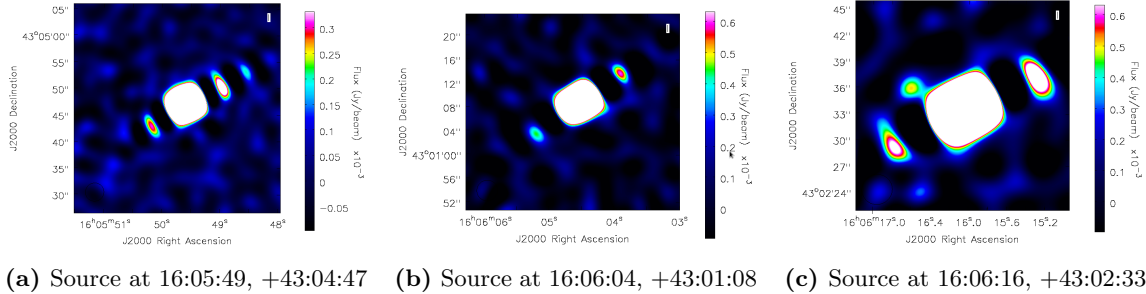


**Figure 13:** Some sources found at the edge of the map. We clearly see the cleaning process has not completely worked well here. The big square blob in the middle is the actual source whereas the sidelobes are a product of the interferometer.

$\sigma = \frac{1}{0.5} 0.011 \text{ mJy} = 0.022 \text{ mJy}$ . The flux density limit for source detection is in both cases 6 times as high as the noise. This flux density limit is calculated similarly for all points in between the pointing center and the FWHM. In Figure 14b this flux density limit is plotted against the radius from the center and against the primary beam response. Since the radius of the FWHM of the GOODS-N survey is equal to ours we expect all the inbetween points to lie on the same radii as well.

With this information we can start comparing the integrated source counts of our survey with the GOODS-N survey. For every distance (or radius) from the pointing center we took the flux density limit and looked for sources with a flux density higher than that limit within the given radius. The number of these sources were then divided by the area over which they were counted as described in Equation 16,

$$dN = \frac{N(S > \text{limit})}{\pi r^2 [\text{deg}^2]} . \quad (16)$$

**Table 3:** Primary Beam intensity

Flux Intensity	flux density limit $\times 0.011$ mJy	position (deg)		distance to pointing center (deg)
		R.A. (J2000)	Decl. (J2000)	
1	6.00	241.0549625	43.23077778	0
0.9	6.67	241.0531458	43.12189056	0.108902374
0.8	7.50	241.0536208	43.07889139	0.151892315
0.7	8.57	241.05465	43.04247694	0.188301099
0.6	10.00	241.0550458	43.00866111	0.222116685
0.5	12.00	241.0550458	42.97504639	0.255731403

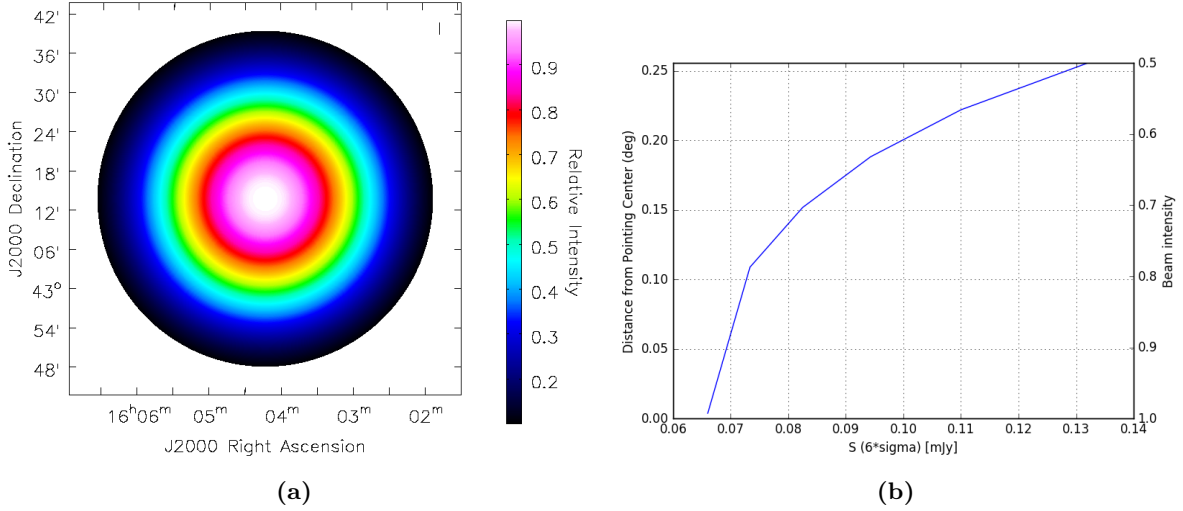


**Figure 14:** *Left:* Primary Beam response. At the center the full flux of the sources is measured whereas on the outer edges only 10% is measured. The FWHM is where 50% of the full flux is measured. *Right:* Flux density limit plotted vs radius from the pointing center and vs the primary beam response.

We decided to take the same flux density limit for the GOODS-N survey as we did for our survey (instead of  $6 \times \frac{1}{r} 0.0039$  mJy) to better compare the results (see Figure 15).

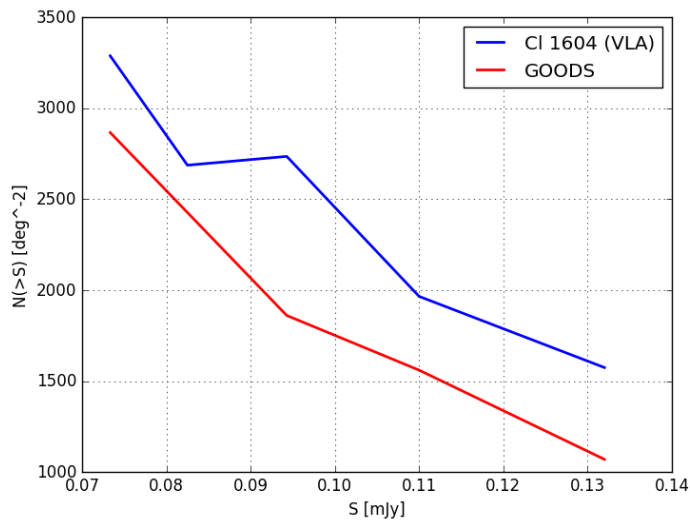


**Figure 15:** Integrated source densities of our survey versus the GOODS-N survey.

In this Figure the red line represents the GOODS-N survey. This line is what we expect to get with no overdensities in the field. The blue line is what we measured. The Figure clearly shows that we measure a higher integrated number count in every part of the flux density spectrum with a significant relative increase to the GOODS survey between  $0.85 - 0.11$  mJy and between  $0.11 > 0.13$  mJy.

We also calculated the total number counts of every source with flux  $> 6 \times 0.022$  mJy =  $6\sigma$ . In Figure 16a the number counts are plotted in a log histogram with bins of binwidth  $10^{-5}$  Jy. We can see that most sources have small flux densities where the highest bin is 8 sources. Figure 16b shows the cumulative number counts. In accordance with Figure 16a we see a steep rise in the function at the lower flux densities.

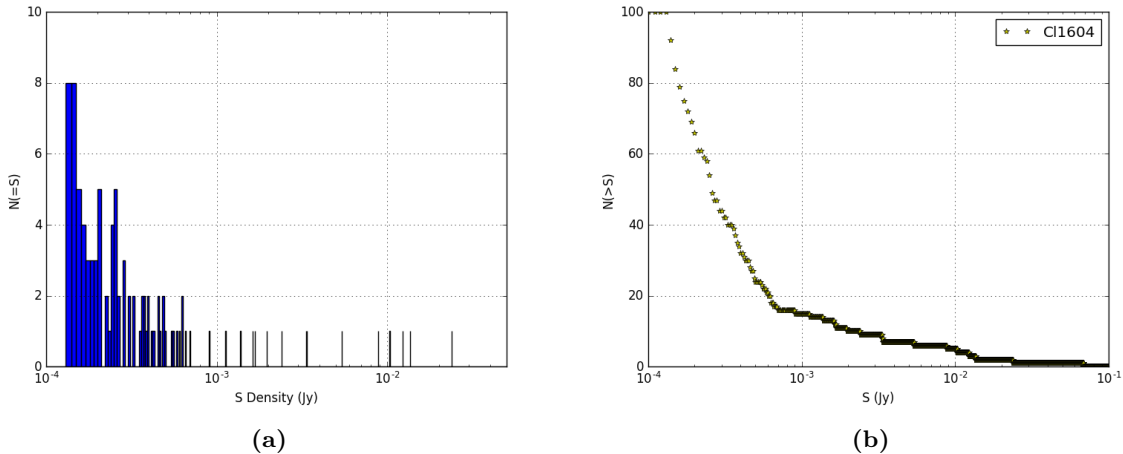


**Figure 16:** Number counts for the supercluster Cl1604. *Left:* Number count per bin of width =  $10^{-5}$  Jy. *Right:* Cumulative number count for Cl1604 (yellow), NVSS (blue) and FIRST (red).

It is also interesting to see how the number densities change in the vicinity of the clusters. From four different papers (Gal et al., 2004, 2005 and 2008 and Kocevski et al. 2009) we establish the averaged positions of the eight confirmed clusters (see Table 4).

**Table 4:** Positions of the clusters of Cl1604

Cluster ID	R.A. (J2000)	Dec. (J2000)	z	distance to pointing center
A	241.09292	43.07955	0.898	0.156
B	241.10292	43.24051	0.865	0.049
C	241.02769	43.26294	0.935	0.042
D	241.14370	43.35294	0.923	0.151
E	241.02083	43.22553		0.035
F	241.20909	43.37150	0.936	0.209
G	240.93835	43.40357	0.899	0.209
H	240.89587	43.37692	0.853	0.216
I	240.79691	43.39176	0.902	0.304
J	240.91905	43.51648		0.317

We then checked how many sources we could find within the immediate vicinity of the clusters with a radius of  $< 1$  Mpc and  $1 < r < 2$  Mpc. The results of these number counts and the densities per region are shown in Table 5. Officially, the clusters are defined to have a radius of 1 Mpc. We would therefore expect the densities of the inner radii of the clusters to be significantly larger than the densities in the outer radii. For 5 of the clusters (A, B, D, E and H) this seems to be the case. For the clusters I and J we find no sources in the inner radii since they are further away than 15 arcminutes from our pointing

center. The outer radius of I however appears to just be inside our 15 arcminutes radius. We can therefore not say anything about the seemingly increasing density with radius of cluster I.

If we want to know whether the overdensities we found are actually cluster detections, we need to know the overall density. With 100 sources within a radius of 15 arcminutes ( $\approx 7$  Mpc), we find an overall source density of  $\approx 0.650$  sources  $\text{Mpc}^{-2}$ . 5 clusters (A, B, D, F and H) have a density higher than this, but only 3 of these (A, B and D) show a significant increase in density ( $> \times 2$ ) at  $r \leq 1$  Mpc and 3 (B, D and F) show a significant increase in density at  $r \leq 2$  Mpc.

**Table 5:** Number counts at different distances from the clusters

Cluster	N at $r < 1$ Mpc	Number density (N $\text{Mpc}^{-2}$ )	N at 1 Mpc $> r > 2$ Mpc	Number density (N $\text{Mpc}^{-2}$ )	Net count at Mpc $r < 2$	Number density (N $\text{Mpc}^{-2}$ )
A	5	1.592	7	0.743	12	0.955
B	4	1.273	11	1.167	15	1.194
C	1	0.318	11	1.167	12	0.955
D	7	2.228	8	0.849	15	1.194
E	2	0.637	3	0.318	5	0.398
F	3	0.955	12	1.273	15	1.194
G	1	0.318	5	0.531	6	0.477
H	3	0.955	3	0.318	6	0.477
I	0	0	2	0.212	2	0.159
J	0	0	0	0	0	0

### 4.3 Comparing with other surveys

We wanted to cross reference the sources we have found to the results of the 'FIRST' and 'NVSS' sky surveys of the same area.

The National Radio Astronomy Observatory VLA Sky Survey (NVSS) is a continuum survey at 1.4 GHz covering the entire sky north of  $-40$  deg declination (Condon et al., 1998). The survey consisted of 2326 continuum images, each of  $4^\circ \times 4^\circ$  degrees. A high surface-brightness sensitivity was obtained using a relatively large restoring beam (45 arcsec FWHM).

In the same area that we investigated, the NVSS found a total of 14 sources of which 5 could be matched to our sources with an error of  $\pm 5.1$  arcseconds. The flux densities of both surveys were then compared and the result can be seen in Figure 17. Since both surveys measured the same objects, we would expect the sources to lay on a straight line through the diagram. The errors measured by both our survey and the NVSS are extremely small, making the errorbars hard to see. Not all the sources lay on the straight line through the origin or even touch it with the errorbars. They are however close to it and small differences in flux can be due to many factors since the flux is easily disturbed.

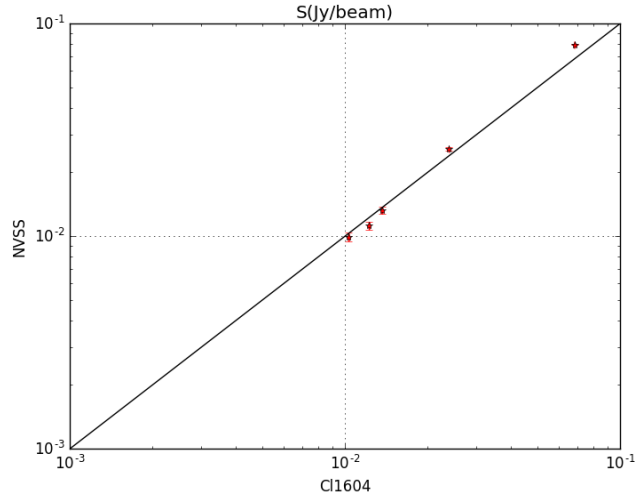


**Figure 17:** Flux density as measured by the NVSS (y-axis) compared to our survey of the supercluster Cl1604 (x-axis). Both flux densities are in units of Jy/beam.

The goal of the Faint Images of the Radio Sky at Twenty-cm (FIRST) project was to produce the radio equivalent of the Palomar Observatory Sky Survey over 10,000 square degrees of the North and South Galactic Caps. For this survey the VLA was used in B-configuration. They used two spectral windows at 1.36 and 1.44 GHz with channels of 3 MHz in width, making this survey set-up similar to ours. A final image was made by coadding twelve images adjacent to each pointing center. All maps have 1.8 arcsec pixels with a resolution of 5 arcseconds and a typical rms noise of  $\sigma = 0.15$  mJy/beam, whereas our rms noise is about 0.011 mJy/beam. This difference in noise predicts that we will be able to match less of our sources to the FIRST survey.

In the same area of our survey, FIRST finds 21 sources, of which 14 could be matched to sources we found with an uncertainty of  $\pm 5.1$  arcseconds. The comparison of flux densities between our research and FIRST can be seen in Figure 18. For this survey we already see a few more sources that lie on the straight line through the origin, which is also to be expected since we have found more sources. But we do see a trend where we measured a higher flux density for the majority of the sources.

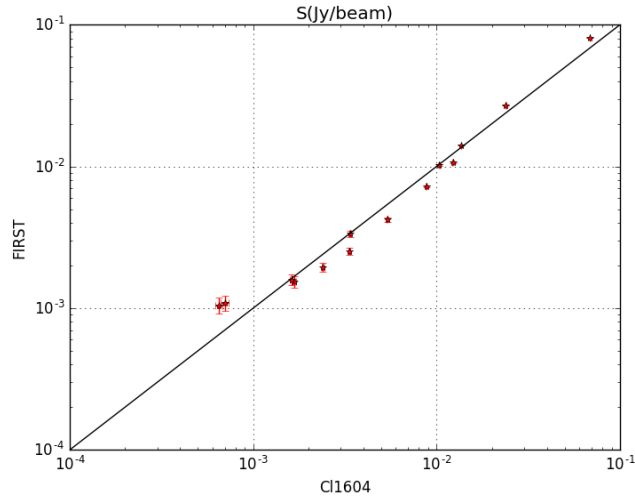


**Figure 18:** Flux density as measured by FIRST (y-axis) compared to our survey of the supercluster Cl1604 (x-axis). Both flux densities are in units of Jy/beam.

We have also compared our data with their X-ray counterparts found with Chandra by Kocevski et

**Table 6:** Catalog of the positions of the 15 sources matched to X-ray and Optical counterparts

Source Name	Radio R.A. (J2000)	Radio Decl (J2000)	X-Ray R.A. (J2000)	X-Ray Decl (J2000)	Optical R.A. (J2000)	Optical Decl (J2000)
J160329.4+432059	16:03:29.3	43:20:59.5	16:03:29.4	43:20:59.5	16:03:29.3	43:21:00.1
J160339.6+431601	16:03:39.6	43:16:02.2	16:03:39.6	43:16:01.1	16:03:39.6	43:16:02.4
J160356.7+432358	16:03:56.7	43:23:59.2	16:03:56.7	43:23:58.9	16:03:56.7	43:23:59.0
J160406.1+430532	16:04:06.3	43:05:24.8	16:04:06.1	43:05:32.8	16:04:06.1	43:05:31.8
J160406.6+431807	16:04:06.4	43:18:08.5	16:04:06.0	43:18:07.6	16:04:06.1	43:18:08.0
J160407.5+432640	16:04:07.5	43:26:34.3	16:04:07.5	43:26:40.0	16:04:07.5	43:26:40.3
J160408.9+431825	16:04:08.4	43:18:14.8	16:04:08.9	43:18:25.8	16:04:08.9	43:18:26.5
J160410.2+432614	16:04:10.3	43:26:14.6	16:04:10.2	43:26:14.6	16:04:10.2	43:26:15.0
J160412.8+432627	16:04:12.8	43:26:28.0	16:04:12.8	43:26:27.8	16:04:12.8	43:26:28.4
J160421.8+432354	16:04:21.8	43:23:54.7	16:04:21.8	43:12:45.7	16:04:21.8	43:23:55.0
J160425.9+431245	16:04:25.9	43:12:45.4	16:04:25.9	43:12:45.2	16:04:25.9	43:12:45.5
J160435.5+432112	16:04:35.9	43:21:06.4	16:04:35.5	43:21:12.3	16:04:35.5	43:21:12.2
J160435.5+432112					16:04:35.5	43:21:13.3
J160441.7+432057	16:04:41.7	43:20:57.7	16:04:41.7	43:20:57.8	16:04:41.7	43:20:58.2
J160444.6+432026	16:04:44.7	43:20:27.0	16:04:44.6	43:20:26.8	16:04:44.6	43:20:27.4
J160444.6+432026					16:04:44.6	43:20:27.0
J160448.4+430807	16:04:48.5	43:08:06.9	16:04:48.4	43:08:07.3	16:04:48.5	43:08:07.2

al. (2009). For our 100 objects we found 18 X-ray counterparts. The data obtained by Kocevski et al. was later also compared with optical data. From our sources, a total of 15 could also be matched with these optical counterparts. Their relative positions from each of these researches can be found in Table 6. More details of these sources can be found in Table 7. A visual representation of these sources can be found in Figure 19.

The redshifts presented here are taken from the Kocevski et al. (2008). With the use of

$$L_{REST, 1.4\text{ GHz}} = 4\pi D_L^2 S_{1.4\text{ GHz}} (1+z)^2 \quad (17)$$

we found the luminosities for the seven sources for which we have redshifts. With the exception of one (J160421.8+432354), we find that all these sources have luminosities of  $L > 10^{24}$  W Hz<sup>-1</sup>. We can therefore conclude that all these sources are dominated by AGN activity, consistent with the X-ray detections.

In the introduction we presented several studies that argued that AGN were to be found at the edges of clusters and in regions of moderate densities. Knowing the redshift of 8 from the 10 clusters, we found the distances of these AGN to the clusters in 3D space and which cluster they are closest to (columns 5 & 6 from Table 7). Here we can see that 2 of the 7 AGN lie relatively close to a cluster (J160406.6+431807 at 25.8 Mpc from cluster D and J160425.9+431245 at 15.7 Mpc from cluster B). We also see that most AGN lie closest to cluster F. This makes sense since F is the cluster with the highest redshift and all these AGN have redshifts  $z > 0.99$ . The same can be said for J160421.8+432354 which has a particularly low redshift and thus lies closer to the cluster with the lowest redshift. We can thus only really say of 2 AGN (J160406.6+431807 and J160425.9+431245) that they belong to the clusters they are closest to (D and B respectively).

We then proceeded to check the number density of sources within a 1 Mpc radius of the AGN. The results can be found in the 7th column of Table 7. We see that 1 of the 7 AGN (J160408.9+431825) is in a relatively sparsely populated area, two (J160421.8+432354 and J160425.9+431245) are in moderately populated areas (with a density approximately equal to the background density) and the rest are in areas with a density twice as high as the background density. This population is however only measured in 2D space, not 3D since we don't know the redshift of our sources.

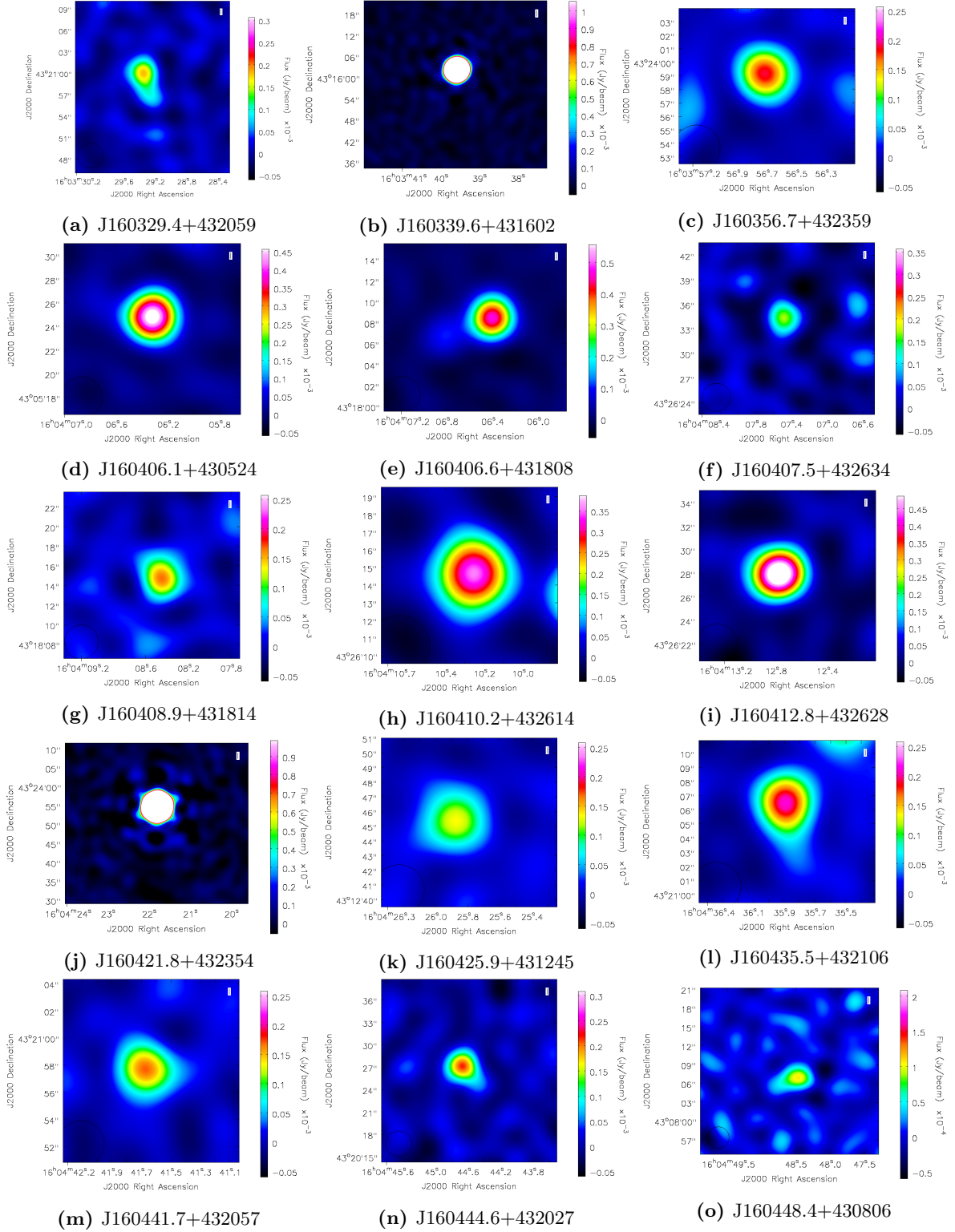


Figure 19: Visual representation of all the sources matched with their X-ray and optical counterparts.

## 5 Discussion

When comparing our results to the GOODS-N survey, we started out by finding the points where the primary beam intensity was at 1 (full flux measured) and where it was at 0.5 (FWHM). We found out

**Table 7:** Catalog of the the 15 sources matched to X-ray and Optical counterparts

Source Name	$z$	$S_{1.4\text{ GHz}}$ (Jy)	$\log(L_{1.4\text{ GHz}})$ [W Hz $^{-1}$ ]	Closest cluster	Distance (Mpc) to cluster	Source density (Mpc $^{-2}$ ) for $r < 1$ Mpc
J160329.4+432059	1.118	0.000177654	24.7	F	436.1	1.27
J160339.6+431601		0.023874889				
J160356.7+432358		0.000189095				
J160406.1+430532		0.000481702				
J160406.6+431807	0.913	0.000455517	24.8	D	25.8	1.91
J160407.5+432640	1.285	0.000170446	24.9	F	798.3	1.91
J160408.9+431825	1.285	0.000164676	24.9	F	798.3	0.32
J160410.2+432614		0.000353902				
J160412.8+432627		0.0005814				
J160421.8+432354	0.055	0.068314139	23.7	H	2697.7	0.95
J160425.9+431245	0.871	0.000133143	24.2	B	15.7	0.64
J160435.5+432112		0.00020861				
J160441.7+432057	0.991	0.000168748	24.5	F	136.7	2.86
J160444.6+432026		0.00021532				
J160448.4+430807		0.000107063				

that the radius of the FWHM was an elliptical with a major axis at 21 arcseconds from the pointing center. However, the National Radio Astronomy Observatory (NRAO) gives an approximate formula to find the diameter of the FWHM,

$$\theta_{FWHM} = \frac{45}{\nu_{GHz}} = \frac{45}{1.4} \approx 32', \quad (18)$$

which gives a radius from the pointing center of  $\approx 16$  arcminutes. This radius corresponds with the minor axis of the FWHM, which we measured at 15 arcseconds. We therefore chose the minor axis as distance from the pointing center to the FWHM, so that we are sure to have a maximum rms background noise of  $\sigma = 22 \mu\text{Jy}$ .

We then compared our integrated number densities to the GOODS-N survey. We found that for  $0.08 - 0.11$  mJy and for  $0.11 - > 0.13$  mJy we measured significant overdensities compared to the GOODS-N survey. When comparing these fluxes with Figure 14b we see that they compare to radii from the pointing center of  $0.15 - 0.22$  deg and  $0.22 - > 0.25$  deg, respectively. We know that the GOODS-N survey was a continuum search with no intention of measuring a certain cluster, whereas we were specifically looking at the supercluster Cl1604. We can therefore compare the radii where these relative overdensities were measured to the radii from the pointing center where we can find the different clusters in column 4 of Table 4. This tells us that in the specific radii of these significant overdensities we find 5 out of 10 identified clusters (A, D, F, G and H) that all fall into the first part (radius of  $0.15 - 0.22$  deg). When we look at Table 5 we see that the 3 of these clusters (A, D, F) have earlier been identified as having significant overdensities compared to the background source density. We can thus conclude due to the measured relative overdensities that we have indeed found at least three clusters within the observed region.

When looking at our number counts we also see an excess of sources with low ( $10^{-4} < \text{Jy/beam} < 10^{-3}$ ) flux densities. This can be because there are just a lot of fainter sources in the region we looked at but since we are looking in the direction of a supercluster it is more likely that the majority of these sources are found at approximately the same redshift. Unfortunately since we do not have the actual redshifts of the sources we measured we can not be sure of this.

When checking the number densities of the ten different clusters we found overdensities for 3 out of 10 (A, B and D) within 1 Mpc of the cluster center. Within 2 Mpc we also found overdensities for 3 clusters, although now these are B, D and F. Looking back at the comparison with the GOODS-N survey we already suggested A, D and F could be the cause of the measured relative overdensities.

We also compared our survey to two similar surveys of the same supercluster. When comparing to the NVSS 8 sources could be matched. In Figure 17 we see that our results for the flux densities are pretty consistent with the NVSS. To see if this is a consistent trend we decided to check our results with the NVSS for a radius of 21 arcminutes to the pointing center (the major axis of the FWHM). In this bigger region the NVSS finds 25 sources in stead of 14, and we can now match 8 sources to ours. The comparative fluxes of this plot can be seen in Figure 20.

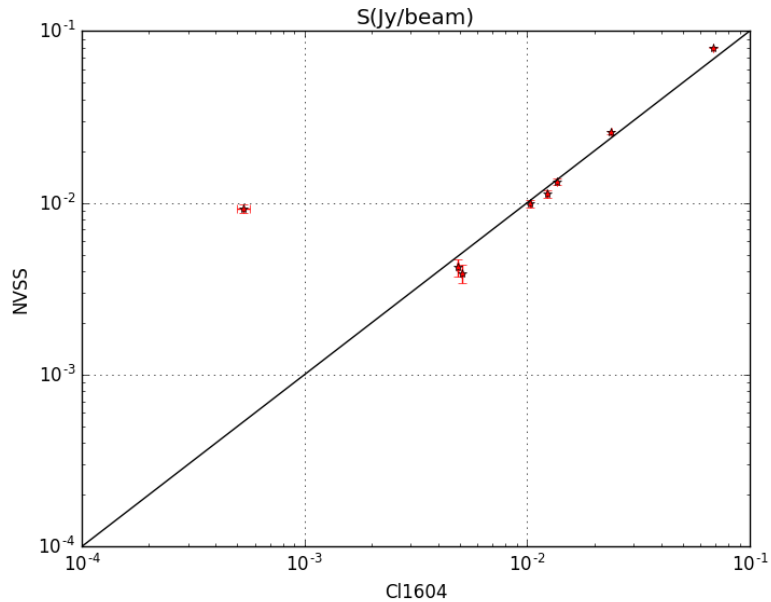


**Figure 20:** Here we again plot the flux densities of 8 sources measured by us (x-axis) and compare them to the same sources measured by the NVSS (y-axis).

Here we see that our results stay consistent with the results of the NVSS with the exception of one source where we measured a significantly lower flux density. When looking into this source we found that there were three sources found by PyBDSM that were close to each other, at (16:05:22.2, +43:17:25.8), (16:05:22.7, +43:17:10.9), and (16:05:22.1, +43:17:37.7). On our skymap we can check where this is (see Figure 21).

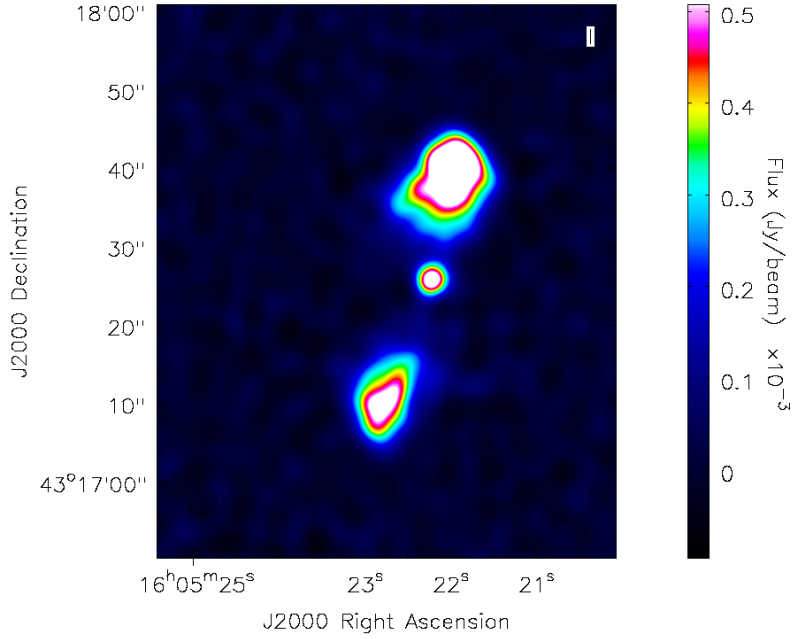


**Figure 21:** In the middle the host galaxy of the AGN is visible with two jets in the north-east and south-west direction. All three objects have been counted as separate sources by PyBDSM.

It looks like we are dealing with an AGN here. The host galaxy is clearly visible in the middle and two jets are shot out at north-east and south-west. We know that the NVSS data was taken in 1998, 8 years before our data was taken. It is possible that the AGN we are looking at was more active a few years before. Looking at the jets we see that they are no longer attached to the source, meaning that the source has stopped shooting them out. We also notice that for the jets we measure a significantly higher flux density (2 and 5 mJy/beam for the jets against 0.5 mJy/beam for the host galaxy). The brighter one of these jets corresponds very well with the flux density measured by the NVSS. It can therefore also be that they measured the wrong source.

A quick look at our skymap and detections by PyBDSM tells us that we also have a few sources with double detections (see Figure 22). Double detections mostly happen for elongated sources. However we have checked for time and bandwidth smearing and found that the equations for both were satisfied in such a way that smearing should not be an issue. Since none of the sources lie on the outskirts of our beam width it is improbable that smearing is the issue. It is therefore likely that these sources are naturally elongated by merging activities.

When comparing with the FIRST survey we see that we mostly measured a higher flux density for the same sources. Here we decided to do the same as for the NVSS, expand the region we look at to the major axis of our FWHM of 21 arcminutes. The result can be seen in Figure 23.

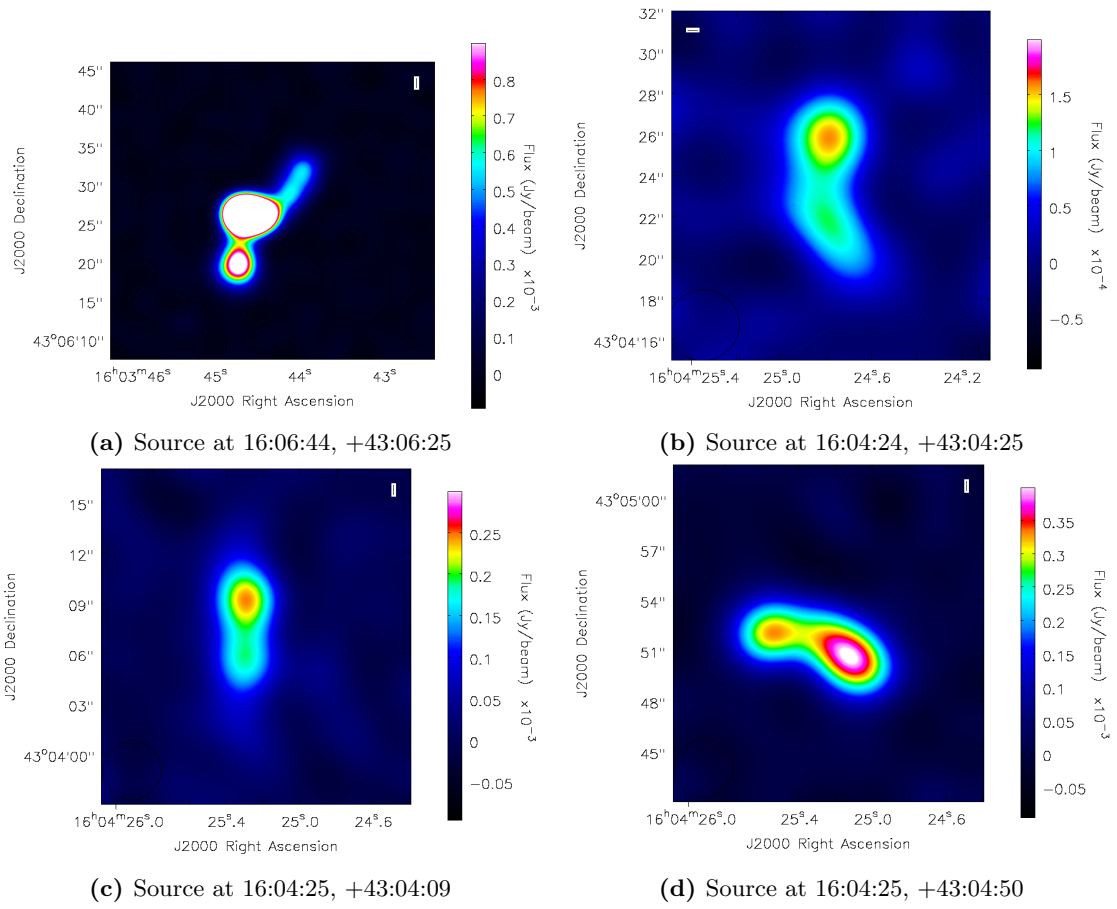


**Figure 22:** Different elongated sources with double detections by PyBDSM

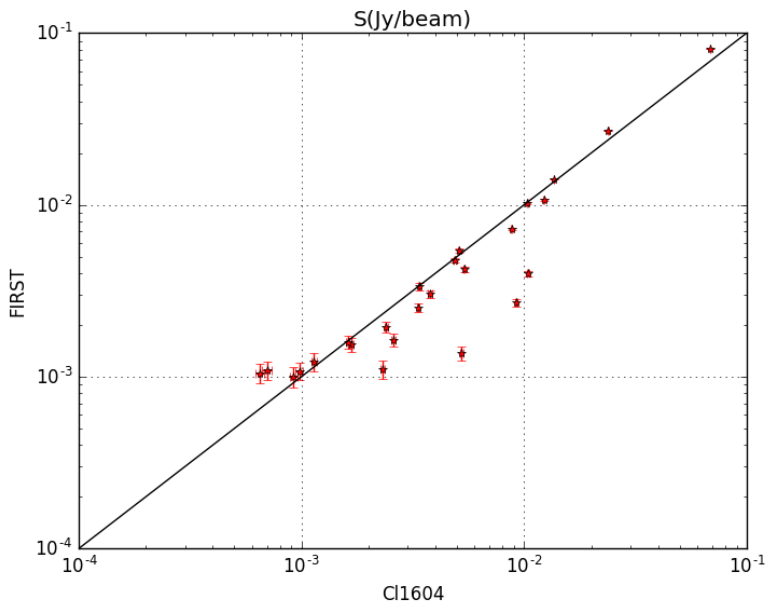


**Figure 23:** Here we again plot the flux densities of 25 sources measured by us (x-axis) and compare them to the same sources measured by FIRST (y-axis).

Here we see the trend even clearer where we measure higher flux densities for the same sources than FIRST does. We know that measuring flux is heavily dependent on the atmosphere. It is therefore possible that something has gone wrong when calibrating the flux and these flux densities have come out a little higher than the FIRST survey.

The results we have found with respect to the AGN does not completely correlate with the theory. We do have to note however that for the finding of AGN we are strongly dependent on other papers since we did not measure redshifts ourselves. If we want to continue researching the sources we found with the VLA we would need to measure the spectra of the sources and determine redshifts. This would not only help us find the positions of our sources with respect to the clusters but also determine the luminosities of the found sources. This will be very helpful to determine the nature of a source.

## 6 Conclusions

In this project we took data from the VLA archive that was taken in 2006 from the supercluster Cl1604. We calibrated the data and made a wide-field image. We used PyBDSM on the primary beam corrected image to get the proper fluxes for all the sources that would be found. Since this gave a very high noise level on the outer edges of the image and PyBDSM counted an increasing amount of false positives at the edges we decided to decrease our field of view to the FWHM at a radius of 15 arcminutes ( $\approx 7$  Mpc at  $z = 0.9$ ). We determined an average noise in the center of the image of  $\sigma = 11 \mu\text{Jy}$  and a dynamic range of 6200. Since at the FWHM this rms noise is twice as much, we assumed for completeness an rms noise of  $\sigma = 22 \mu\text{Jy}$ . We then decided to eliminate all sources with detections of  $< 6\sigma$ . This left us with 100 sources out of the 538 original detections by PyBDSM.

We then checked the literature for the positions of the 10 different clusters within the supercluster and tried to find those on our map. For these clusters we tried to find sources within a radius of 1 and 2 Mpc and see if the number densities would decrease. The clusters I and J were not completely inside our FWHM range and thus have no reliable number counts. We found that the number densities decrease at bigger radii for 5 of the 8 clusters (A, B, D, E and H). For 2 other clusters (F, and G) the density only seems to increase very moderately and one cluster (C) seems to have a very steeply increasing source density at  $1 \text{ Mpc} < r < 2 \text{ Mpc}$ . But with an overall source density of  $0.650 \text{ N Mpc}^{-2}$ , we have only

noticed a significant increase in source density in three clusters (A, B and D) at  $r < 1$  Mpc and for B, D and F at  $R < 2$  Mpc.

The results of our research have been compared to two similar surveys in the same area, the NVSS and FIRST. Within a 15 arcminute radius from our pointing center at R.A. 16:04:13.191 and Decl. 43:13:50.80, the NVSS finds 14 sources of which 5 can be linked to a source we found. The FIRST survey finds 21 sources of which 14 can be matched to sources we found with an uncertainty of  $\pm 5.1$  arcseconds. Both surveys show flux densities similar to what we found.

Lastly we compared our results to a research by Kocevski et al. (2009) who searched Cl1604 for X-Ray sources. We matched 18 of our sources to their X-ray counterparts and 15 of those could also be matched to their optical counterparts. From the paper of Kocevski we find 7 redshifts for these 15 sources, with which we could find the distances of these sources to the clusters. All have luminosities of  $L_\nu \approx 10^{24}$  W  $\text{Hz}^{-1}$  and can thus be called AGN. We find that only 2 have redshifts that corresponds to the clusters with distances to a cluster center of 25.8 and 15.7 Mpc. We can thus say that these AGN do probably belong to these clusters but lie on the outskirts as predicted in the introduction.

However, we have not measured the redshifts of our sources ourselves. For this we are thus dependend on other researches. If we were to know the redshifts of all of our sources, we could find their luminosities and so find out their nature. Knowing their redshifts also would help in finding their relative positions with respect to the clusters within the supercluster Cl1604 and the densities in their surroundings.

## References

- Alfven, H., Herlofson, N. 1950, Phys. Rev., 78, 616  
Branchesi, M., Gioia, I. M., Fanti, C., Fanti, R., & Cappelluti, N. 2007, A&A, 462, 449  
Burke, B.F., Graham-Smith, F., An Introduction to Radio Astronomy, 1996, Third edition  
Cappelluti, N., Cappi, M., Dadina, M., Malaguti, G., Branchesi, M., D'Elia, V., & Palumbo, G. G. C. 2005, A&A, 430, 39  
Cappi, M., Mazzotta, P., Elvis, M., Burke, D. J., Comastri, A., Fiore, F., Forman, W., Fruscione, A., et al. 2001, ApJ, 548, 624  
Casa User Reference & Cookbook,  
Condon, J. J. 1992, Ann. Rev. A&A, 30, 575  
Condon, J. J., Cotton, W. D., Greisen, E. W., Yin, Q. F., Perley, R. A., Taylor, G. B., & Broderick, J. J. 1998, AJ, 115, 1693  
D'Elia, V., Fiore, F., Elvis, M., Cappi, M., Mathur, S., Mazzotta, P., Falco, E., & Cocchia, F. 2004, A&A, 422, 11  
Fath E. H., 1909, Lick Obs. Bull., 5, 71  
Gal, R. R., Lemaux, B. C., Lubin, L. M., Kocevski, D., & Squires, G. K. 2008, ArXiv e-prints, 0803.3842  
Gal R. R., Lubin L.M. 2004, ApJ, 607, L1  
Garrett M., ASTRON Leiden Swinburne, Radio Astronomy lectures  
Gilmour, R., Gray, M. E., Almaini, O., Best, P., Wolf, C., Meisenheimer, K., Papovich, C., & Bell, E. 2007, MNRAS, 380, 1467  
Gunn J. E., Hoessel J. G., Oke, J. B. 1986, ApJ, 306, 30  
Henry, J. P. & Briel, U. G. 1991, A&A, 246, L14  
Hubble, E. P. 1926, ApJ, 624, 321  
Hudaverdi, M., Kunieda, H., Tanaka, T., Haba, Y., Furuzawa, A., Tawara, Y., & Ercan, E. N. 2006, PASJ, 58, 931  
Jansky, K. G. 1932, Proc. IRE, 20, 1920  
Johnson, O., Best, P. N., & Almaini, O. 2003, MNRAS, 343, 924  
Kutner M. L., 1987, Astronomy A Physical Perspective  
Lubin L. M., Brunner R., Metzger M. R., Postman M., Oke J. B., 200, ApJ, 531, L5  
Martini, P., Kelson, D. D., Kim, E., Mulchaey, J. S., & Athey, A. A. 2006, ApJ, 644, 116  
Martini, P., Kelson, D. D., Mulchaey, J. S., & Trager, S. C. 2002, ApJ, 576, L109  
Miyoshi M., Moran J., Herrnstein J. et al., 1995, Nature, 373, 127  
Molnar, S. M., Hughes, J. P., Donahue, M., & Joy, M. 2002, ApJ, 573, L91

Pentericci, L., Kurk, J. D., Carilli, C. L., Harris, D. E., Miley, G. K., & Rottgering, H. J. A. 2002, *A&A*, 396, 109  
Postman, M., Lubin, L. M., & Oke, J. B. 1998, *AJ*, 116, 560  
Postman, M., Lubin, L. M., & Oke, J. B. 2001, *AJ*, 122, 1125  
Reber, G. 1944, *ApJ*, 100, 279  
Ruderman, J. T. & Ebeling, H. 2005, *ApJ*, 623, L81  
Seyfert, C. K. 1943, *ApJ*, 97, 28  
Slipher, V. M. 1917, *Lowell Obs. Bull.*, 3, 59

# Appendices

## A Images

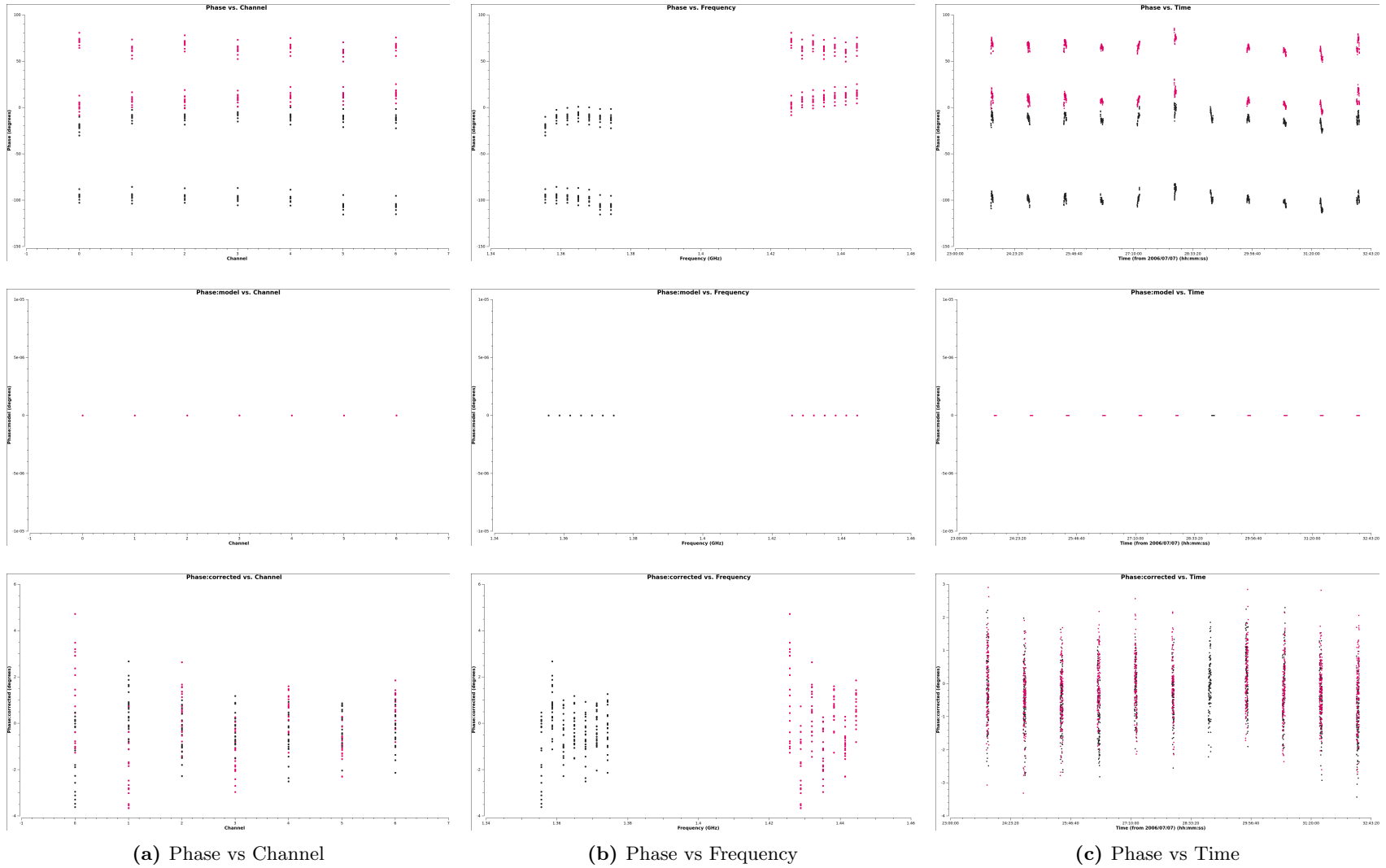


**Figure 24:** In this figure, the phase of field 1 (phase calibrator 1635+381) is being shown before (up) and after calibration (down), with in the middle the model. The phase as a function of channel (24a), frequency (24b) and time (24c) has been compared and equalized to the available model and scaled accordingly.

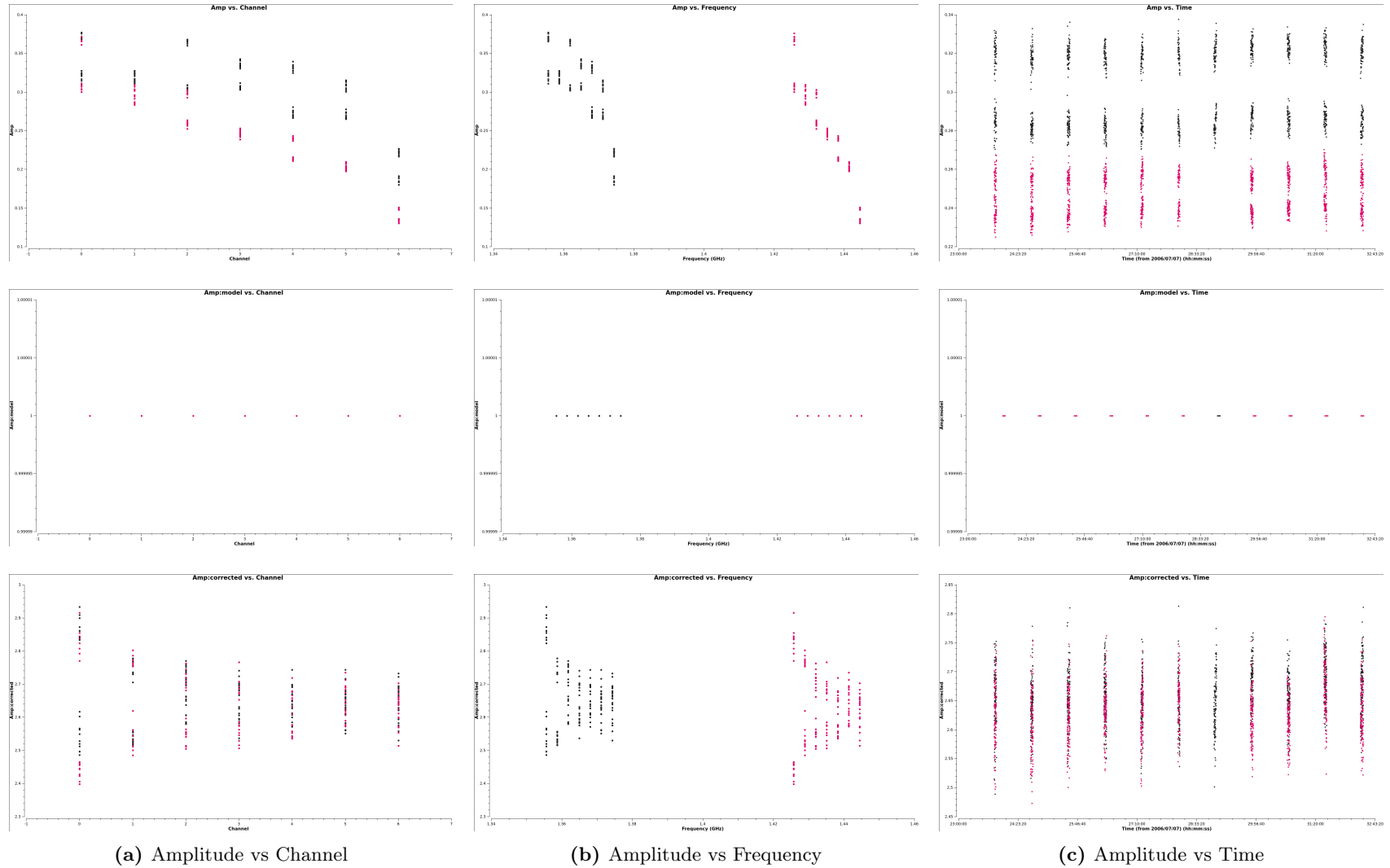


**Figure 25:** In this figure, the amplitude of field 1 (phase calibrator 1635+381) is being shown before (up) and after calibration (down), with in the middle the model. The phase as a function of channel (24a), frequency (24b) and time (24c) has been compared and equalized to the available model and scaled accordingly.

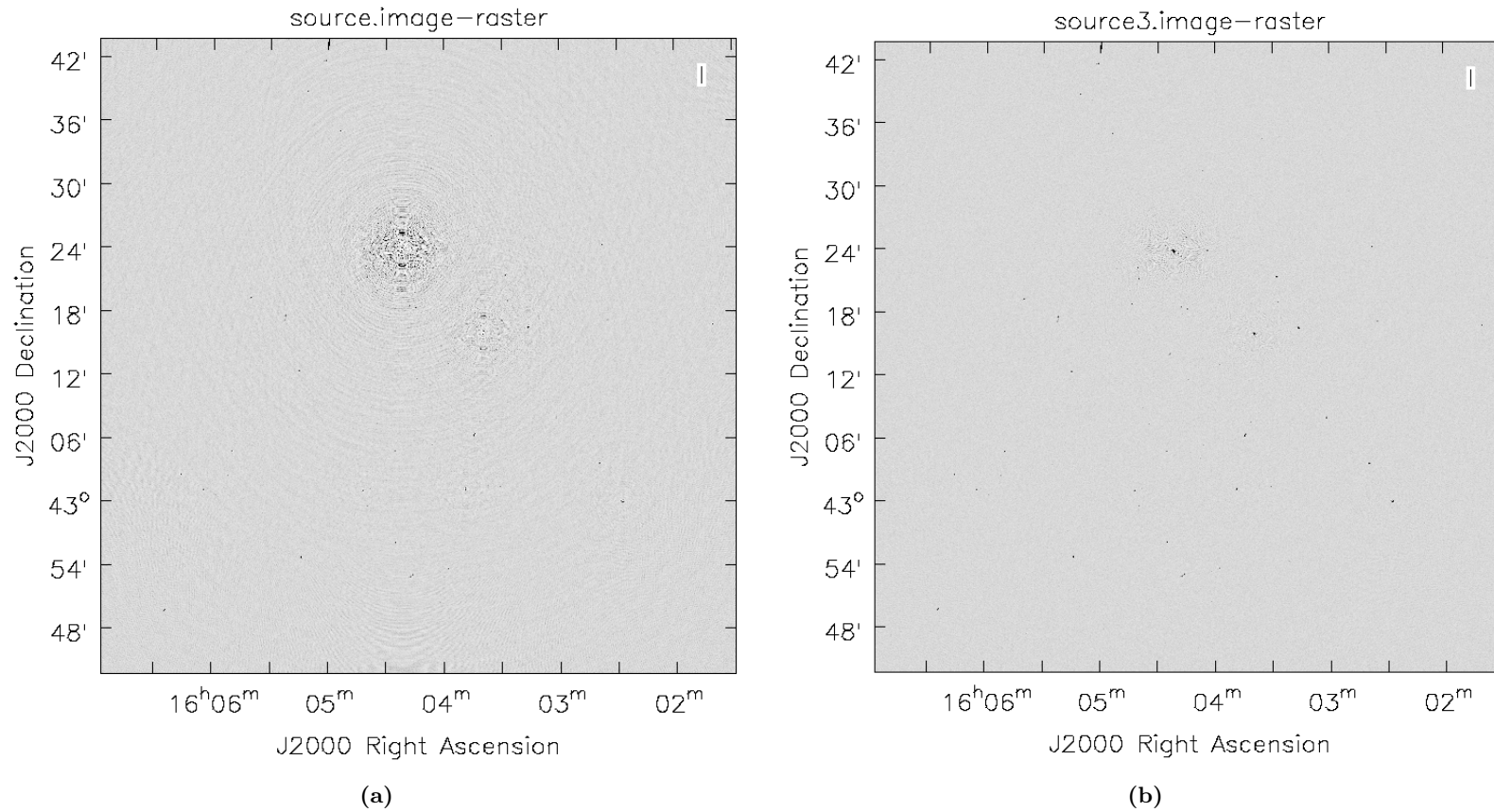


**Figure 26:** *Left:* First Dirty Image made after initial calibration. Strong sidelobes from the brightest sources are visible at R.A. (J2000) 16<sup>h</sup>04<sup>m</sup>21<sup>s</sup>, decl. (J2000) 43<sup>o</sup>23'52" and at R.A. (J2000) 16<sup>h</sup>03<sup>m</sup>39<sup>s</sup>, decl. (J2000) 43<sup>o</sup>16'02", which overshadow all underlying sources. Image needs to be 'cleaned' in order to show more sources. *Right:* Intensity of the sidelobes has decreased, revealing new sources underneath. Sources can be 'boxed' and clean process continued.

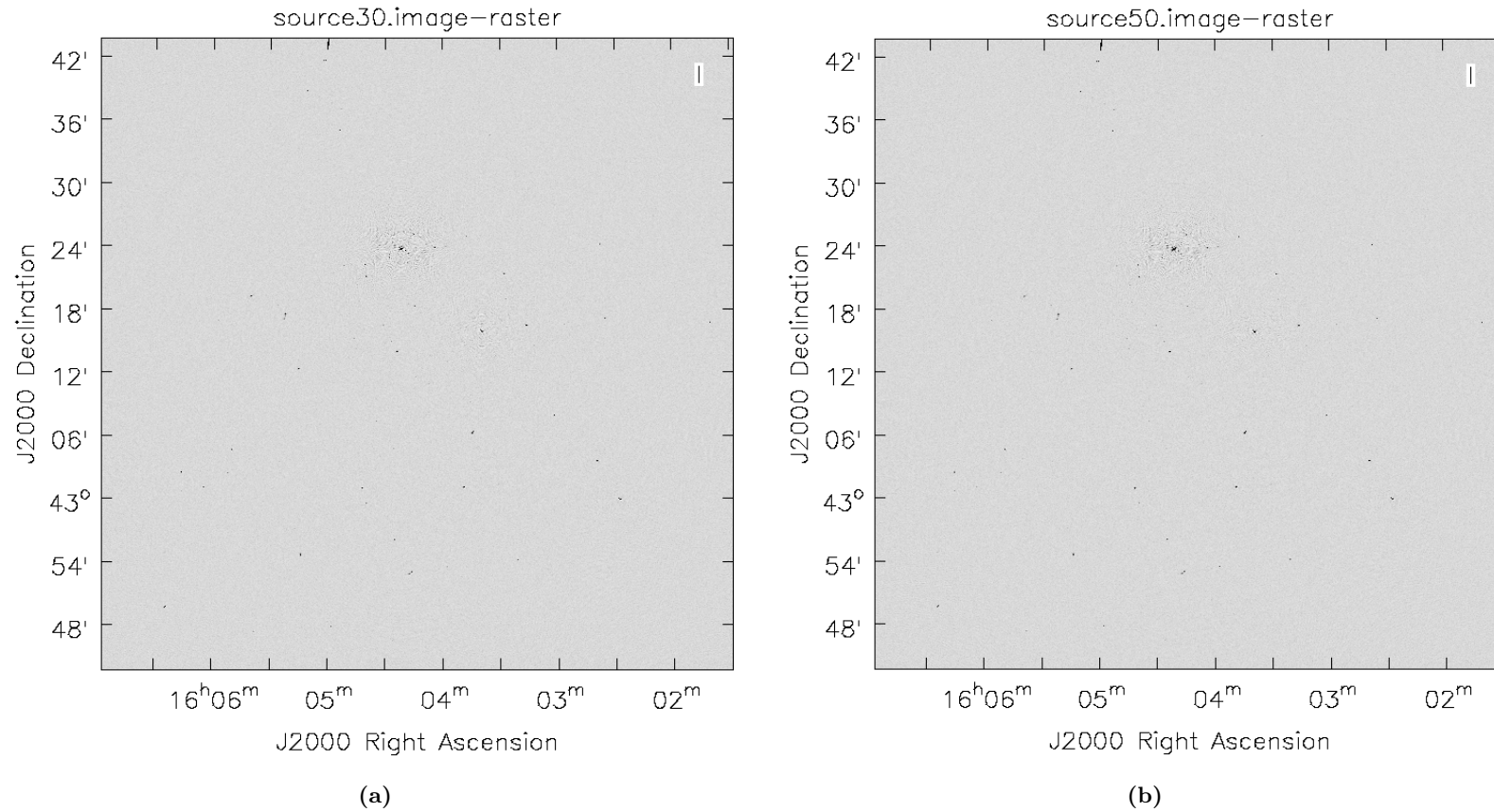


**Figure 27:** *Left:* After several cleaning and self-calibration cycles lots of new sources have appeared and the 'old' sources seem brighter. The background noise has also gone down ever so slightly. *Right:* Final image. No new sources appear upon further cleaning or calibration. The background noise is at its lowest and the flux density of the present sources at its highest. Unfortunately, we can see that since image 26b the noise of the two brightest sources has not gone down much. We expect some sources are still hidden behind this noise.

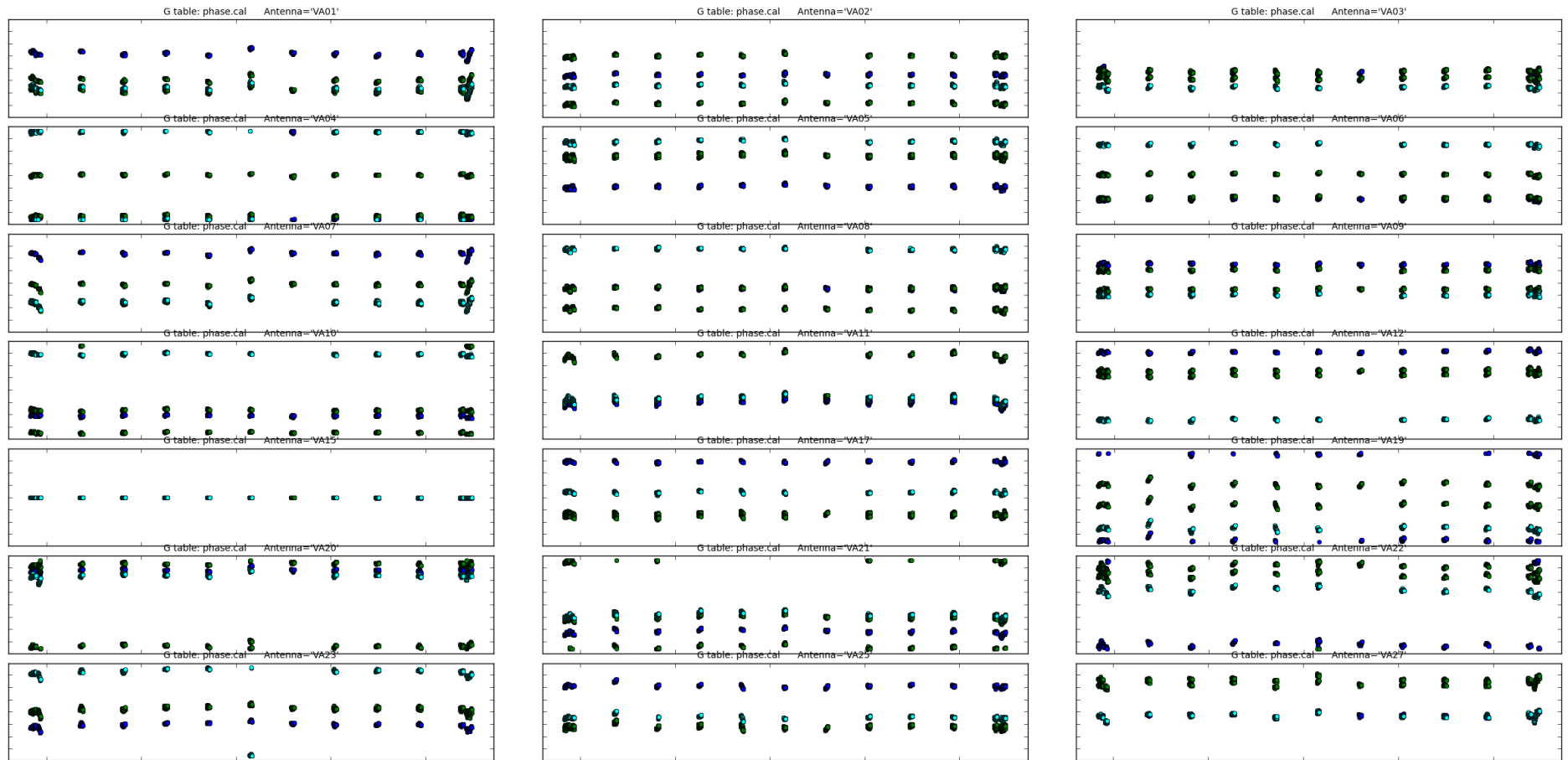


**Figure 28:** Phase offset per antenna. The four different colours represent the two spws and the two correlations. VL15 is the reference antenna, thus the offset should be 0 here. All other antennas have quite a big offset with respect to VL15, but are constant in time.

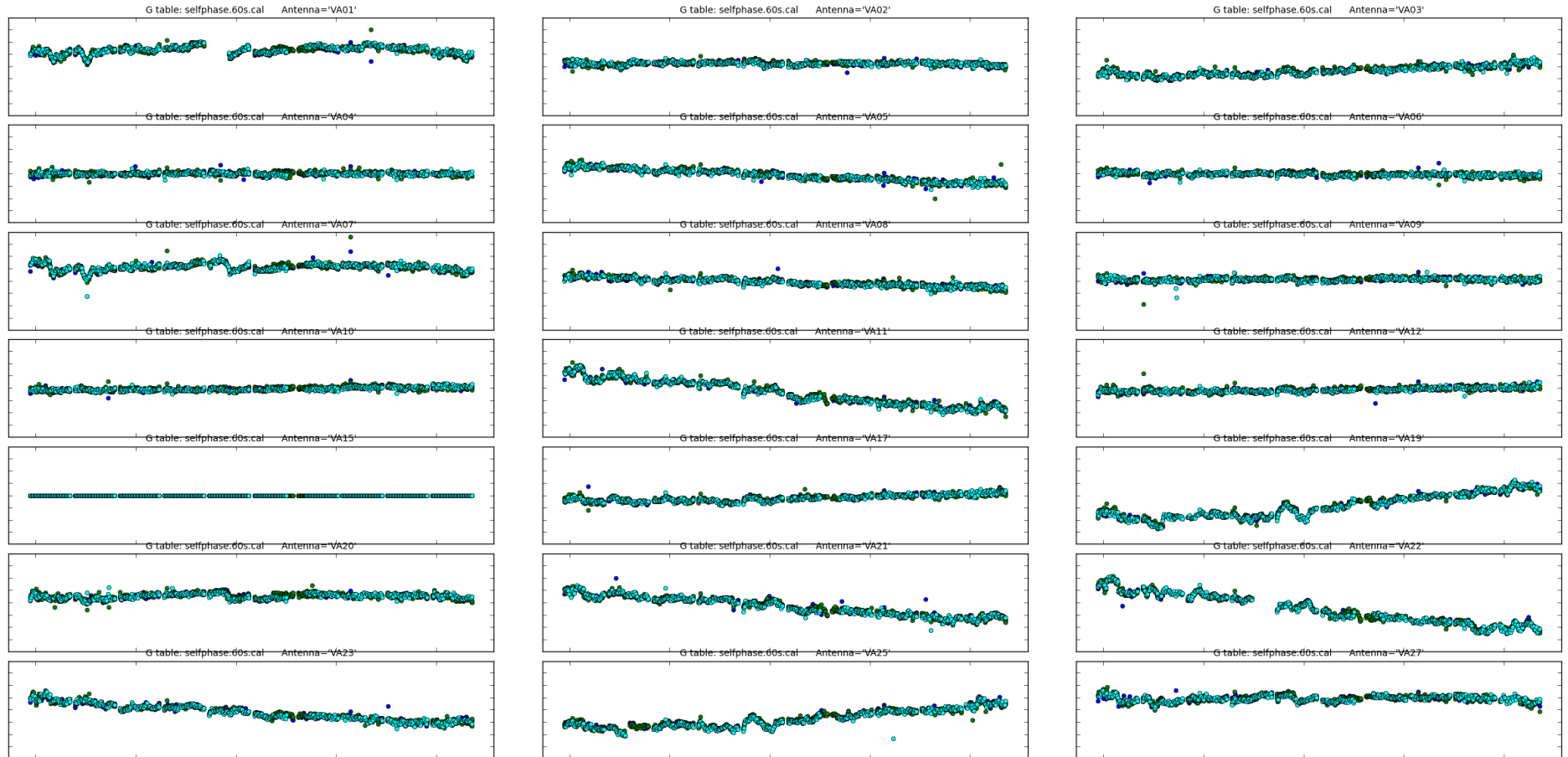


**Figure 29:** Phase offset per antenna. The four different colours represent the two spws and the two correlations. VL15 is the reference antenna, thus the offset should be 0 here. The phases of the other antennas have been averaged per 60 seconds and referenced to VL15. We see that not all the phase offsets are at 0, and some show a pretty big spread.

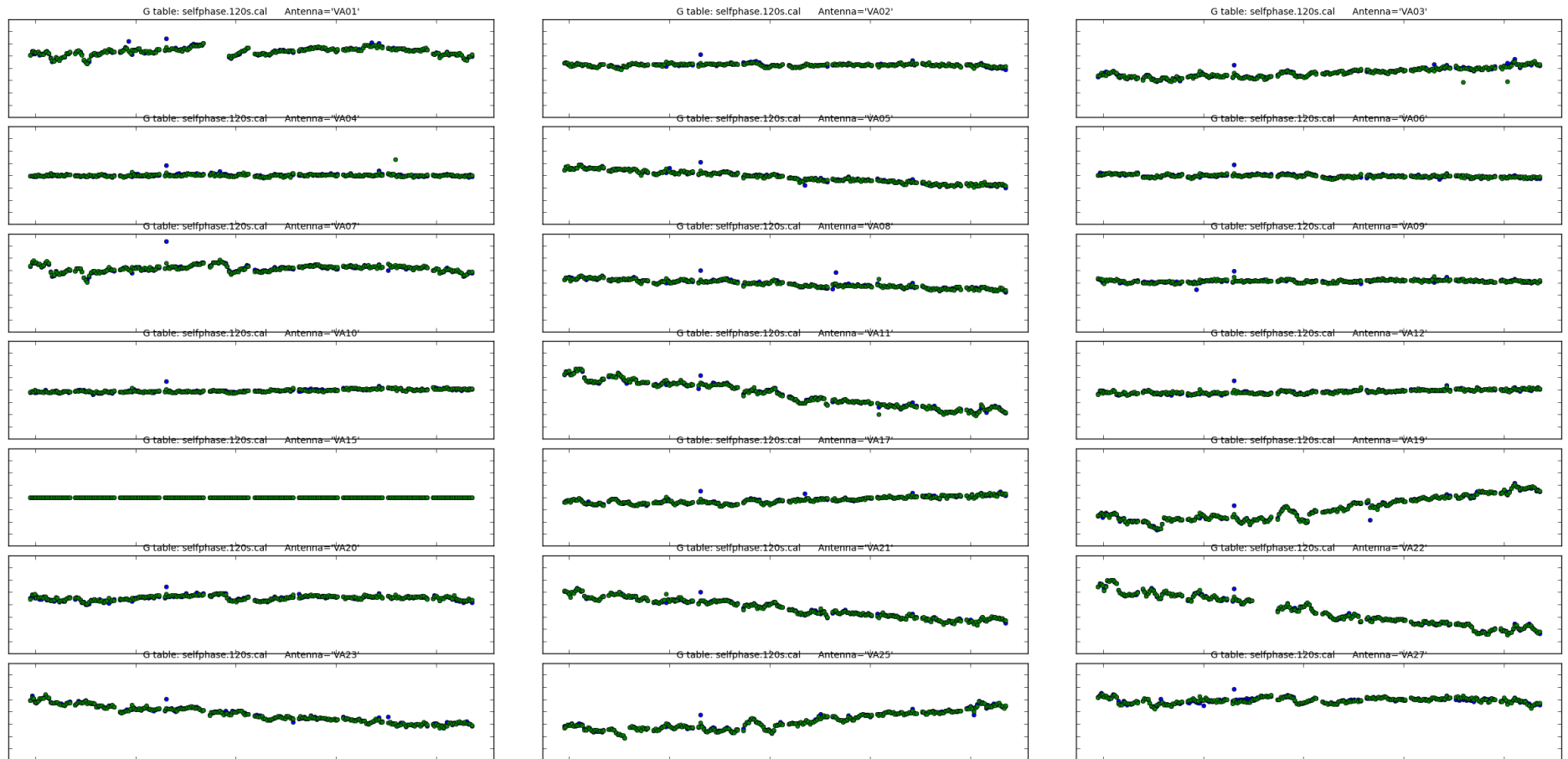
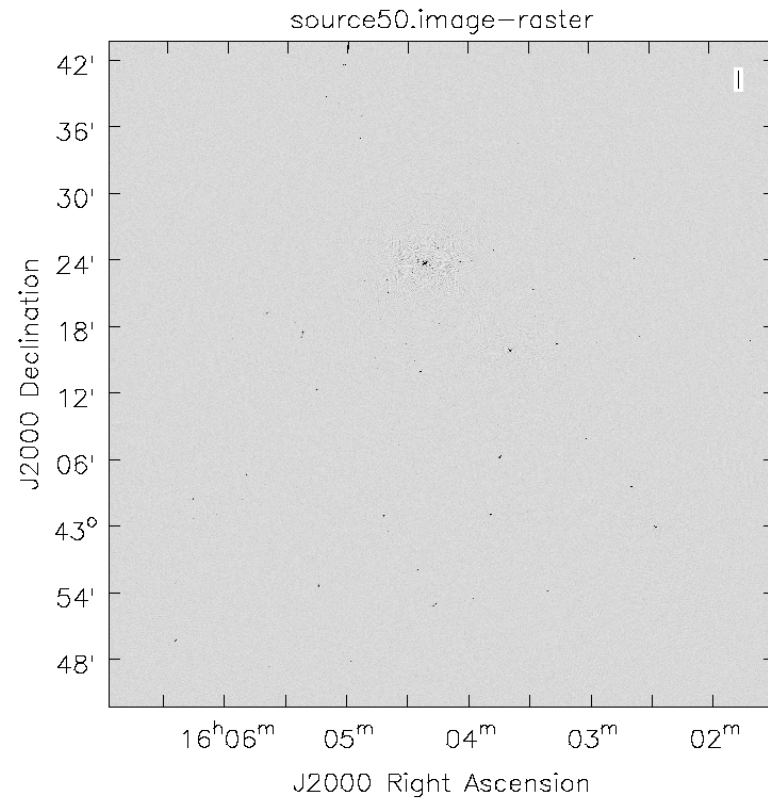
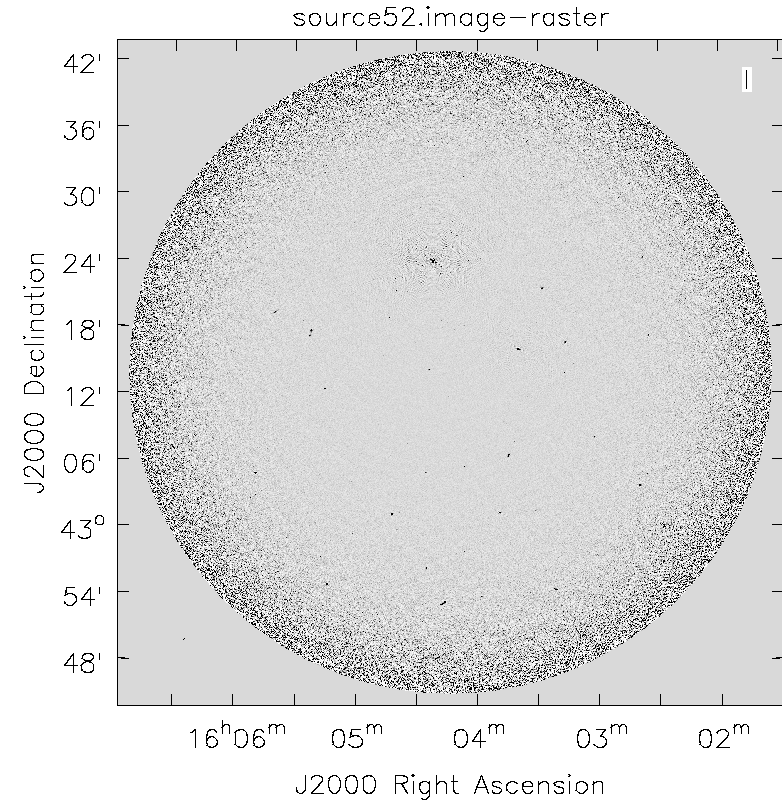


**Figure 30:** Phase offset per antenna. The three different colours represent the combined spws and the two correlations. VL15 is the reference antenna, thus the offset should be 0 here. The phases of the other antennas have been averaged per 120 seconds and per spw, and referenced to VL15. In comparison with figure 29 we see that the spread is less thick, but still not all the offsets are at 0.

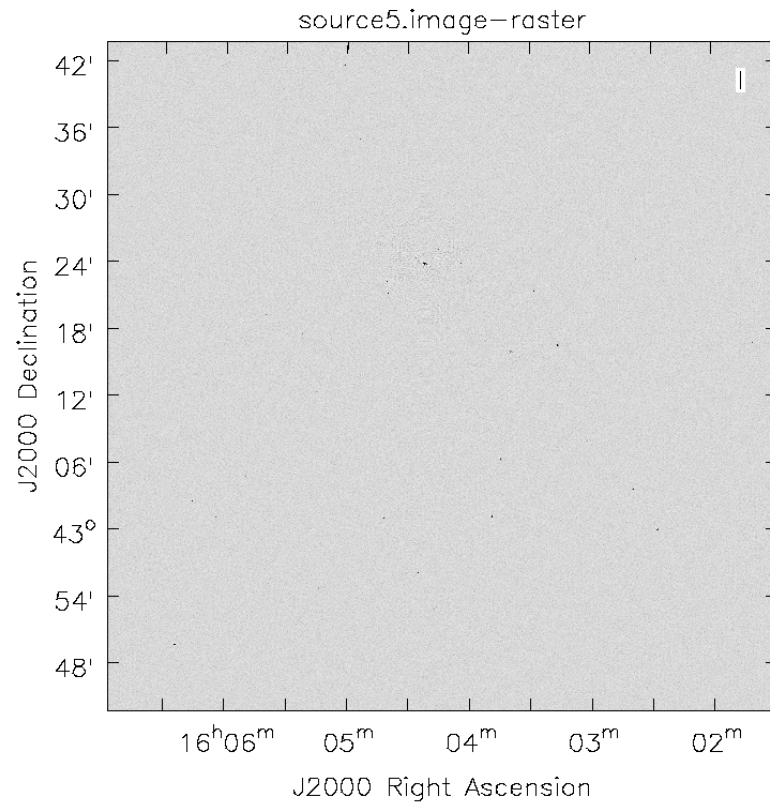


(a)

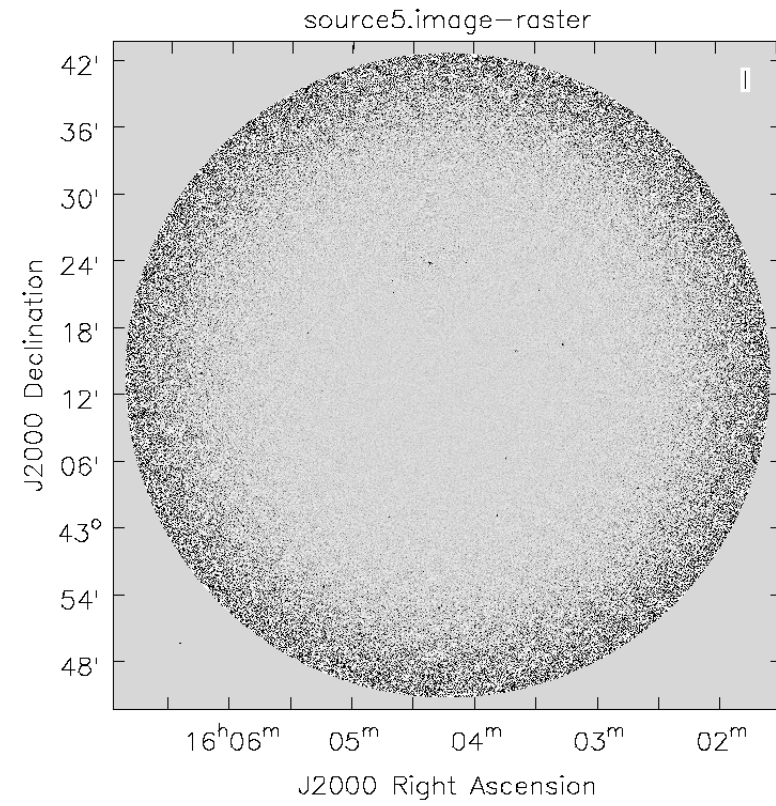


(b)

Figure 31: Dataset A

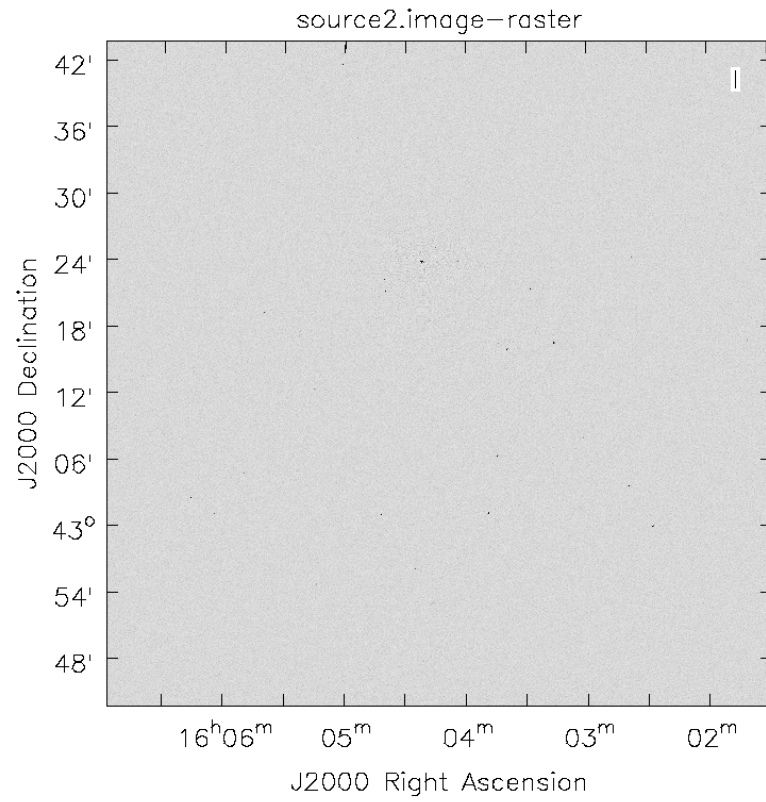


(a)

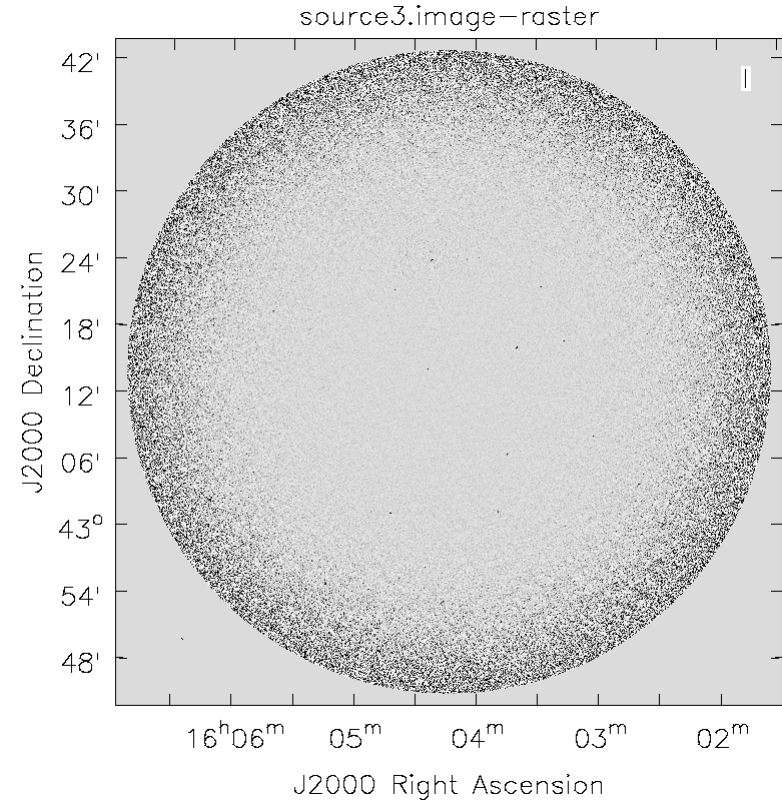


(b)

**Figure 32:** Dataset B

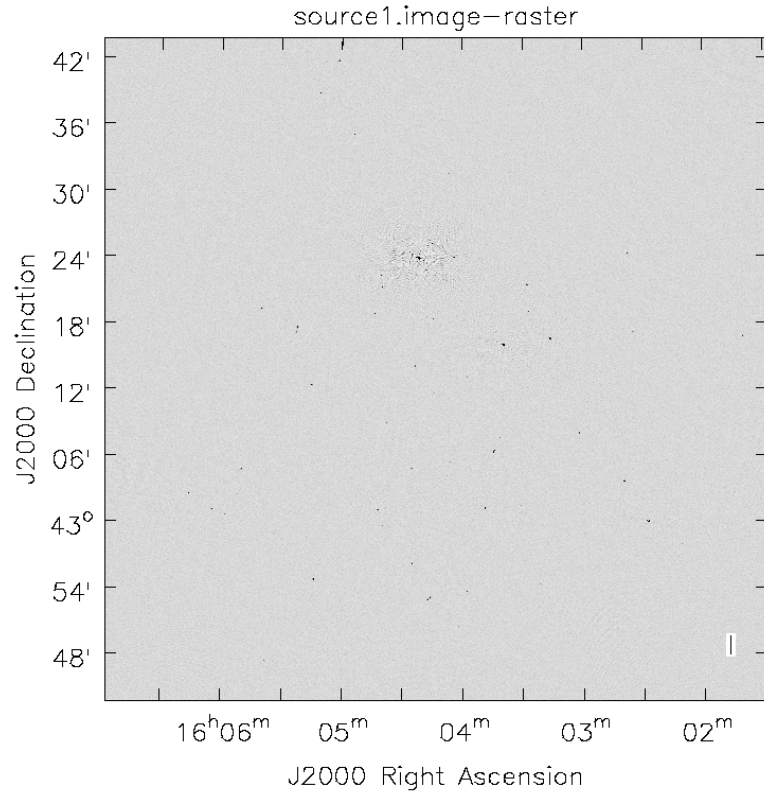


(a)

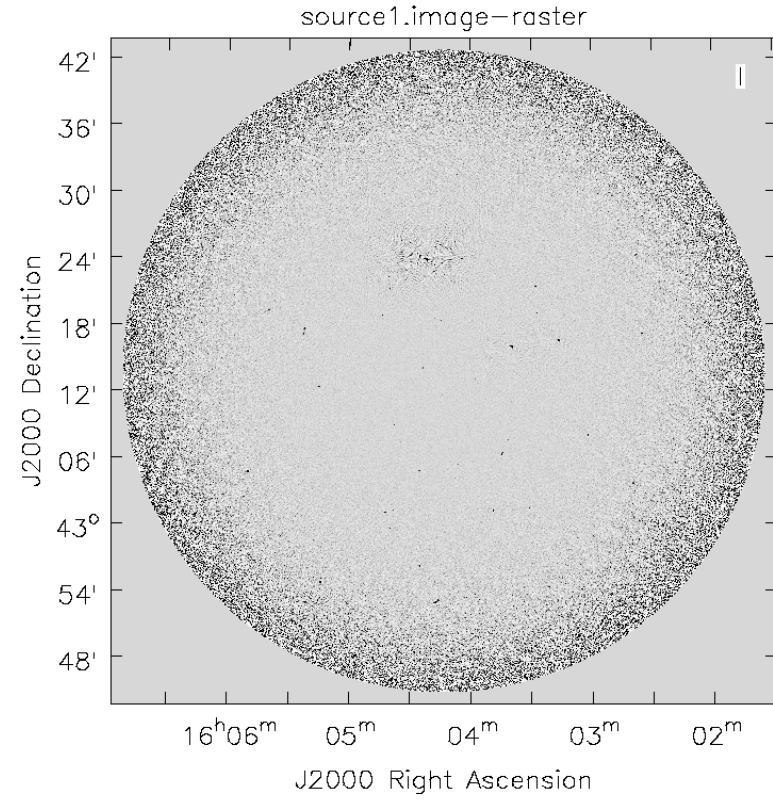


(b)

Figure 33: Dataset C

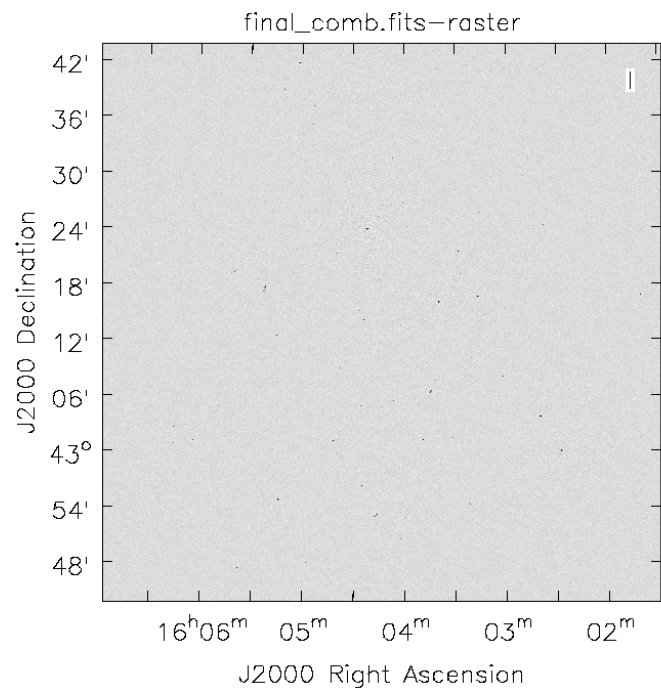


(a)

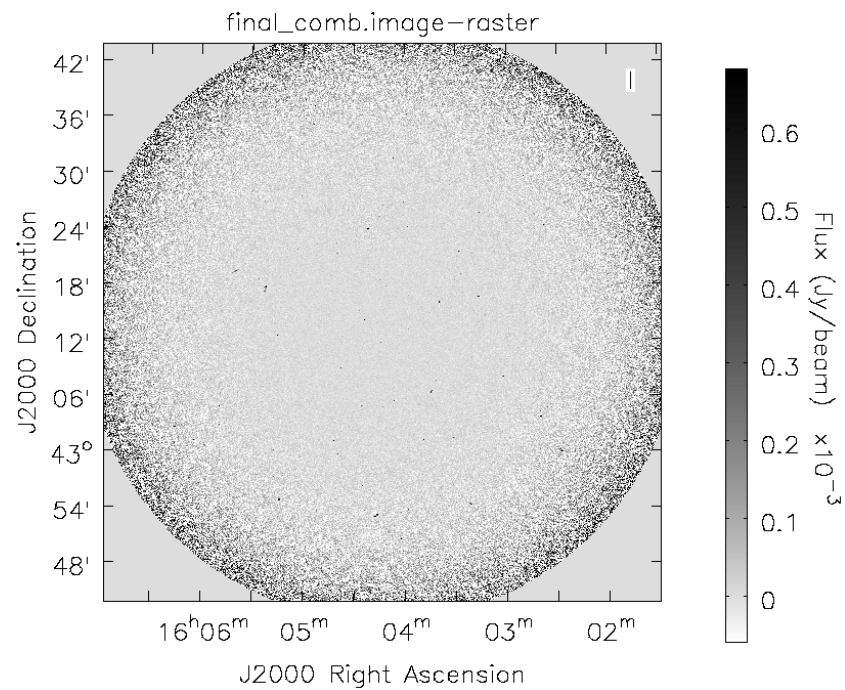


(b)

Figure 34: Dataset D



(a)



(b)

Figure 35: The Final image

## B MS details of dataset A

MeasurementSet Name:		/data/users/hopma/VLA/A/S7218.A.ms		MS Version 2			
Observer: unavailable		Project: S7218					
Observation: VLA							
Telescope	Observation Date	Observer	Project				
VLA	[	4.65903e+09,	4.65903e+09]	unavailable	S7218		
VLA	[	4.65903e+09,	4.65906e+09]	unavailable	S7218		
Data records: 6587568		Total elapsed time = 32193.3 seconds					
Observed from 07-Jul-2006/23:40:06.7		to 08-Jul-2006/08:36:40.0		(TAI)			
ObservationID = 0		ArrayID = 0					
Date	Timerange (TAI)	Scan	FldId	FieldName	nRows SpwIds Average Interval(s) ScanIntent		
07-Jul-2006	23:40:06.7 - 23:47:46.7	1	0	1331+305	96876 [0,1] [3.33, 3.33]		
	23:49:16.7 - 23:52:46.7	2	1	1635+381	44226 [0,1] [3.33, 3.33]		
	23:53:16.7 - 23:59:56.7	3	2	CL1604+432	84240 [0,1] [3.33, 3.33]		
ObservationID = 1		ArrayID = 0					
Date	Timerange (TAI)	Scan	FldId	FieldName	nRows SpwIds Average Interval(s) ScanIntent		
07-Jul-2006	23:59:56.7 - 00:39:46.7	4	2	CL1604+432	503334 [0,1] [3.33, 3.33]		
08-Jul-2006	00:40:16.7 - 00:44:06.7	5	1	1635+381	48438 [0,1] [3.33, 3.33]		
	00:44:26.7 - 01:31:06.7	6	2	CL1604+432	589680 [0,1] [3.33, 3.33]		
	01:31:26.7 - 01:35:36.7	7	1	1635+381	51948 [0,1] [3.33, 3.33]		
	01:35:56.7 - 02:22:26.7	8	2	CL1604+432	587574 [0,1] [3.33, 3.33]		
	02:22:56.7 - 02:26:56.7	9	1	1635+381	50544 [0,1] [3.33, 3.33]		
	02:27:26.7 - 03:13:46.7	10	2	CL1604+432	585468 [0,1] [3.33, 3.33]		
	03:14:26.7 - 03:18:16.7	11	1	1635+381	48438 [0,1] [3.33, 3.33]		
	03:18:56.7 - 04:05:06.7	12	2	CL1604+432	583362 [0,1] [3.33, 3.33]		
	04:06:26.7 - 04:09:36.7	13	1	1635+381	40014 [0,1] [3.33, 3.33]		
	04:10:56.7 - 04:56:26.7	14	2	CL1604+432	574938 [0,1] [3.33, 3.33]		
	04:56:56.7 - 05:00:56.7	15	1	1635+381	50544 [0,1] [3.33, 3.33]		
	05:01:26.7 - 05:47:46.7	16	2	CL1604+432	585468 [0,1] [3.33, 3.33]		
	05:48:16.7 - 05:52:16.7	17	1	1635+381	50544 [0,1] [3.33, 3.33]		
	05:52:36.7 - 06:39:16.7	18	2	CL1604+432	589680 [0,1] [3.33, 3.33]		
	06:39:36.7 - 06:43:46.7	19	1	1635+381	52650 [0,1] [3.33, 3.33]		
	06:44:06.7 - 07:30:36.7	20	2	CL1604+432	587574 [0,1] [3.33, 3.33]		
	07:30:56.7 - 07:35:06.7	21	1	1635+381	52650 [0,1] [3.33, 3.33]		
	07:35:26.7 - 08:21:56.7	22	2	CL1604+432	587574 [0,1] [3.33, 3.33]		
	08:22:16.7 - 08:26:26.7	23	1	1635+381	52650 [0,1] [3.33, 3.33]		
	08:29:36.7 - 08:36:40.0	24	3	0137+331	89154 [0,1] [3.33, 3.33]		
(nRows = Total number of rows per scan)							
Fields: 4							
ID	Code Name	RA	Decl	Epoch	SrcId nRows		
0	A 1331+305	13:31:08.287900	+30.30.32.95800	J2000	0 96876		
1	A 1635+381	16:35:15.492900	+38.08.04.50000	J2000	1 542646		
2	CL1604+432	16:04:13.191000	+43.13.50.80000	J2000	2 5858892		
3	B 0137+331	01:37:41.299400	+33.09.35.13200	J2000	3 89154		
Spectral Windows: (2 unique spectral windows and 1 unique polarization setups)							
SpwID	Name	#Chans	Frame	Ch0(MHz)	ChanWid(kHz) TotBW(kHz) CtrFreq(MHz) Corrs		
0	7*3.12 MHz channels @ 1.36 GHz (TOPO)	7	TOPO	1355.525	3125.000 21875.0 1364.9000 RR LL		
1	7*3.12 MHz channels @ 1.44 GHz (TOPO)	7	TOPO	1425.725	3125.000 21875.0 1435.1000 RR LL		
Sources: 4							
ID	Name	SpwID	RestFreq(MHz)	SysVel(km/s)			
0	1331+305	any	0	112.5			
1	1635+381	any	0	112.5			
2	CL1604+432	any	0	112.5			
3	0137+331	any	0	112.5			
Antennas: 27:							
ID	Name	Station	Diam.	Long.	Lat.	Offset from array center (m)	ITRF Geocentric coordinates (m)
						East North Elevation	x y z
0	VA01	VLA:_N36	25.0 m	-107.37.25.6	+33.57.07.6	-502.9595 5742.2455	-15.2450 -1600690.564679 -5038758.763935 3559632.019372
1	VA02	VLA:_N12	25.0 m	-107.37.09.0	+33.54.30.0	-76.3089 871.7642	-3.5944 -1601110.000684 -5041488.140172 3555597.402413
2	VA03	VLA:_E20	25.0 m	-107.35.43.6	+33.53.29.9	2113.0099 -985.5189	13.1843 -1599340.793422 -5043151.030286 3554065.191265
3	VA04	VLA:_W4	25.0 m	-107.37.10.8	+33.53.59.1	-122.0116 -82.2988	1.2784 -1601315.868658 -5041985.375637 3554808.274136
4	VA05	VLA:_W20	25.0 m	-107.38.21.4	+33.53.19.5	-1932.7164 -1304.0637	7.8260 -1603249.655427 -5042091.458312 3553797.776537
5	VA06	VLA:_W8	25.0 m	-107.37.21.6	+33.53.53.0	-401.2642 -270.6288	2.2222 -1601614.057594 -5042001.693450 3554652.482238
6	VA07	VLA:_N32	25.0 m	-107.37.22.0	+33.56.33.6	-410.8593 4691.4813	-13.2098 -1600780.997940 -5039347.481068 3558761.495627
7	VA08	VLA:_W16	25.0 m	-107.37.57.4	+33.53.33.0	-1317.8702 -889.1019	5.0328 -1602592.832932 -5042055.037107 3554140.680613
8	VA09	VLA:_N8	25.0 m	-107.37.07.5	+33.54.15.8	-38.0429 434.7090	-1.3234 -1601147.899029 -5041733.887153 3555235.935218
9	VA10	VLA:_E8	25.0 m	-107.36.48.9	+33.53.55.1	438.6922 -204.4956	0.5127 -1600801.886033 -5042219.424465 3554706.421206

10	VA11	VLA:_W32	25.0	m	-107.39.54.8	+33.52.27.2	-4328.6059	-2921.5887	15.4661	-1605808.610365	-5042230.088524	3552459.176260
11	VA12	VLA:_E12	25.0	m	-107.36.31.7	+33.53.48.5	879.5579	-410.0949	1.0026	-1600416.485000	-5042462.494078	3554536.039941
12	EA13	EVLA:W12	25.0	m	-107.37.37.4	+33.53.44.2	-804.5130	-542.7145	4.3146	-1602044.865201	-5042025.865459	3554427.806117
13	EA14	EVLA:N16	25.0	m	-107.37.10.9	+33.54.48.0	-124.9782	1428.1587	-5.6624	-1601061.901682	-5041175.923155	3556058.003936
14	VA15	VLA:_E4	25.0	m	-107.37.00.8	+33.53.59.7	133.6464	-62.2723	1.0919	-1601068.772930	-5042051.964001	3554824.792372
15	EA16	EVLA:E24	25.0	m	-107.35.13.4	+33.53.18.1	2889.0201	-1347.6429	17.4779	-1598663.081750	-5043581.464690	3553766.982074
16	VA17	VLA:_E16	25.0	m	-107.36.09.8	+33.53.40.0	1440.8788	-671.9522	2.9537	-1599926.085477	-5042773.020759	3554319.772057
17	EA18	EVLA:N4	25.0	m	-107.37.06.5	+33.54.06.1	-11.7523	134.3610	0.1852	-1601173.929543	-5041902.710315	3554987.493192
18	VA19	VLA:_E32	25.0	m	-107.34.01.5	+33.52.50.3	4732.4996	-2208.2291	28.9796	-1597053.111826	-5044604.778050	3553058.965002
19	VA20	VLA:_N20	25.0	m	-107.37.13.2	+33.55.09.5	-183.3636	2094.3889	-7.0383	-1601004.664081	-5040802.861410	3556610.109116
20	VA21	VLA:_W28	25.0	m	-107.39.20.2	+33.52.46.6	-3442.4326	-2323.1211	26.7532	-1604865.604209	-5042190.064262	3552962.339391
21	VA22	VLA:_W36	25.0	m	-107.40.32.6	+33.52.06.0	-5297.7685	-3576.2398	10.7382	-1606841.921881	-5042279.707478	3551912.988731
22	VA23	VLA:_W24	25.0	m	-107.38.49.0	+33.53.04.0	-2642.4982	-1783.0764	14.1997	-1604008.712833	-5042135.851614	3553403.680659
23	EA24	EVLA:MPD	25.0	m	-107.37.41.3	+33.53.42.0	-904.8851	-610.2588	4.9402	-1602152.094393	-5042031.862177	3554372.089241
24	VA25	VLA:_E28	25.0	m	-107.34.39.3	+33.53.04.9	3763.6229	-1755.8320	25.1893	-1597899.879795	-5044068.762074	3553432.424884
25	VA27	VLA:_N28	25.0	m	-107.37.18.7	+33.56.02.5	-326.7425	3730.7384	-11.6800	-1600863.633555	-5039885.356186	3557965.281676
26	VA28	VLA:_E36	25.0	m	-107.33.20.2	+33.52.34.3	5792.2240	-2703.1828	36.7907	-1596127.714111	-5045193.838185	3552652.395292

## C The code for dataset A

```
#!/usr/bin/env python
# -*- coding: utf-8 -*-

# VLA data reduction script for CL1604 at z = 0.9 (2 spws x 7 channels) in CASA 4.6.1
# Must be run with an internet connection to determine antenna offsets and opacity measurements

#Calibration steps

thesteps = [0]
step_title = {0: 'Set the variables and initial split (split)',
              1: 'A priori correction of opacity, antenna elevation and antenna positions (gencal)',
              2: 'Flag bad data (flagdata)',
              3: 'Insert model of the flux calibrator (setjy)',
              4: 'Short phase correction (gaincal)',
              5: 'Delay correction (gaincal)',
              6: 'Bandpass calibration (bandpass)',
              7: 'Gain (Amplitude and Phase) calibration (gaincal)',
              8: 'Determine the absolute flux-scale of the calibrators (fluxscale)',
              9: 'Applying the calibration tables (applycal)',
              10: 'Split target (split)',
              11: 'Insert model (ft)',
              12: 'Self-calibrate (phase) and clean (clean) 20 mins',
              13: 'Self-calibrate (phase) and clean (clean) 10 mins',
              14: 'Self-calibrate (phase) and clean (clean) 5 mins',
              15: 'Self-calibrate (phase) and clean (clean) 2 mins',
              16: 'Self-calibrate (phase) and clean (clean) 2 mins',
              17: 'Final clean (clean)'}

try:
    print 'List of steps to be executed...', mysteps
    thesteps = mysteps
except:
    print 'global variable mysteps not set.'
if (thesteps == []):
```

```

thesteps = range(0, len(step_title))
print 'Executing all steps:', thesteps

# The Python variable 'mysteps' will control which steps
# are executed when you start the script using
#   execfile('scriptForCalibration.py')
# e.g. setting
#   mysteps = [2,3,4]# before starting the script will make the script execute
# only steps 2, 3, and 4
# Setting mysteps = [] will make it execute all steps.

print 'Write the value for variables and do a priori flagging -> run the script from the beginning'
#definitions

archivefile = ['S7218_A060707.xpl', 'S7218_B060708.xpl'] #ms multisource file
myspw = '0,1' #spw of interest
msfile = 'S7218.A.ms' #ms file with the interesting sources
msscans = 'S7218.A.ms.txt' #text file to write listobs output to
antevla = '12,13,15,17,23'
mytarget = 'CL1604+432.A.ms' #ms file of the target

myimage1 = 'source1'
myimage2 = 'source2'
myimage3 = 'source3'
myimage4 = 'source4'
myimage5 = 'source5'
myimage6 = 'final_A'
mymask1 = 'skymask.mask'
mymodel1 = 'skymodel.model'

myrefant = 'ea22'

mystep = 0
if(mystep in thesteps):
    casalog.post('Step '+str(mystep)+' '+step_title[mystep], 'INFO')

```

```

print 'Step_', mystep, step_title[mystep]

# msfile = raw_input(" Msfile , please: ")
# myfield = raw_input(" Fields , please: ")
# mspw = raw_input(" Spectral windows, please: ")
# mssplit = raw_input(" Write the name of the mssplit file , please: ")
# myTau = raw_input(" Opacity parameter, please: ")

importvla(archivefiles=archivefile , vis=msfile , bandname="", frequencytol="150000.0Hz" , project="",
starttime="", stoptime="", applysys=True, autocorr=False , antnamescheme="new" , keepblanks=False , evlabands
=False)

listobs( vis=msfile , selectdata=True, spw="", field="", antenna="", uvrange="", timerange="", correlation=""
, scan="", intent="", feed="", array="", observation="", verbose=True, listfile=msscans , listunfl=False ,
cachesize=50, overwrite=True)

plotuv( vis=msfile , field=0, antenna="", spw="", observation="", array="", maxnpts=1000000000000, colors=['r' ,
'y' , 'g' , 'b' ] , symb="," , ncycles=1, figfile="uv0.png")

plotuv( vis=msfile , field=1, antenna="", spw="", observation="", array="", maxnpts=1000000000000, colors=['r' ,
'y' , 'g' , 'b' ] , symb="," , ncycles=1, figfile="uv1.png")

plotuv( vis=msfile , field=2, antenna="", spw="", observation="", array="", maxnpts=1000000000000, colors=['r' ,
'y' , 'g' , 'b' ] , symb="," , ncycles=1, figfile="uv2.png")

plotuv( vis=msfile , field=3, antenna="", spw="", observation="", array="", maxnpts=1000000000000, colors=['r' ,
'y' , 'g' , 'b' ] , symb="," , ncycles=1, figfile="uv3.png")

# step a priori splitting and calibration
mystep = 1
if(mystep in thesteps):
    casalog.post( 'Step_'+str(mystep)+'_' +step_title[mystep] , 'INFO')
    print 'Step_', mystep, step_title[mystep]

gencal( vis=msfile , caltable="antpos.cal" , caltype="antpos" , infile="" , spw="" , antenna="17" , pol="" , parameter
=[0.021, -0.022, 0.0])

```

```

gencal(vis=msfile , caltable="gaincurve.cal" , caltype="gceff" , infile="" , spw="" , antenna="" , pol="" , parameter
=[])

# step flagging
mystep = 2
if(mystep in thesteps):
    casalog.post('Step_' + str(mystep) + '_' + step_title[mystep] , 'INFO')
    print 'Step_' , mystep , step_title[mystep]

# plotms amp vs time (single baseline)
# plotms phase v time
# flag regular off-source
flagdata(vis=msfile , mode="quack" , autocorr=False , infile="" , reason="any" , tbuff=0.0 , spw="" , field="" ,
antenna="" , uvrange="" , timerange="" , correlation="" , scan="" , intent="" , array="" , observation="" , feed="" ,
clipminmax=[] , datacolumn="DATA" , clipoutside=True , channelavg=False , clipzeros=False , quackinterval=21 ,
quackmode="beg" , quackincrement=False , tolerance=0.0 , addantenna="" , lowerlimit=0.0 , upperlimit=90.0 , ntime=
"scan" , combinescans=False , timecutoff=4.0 , freqcutoff=3.0 , timefit="line" , freqfit="poly" , maxnpieces=7 ,
flagdimension="freqtime" , usewindowstats="none" , halfwin=1 , extendflags=True , winsize=3 , timedev="" , freqdev=
"" , timedevscale=5.0 , freqdevscale=5.0 , spectralmax=1000000.0 , spectralmin=0.0 , extendpols=True , growtime=
50.0 , growfreq=50.0 , growaround=False , flagneartime=False , flagnearfreq=False , minrel=0.0 , maxrel=1.0 , minabs=
0 , maxabs=-1 , spwchan=False , spwcorr=False , basecnt=False , name="Summary" , action="apply" , display="" ,
flagbackup=True , savepars=False , cmdreason="" , outfile="")

# plotms amp vs time (single baseline)
# plotms phase v time
# flag EVLA antennas

flagdata(vis=msfile , mode="manual" , autocorr=False , infile="" , reason="any" , tbuff=0.0 , spw="" , field="" ,
antenna=antevla , uvrange="" , timerange="" , correlation="" , scan="" , intent="" , array="" , observation="" , feed=
"" , clipminmax=[] , datacolumn="DATA" , clipoutside=True , channelavg=False , timeavg=False , timebin="0s" ,
clipzeros=False , quackinterval=1.0 , quackmode="beg" , quackincrement=False , tolerance=0.0 , addantenna="" ,
lowerlimit=0.0 , upperlimit=90.0 , ntime="scan" , combinescans=False , timecutoff=4.0 , freqcutoff=3.0 , timefit=
"line" , freqfit="poly" , maxnpieces=7 , flagdimension="freqtime" , usewindowstats="none" , halfwin=1 , extendflags=
True , winsize=3 , timedev="" , freqdev="" , timedevscale=5.0 , freqdevscale=5.0 , spectralmax=1000000.0 , spectralmin
=0.0 , extendpols=True , growtime=50.0 , growfreq=50.0 , growaround=False , flagneartime=False , flagnearfreq=False ,
minrel=0.0 , maxrel=1.0 , minabs=0 , maxabs=-1 , spwchan=False , spwcorr=False , basecnt=False , fieldcnt=None , name=
"Summary" , action="apply" , display="" , flagbackup=True , savepars=False , cmdreason="" , outfile="" , writeflags=

```

None)

```
flagdata(vis=msfile,mode="manual",autocorr=False,inpfile="",reason="any",tbuff=0.0,spw="",field="",
,antenna="16",uvrange="",timerange="23:49:41~23:50:06",correlation="",scan="",intent="",array="",
observation="",feed="",clipminmax=[],datacolumn="DATA",clipoutside=True,channelavg=False,clipzeros=
False,quackinterval=1.0,quackmode="beg",quackincrement=False,tolerance=0.0,addantenna="",lowerlimit=0.0,
upperlimit=90.0,ntime="scan",combinescans=False,timecutoff=4.0,freqcutoff=3.0,timefit="line",freqfit=
"poly",maxnpieces=7,flagdimension="freqtime",usewindowstats="none",halfwin=1,extendflags=True,winsize=3,
timedev="",freqdev="",timedevscale=5.0,freqdevscale=5.0,spectralmax=1000000.0,spectralmin=0.0,extendpols
=True,growtime=50.0,growfreq=50.0,growaround=False,flagneartime=False,flagnearfreq=False,minrel=0.0,
maxrel=1.0,minabs=0,maxabs=-1,spwchan=False,spwcorr=False,basecnt=False,name="Summary",action="apply",
display="",flagbackup=True,savepars=False,cmdreason="",outfile="")
```

```
flagdata(vis=msfile,mode="manual",autocorr=False,inpfile="",reason="any",tbuff=0.0,spw="",field="",
,antenna="16",uvrange="",timerange="32:25:14~32:25:56",correlation="",scan="",intent="",array="",
observation="",feed="",clipminmax=[],datacolumn="DATA",clipoutside=True,channelavg=False,clipzeros=
False,quackinterval=1.0,quackmode="beg",quackincrement=False,tolerance=0.0,addantenna="",lowerlimit=0.0,
upperlimit=90.0,ntime="scan",combinescans=False,timecutoff=4.0,freqcutoff=3.0,timefit="line",freqfit=
"poly",maxnpieces=7,flagdimension="freqtime",usewindowstats="none",halfwin=1,extendflags=True,winsize=3,
timedev="",freqdev="",timedevscale=5.0,freqdevscale=5.0,spectralmax=1000000.0,spectralmin=0.0,extendpols
=True,growtime=50.0,growfreq=50.0,growaround=False,flagneartime=False,flagnearfreq=False,minrel=0.0,
maxrel=1.0,minabs=0,maxabs=-1,spwchan=False,spwcorr=False,basecnt=False,name="Summary",action="apply",
display="",flagbackup=True,savepars=False,cmdreason="",outfile="")
```

```
flagdata(vis=msfile,mode="manual",autocorr=False,inpfile="",reason="any",tbuff=0.0,spw="",field="",
,antenna="25",uvrange="",timerange="23:40:00~23:41:30",correlation="",scan="",intent="",array="",
observation="",feed="",clipminmax=[],datacolumn="DATA",clipoutside=True,channelavg=False,clipzeros=
False,quackinterval=1.0,quackmode="beg",quackincrement=False,tolerance=0.0,addantenna="",lowerlimit=0.0,
upperlimit=90.0,ntime="scan",combinescans=False,timecutoff=4.0,freqcutoff=3.0,timefit="line",freqfit=
"poly",maxnpieces=7,flagdimension="freqtime",usewindowstats="none",halfwin=1,extendflags=True,winsize=3,
timedev="",freqdev="",timedevscale=5.0,freqdevscale=5.0,spectralmax=1000000.0,spectralmin=0.0,extendpols
=True,growtime=50.0,growfreq=50.0,growaround=False,flagneartime=False,flagnearfreq=False,minrel=0.0,
maxrel=1.0,minabs=0,maxabs=-1,spwchan=False,spwcorr=False,basecnt=False,name="Summary",action="apply",
display="",flagbackup=True,savepars=False,cmdreason="",outfile="")
```

```
flagdata(vis=msfile,mode="manual",autocorr=False,inpfile="",reason="any",tbuff=0.0,spw="",field="",
,antenna="20",uvrange="",timerange="32:35:00~32:35:08",correlation="",scan="",intent="",array="",
observation="",feed="",clipminmax=[],datacolumn="DATA",clipoutside=True,channelavg=False,clipzeros=
```

```

False , quackinterval=1.0,quackmode="beg" , quackincrement=False , tolerance =0.0,addantenna="",lowerlimit=0.0,
upperlimit=90.0,ntime="scan" , combinescans=False , timecutoff=4.0, freqcutoff=3.0, timefit="line" , freqfit=
"poly" , maxnpieces=7,flagdimension="freqtime" , usewindowstats="none" , halfwin=1,extendflags=True, winsize=3,
timedev="", freqdev="" , timedevscale=5.0, freqdevscale=5.0, spectralmax=1000000.0, spectralmin=0.0, extendpols
=True, growtime=50.0, growfreq=50.0, growaround=False , flagneartime=False , flagnearfreq=False , minrel=0.0,
maxrel=1.0, minabs=0, maxabs=-1, spwchan=False , spwcorr=False , basecnt=False , name="Summary" , action="apply" ,
display="" , flagbackup=True, savepars=False , cmdreason="" , outfile="")

```

```

flagdata ( vis=msfile , mode="manual" , autocorr=False , infile="" , reason="any" , tbuff=0.0, spw="" , field="" ,
antenna="20" , uvrage="" , timerange="32:36:26~32:36:30" , correlation="" , scan="" , intent="" , array="" ,
observation="" , feed="" , clipminmax=[] , datacolumn="DATA" , clipoutside=True, channelavg=False , clipzeros=
False , quackinterval=1.0,quackmode="beg" , quackincrement=False , tolerance =0.0,addantenna="",lowerlimit=0.0,
upperlimit=90.0,ntime="scan" , combinescans=False , timecutoff=4.0, freqcutoff=3.0, timefit="line" , freqfit=
"poly" , maxnpieces=7,flagdimension="freqtime" , usewindowstats="none" , halfwin=1,extendflags=True, winsize=3,
timedev="" , freqdev="" , timedevscale=5.0, freqdevscale=5.0, spectralmax=1000000.0, spectralmin=0.0, extendpols
=True, growtime=50.0, growfreq=50.0, growaround=False , flagneartime=False , flagnearfreq=False , minrel=0.0,
maxrel=1.0, minabs=0, maxabs=-1, spwchan=False , spwcorr=False , basecnt=False , name="Summary" , action="apply" ,
display="" , flagbackup=True, savepars=False , cmdreason="" , outfile="")

```

```

flagdata ( vis=msfile , mode="manual" , autocorr=False , infile="" , reason="any" , tbuff=0.0, spw="1" , field="" ,
antenna="" , uvrage="" , timerange="28:48:20~29:10:00" , correlation="" , scan="" , intent="" , array="" ,
observation="" , feed="" , clipminmax=[] , datacolumn="DATA" , clipoutside=True, channelavg=False , clipzeros=
False , quackinterval=1.0,quackmode="beg" , quackincrement=False , tolerance =0.0,addantenna="",lowerlimit=0.0,
upperlimit=90.0,ntime="scan" , combinescans=False , timecutoff=4.0, freqcutoff=3.0, timefit="line" , freqfit=
"poly" , maxnpieces=7,flagdimension="freqtime" , usewindowstats="none" , halfwin=1,extendflags=True, winsize=3,
timedev="" , freqdev="" , timedevscale=5.0, freqdevscale=5.0, spectralmax=1000000.0, spectralmin=0.0, extendpols
=True, growtime=50.0, growfreq=50.0, growaround=False , flagneartime=False , flagnearfreq=False , minrel=0.0,
maxrel=1.0, minabs=0, maxabs=-1, spwchan=False , spwcorr=False , basecnt=False , name="Summary" , action="apply" ,
display="" , flagbackup=True, savepars=False , cmdreason="" , outfile="")

```

```

flagdata ( vis=msfile , mode="manual" , autocorr=False , infile="" , reason="any" , tbuff=0.0, spw="" , field="" ,
antenna="9&14" , uvrage="" , timerange="30:40:00~30:44:10" , correlation="" , scan="" , intent="" , array="" ,
observation="" , feed="" , clipminmax=[] , datacolumn="DATA" , clipoutside=True, channelavg=False , clipzeros=
False , quackinterval=1.0,quackmode="beg" , quackincrement=False , tolerance =0.0,addantenna="",lowerlimit=0.0,
upperlimit=90.0,ntime="scan" , combinescans=False , timecutoff=4.0, freqcutoff=3.0, timefit="line" , freqfit=
"poly" , maxnpieces=7,flagdimension="freqtime" , usewindowstats="none" , halfwin=1,extendflags=True, winsize=3,
timedev="" , freqdev="" , timedevscale=5.0, freqdevscale=5.0, spectralmax=1000000.0, spectralmin=0.0, extendpols
=True, growtime=50.0, growfreq=50.0, growaround=False , flagneartime=False , flagnearfreq=False , minrel=0.0,

```

```
maxrel=1.0,minabs=0,maxabs=-1,spwchan=False,spwcorr=False,basecnt=False,name="Summary",action="apply",
display="",flagbackup=True,savepars=False,cmdreason="",outfile="")
```

```
flagdata(vis=msfile,mode="manual",autocorr=False,inpfile="",reason="any",tbuff=0.0,spw="",field="",
antenna="9&11",uvrange="",timerange="30:40:00~30:44:10",correlation="",scan="",intent="",array="",
observation="",feed="",clipminmax=[],datacolumn="DATA",clipoutside=True,channelavg=False,clipzeros=
False,quackinterval=1.0,quackmode="beg",quackincrement=False,tolerance=0.0,addantenna="",lowerlimit=0.0,
upperlimit=90.0,ntime="scan",combinescans=False,timecutoff=4.0,freqcutoff=3.0,timefit="line",freqfit=
"poly",maxnpieces=7,flagdimension="freqtime",usewindowstats="none",halfwin=1,extendflags=True,winsize=3,
timedev="",freqdev="",timedevscale=5.0,freqdevscale=5.0,spectralmax=1000000.0,spectralmin=0.0,extendpols
=True,growtime=50.0,growfreq=50.0,growaround=False,flagneartime=False,flagnearfreq=False,minrel=0.0,
maxrel=1.0,minabs=0,maxabs=-1,spwchan=False,spwcorr=False,basecnt=False,name="Summary",action="apply",
display="",flagbackup=True,savepars=False,cmdreason="",outfile="")
```

```
flagdata(vis=msfile,mode="manual",autocorr=False,inpfile="",reason="any",tbuff=0.0,spw="1",field="",
antenna="3&14",uvrange="",timerange="30:46:34~30:48:32",correlation="",scan="",intent="",array="",
observation="",feed="",clipminmax=[],datacolumn="DATA",clipoutside=True,channelavg=False,clipzeros=
False,quackinterval=1.0,quackmode="beg",quackincrement=False,tolerance=0.0,addantenna="",lowerlimit=0.0,
upperlimit=90.0,ntime="scan",combinescans=False,timecutoff=4.0,freqcutoff=3.0,timefit="line",freqfit=
"poly",maxnpieces=7,flagdimension="freqtime",usewindowstats="none",halfwin=1,extendflags=True,winsize=3,
timedev="",freqdev="",timedevscale=5.0,freqdevscale=5.0,spectralmax=1000000.0,spectralmin=0.0,extendpols
=True,growtime=50.0,growfreq=50.0,growaround=False,flagneartime=False,flagnearfreq=False,minrel=0.0,
maxrel=1.0,minabs=0,maxabs=-1,spwchan=False,spwcorr=False,basecnt=False,name="Summary",action="apply",
display="",flagbackup=True,savepars=False,cmdreason="",outfile="")
```

```
flagdata(vis=msfile,mode="manual",autocorr=False,inpfile="",reason="any",tbuff=0.0,spw="",field="",
antenna="3&5",uvrange="",timerange="30:52:21.7~30:52:38.3",correlation="",scan="",intent="",array="",
observation="",feed="",clipminmax=[],datacolumn="DATA",clipoutside=True,channelavg=False,clipzeros=
False,quackinterval=1.0,quackmode="beg",quackincrement=False,tolerance=0.0,addantenna="",lowerlimit=0.0,
upperlimit=90.0,ntime="scan",combinescans=False,timecutoff=4.0,freqcutoff=3.0,timefit="line",freqfit=
"poly",maxnpieces=7,flagdimension="freqtime",usewindowstats="none",halfwin=1,extendflags=True,winsize=3,
timedev="",freqdev="",timedevscale=5.0,freqdevscale=5.0,spectralmax=1000000.0,spectralmin=0.0,extendpols
=True,growtime=50.0,growfreq=50.0,growaround=False,flagneartime=False,flagnearfreq=False,minrel=0.0,
maxrel=1.0,minabs=0,maxabs=-1,spwchan=False,spwcorr=False,basecnt=False,name="Summary",action="apply",
display="",flagbackup=True,savepars=False,cmdreason="",outfile="")
```

```
flagdata(vis=msfile,mode="manual",autocorr=False,inpfile="",reason="any",tbuff=0.0,spw="",field="",
antenna="3&9",uvrange="",timerange="30:45:01.7~30:45:11.7",correlation="",scan="",intent="",array="",
```

```

observation="" , feed="" , clipminmax=[] , datacolumn="DATA" , clipoutside=True , channelavg=False , clipzeros=False , quackinterval=1.0 , quackmode="beg" , quackincrement=False , tolerance=0.0 , addantenna="" , lowerlimit=0.0 , upperlimit=90.0 , ntime="scan" , combinescans=False , timecutoff=4.0 , freqcutoff=3.0 , timefit="line" , freqfit="poly" , maxnpieces=7 , flagdimension="freqtime" , usewindowstats="none" , halfwin=1 , extendflags=True , winsize=3 , timedev="" , freqdev="" , timedevscale=5.0 , freqdevscale=5.0 , spectralmax=1000000.0 , spectralmin=0.0 , extendpols=True , growtime=50.0 , growfreq=50.0 , growaround=False , flagneartime=False , flagnearfreq=False , minrel=0.0 , maxrel=1.0 , minabs=0 , maxabs=-1 , spwchan=False , spwcorr=False , basecnt=False , name="Summary" , action="apply" , display="" , flagbackup=True , savepars=False , cmdreason="" , outfile="")

```

```

flagdata ( vis=msfile , mode="manual" , autocorr=False , infile="" , reason="any" , tbuff=0.0 , spw="" , field="" , antenna="9&14" , uvrage="" , timerange="30:44:41.7" , correlation="" , scan="" , intent="" , array="" , observation="" , feed="" , clipminmax=[] , datacolumn="DATA" , clipoutside=True , channelavg=False , clipzeros=False , quackinterval=1.0 , quackmode="beg" , quackincrement=False , tolerance=0.0 , addantenna="" , lowerlimit=0.0 , upperlimit=90.0 , ntime="scan" , combinescans=False , timecutoff=4.0 , freqcutoff=3.0 , timefit="line" , freqfit="poly" , maxnpieces=7 , flagdimension="freqtime" , usewindowstats="none" , halfwin=1 , extendflags=True , winsize=3 , timedev="" , freqdev="" , timedevscale=5.0 , freqdevscale=5.0 , spectralmax=1000000.0 , spectralmin=0.0 , extendpols=True , growtime=50.0 , growfreq=50.0 , growaround=False , flagneartime=False , flagnearfreq=False , minrel=0.0 , maxrel=1.0 , minabs=0 , maxabs=-1 , spwchan=False , spwcorr=False , basecnt=False , name="Summary" , action="apply" , display="" , flagbackup=True , savepars=False , cmdreason="" , outfile="")

```

```

flagdata ( vis=msfile , mode="manual" , autocorr=False , infile="" , reason="any" , tbuff=0.0 , spw="0" , field="" , antenna="16" , uvrage="" , timerange="23:41:38.3" , correlation="" , scan="" , intent="" , array="" , observation="" , feed="" , clipminmax=[] , datacolumn="DATA" , clipoutside=True , channelavg=False , clipzeros=False , quackinterval=1.0 , quackmode="beg" , quackincrement=False , tolerance=0.0 , addantenna="" , lowerlimit=0.0 , upperlimit=90.0 , ntime="scan" , combinescans=False , timecutoff=4.0 , freqcutoff=3.0 , timefit="line" , freqfit="poly" , maxnpieces=7 , flagdimension="freqtime" , usewindowstats="none" , halfwin=1 , extendflags=True , winsize=3 , timedev="" , freqdev="" , timedevscale=5.0 , freqdevscale=5.0 , spectralmax=1000000.0 , spectralmin=0.0 , extendpols=True , growtime=50.0 , growfreq=50.0 , growaround=False , flagneartime=False , flagnearfreq=False , minrel=0.0 , maxrel=1.0 , minabs=0 , maxabs=-1 , spwchan=False , spwcorr=False , basecnt=False , name="Summary" , action="apply" , display="" , flagbackup=True , savepars=False , cmdreason="" , outfile="")

```

```

flagdata ( vis=msfile , mode="manual" , autocorr=False , infile="" , reason="any" , tbuff=0.0 , spw="0" , field="" , antenna="16&20" , uvrage="" , timerange="23:46:01.7" , correlation="" , scan="" , intent="" , array="" , observation="" , feed="" , clipminmax=[] , datacolumn="DATA" , clipoutside=True , channelavg=False , clipzeros=False , quackinterval=1.0 , quackmode="beg" , quackincrement=False , tolerance=0.0 , addantenna="" , lowerlimit=0.0 , upperlimit=90.0 , ntime="scan" , combinescans=False , timecutoff=4.0 , freqcutoff=3.0 , timefit="line" , freqfit="poly" , maxnpieces=7 , flagdimension="freqtime" , usewindowstats="none" , halfwin=1 , extendflags=True , winsize=3 , timedev="" , freqdev="" , timedevscale=5.0 , freqdevscale=5.0 , spectralmax=1000000.0 , spectralmin=0.0 , extendpols=True , growtime=50.0 , growfreq=50.0 , growaround=False , flagneartime=False , flagnearfreq=False , minrel=0.0 , maxrel=1.0 , minabs=0 , maxabs=-1 , spwchan=False , spwcorr=False , basecnt=False , name="Summary" , action="apply" , display="" , flagbackup=True , savepars=False , cmdreason="" , outfile="")

```

```

=True, growtime=50.0, growfreq=50.0, growaround=False, flagneartime=False, flagnearfreq=False, minrel=0.0,
maxrel=1.0, minabs=0, maxabs=-1, spwchan=False, spwcorr=False, basecnt=False, name="Summary", action="apply",
display="", flagbackup=True, savepars=False, cmdreason="", outfile="")

# step: model of the flux calibrator-setjy
# observation at 31.7 GHz, using Ka band model
mystep = 3
if(mystep in thesteps):
    casalog.post('Step_' + str(mystep) + '_' + step_title[mystep], 'INFO')
    print 'Step_', mystep, step_title[mystep]

    setjy(vis=msfile, field="0", spw="", selectdata=True, timerange="", scan="", intent="", observation="",
scalebychan=True, standard="PerleyButler2013", model="3C286_L.im", modimage=None, listmodels=False,
fluxdensity=-1, spix=0.0, reffreq="1GHz", polindex=[], polangle=[], rotmeas=0.0, fluxdict={}, useephemdir=
False, interpolation="nearest", usescratch=False, ismms=None)

    setjy(vis=msfile, field="3", spw="", selectdata=True, timerange="", scan="", intent="", observation="",
scalebychan=True, standard="PerleyButler2013", model="3C48_L.im", modimage=None, listmodels=False,
fluxdensity=-1, spix=0.0, reffreq="1GHz", polindex=[], polangle=[], rotmeas=0.0, fluxdict={}, useephemdir=
False, interpolation="nearest", usescratch=False, ismms=None)

# step: short phase calibration
mystep = 4
if(mystep in thesteps):
    casalog.post('Step_' + str(mystep) + '_' + step_title[mystep], 'INFO')
    print 'Step_', mystep, step_title[mystep]

    gaincal(vis=msfile, caltable="intphase.cal", field="0,1,3", spw="*:
2~4", intent="", selectdata=True, timerange="", uvrage="", antenna="", scan="", observation="", msselect="",
solint="int", combine="", preavg=-1.0, refant="14", minblperant=4, minsnr=3.0, solnorm=False, gaintype="G",
smodel=[], calmode="p", append=False, splintime=3600.0, npointaver=3, phasewrap=180.0, docallib=False, callib
="", gaintable=['antpos.cal', 'gaincurve.cal'], gainfield=[], interp=[], spwmap=[], parang=False)

# step: residual delay calibration
mystep = 5
if(mystep in thesteps):

```

```

casalog.post('Step_' + str(mystep) + '_' + step_title[mystep], 'INFO')
print 'Step_', mystep, step_title[mystep]

gaincal(vis=msfile, caltable="delays.cal", field="0,1,3", spw="", intent="", selectdata=True, timerange="",
uvrange="", antenna="", scan="", observation="", msselect="", solint="inf", combine="scan", preavg=-1.0, refant="14",
minblperant=4, minsnr=3.0, solnorm=False, gaintype="K", smodel=[], calmode="p", append=False, splintime=3600.0,
npointaver=3, phasewrap=180.0, docallib=False, callib="", gaintable=['antpos.cal', 'gaincurve.cal', 'intphase.cal'],
gainfield=[], interp=[], spwmap=[], parang=False)

# step: bandpass calibration
mystep = 6
if(mystep in thesteps):
    casalog.post('Step_' + str(mystep) + '_' + step_title[mystep], 'INFO')
    print 'Step_', mystep, step_title[mystep]

    bandpass(vis=msfile, caltable="bpass.cal", field="0,1,3", spw="", intent="", selectdata=True, timerange="",
uvrange="", antenna="", scan="", observation="", msselect="", solint="inf", combine="scan", refant="14",
minblperant=4, minsnr=3.0, solnorm=True, bandtype="B", smodel=[], append=False, fillgaps=0, degamp=3, degphase=3,
visnorm=False, maskcenter=0, maskedge=5, docallib=False, callib="", gaintable=['antpos.cal', 'gaincurve.cal', 'intphase.cal',
'delays.cal'], gainfield=[], interp=[], spwmap=[], parang=False)

# step: phase & amplitude calibration
mystep = 7
if(mystep in thesteps):
    casalog.post('Step_' + str(mystep) + '_' + step_title[mystep], 'INFO')
    print 'Step_', mystep, step_title[mystep]

    gaincal(vis=msfile, caltable="phase.cal", field="0,1,3", spw="", intent="", selectdata=True, timerange="",
uvrange="", antenna="", scan="", observation="", msselect="", solint="int", combine="", preavg=-1.0, refant="14",
minblperant=4, minsnr=3.0, solnorm=False, gaintype="G", smodel=[], calmode="p", append=False, splintime=3600.0,
npointaver=3, phasewrap=180.0, docallib=False, callib="", gaintable=['antpos.cal', 'gaincurve.cal',
'delays.cal', 'bpass.cal'], gainfield=[], interp=[], spwmap=[], parang=False)

    gaincal(vis=msfile, caltable="amp.cal", field="0,1,3", spw="", intent="", selectdata=True, timerange="",
uvrange="", antenna="", scan="", observation="", msselect="", solint="inf", combine="", preavg=-1.0, refant="14",
minblperant=4, minsnr=3.0, solnorm=False, gaintype="G", smodel=[], calmode="ap", append=False, splintime=

```

```

3600.0,npointaver=3,phaseswrap=180.0,docallib=False,callib="",gaintable=['antpos.cal', 'gaincurve.cal',
'delays.cal', 'bpass.cal', 'phase.cal'],gainfield=[],interp=[],spwmap=[],parang=False)

# step: absolute flux-scale calibration
mystep = 8
if(mystep in thesteps):
    casalog.post('Step_'+str(mystep)+'_'+step_title[mystep], 'INFO')
    print 'Step_', mystep, step_title[mystep]

    fluxscale(vis=msfile, caltable="amp.cal", fluxtable="flux.cal", reference="0,3", transfer="1", listfile="",
    append=False, refspwmap=[-1], gainthreshold=-1.0, antenna="", timerange="", scan="", incremental=True, fitorder
    =1, display=False)

# step: Application of the calibration tables
mystep = 9
if(mystep in thesteps):
    casalog.post('Step_'+str(mystep)+'_'+step_title[mystep], 'INFO')
    print 'Step_', mystep, step_title[mystep]

    applycal(vis=msfile, field="0", spw="", intent="", selectdata=True, timerange="", uvrage="", antenna="", scan=
    "", observation="", msselect="", docallib=False, callib="", gaintable=['antpos.cal', 'gaincurve.cal',
'delays.cal', 'bpass.cal', 'phase.cal', 'amp.cal', 'flux.cal'], gainfield=['', '', '0', '0', '0', '0', '0'],
    interp=['', 'nearest', 'nearest', 'linear', 'nearest', 'nearest'], spwmap=[], calwt=False, parang=False,
    applymode="", flagbackup=True)

    applycal(vis=msfile, field="3", spw="", intent="", selectdata=True, timerange="", uvrage="", antenna="", scan=
    "", observation="", msselect="", docallib=False, callib="", gaintable=['antpos.cal', 'gaincurve.cal',
'delays.cal', 'bpass.cal', 'phase.cal', 'amp.cal', 'flux.cal'], gainfield=['', '', '3', '3', '3', '3', '3'], interp
    =['', 'nearest', 'nearest', 'linear', 'nearest', 'nearest'], spwmap=[], calwt=False, parang=False, applymode="",
    flagbackup=True)

    applycal(vis=msfile, field="1", spw="", intent="", selectdata=True, timerange="", uvrage="", antenna="", scan=
    "", observation="", msselect="", docallib=False, callib="", gaintable=['antpos.cal', 'gaincurve.cal',
'delays.cal', 'bpass.cal', 'phase.cal', 'amp.cal', 'flux.cal'], gainfield=['', '', '1', '1', '1', '1', '1'], interp
    =['', 'nearest', 'nearest', 'linear', 'nearest', 'nearest'], spwmap=[], calwt=False, parang=False, applymode="",
    flagbackup=True)

```

```

applycal(vis=msfile, field="2", spw="", intent="", selectdata=True, timerange="", uvrange="", antenna="", scan=""
, observation="", msselect="", docallib=False, callib="", gaintable=['antpos.cal', 'gaincurve.cal',
'delays.cal', 'bpass.cal', 'phase.cal', 'amp.cal', 'flux.cal'], gainfield=['', '', '1', '1', '1', '1', '1'], interp
=['', 'nearest', 'nearest', 'linear', 'nearest', 'nearest'], spwmap=[], calwt=False, parang=False, applymode="",
flagbackup=True)

```

```

flagdata(vis=msfile, mode="clip", autocorr=False, infile="", reason="any", tbuff=0.0, spw="", field="2",
antenna="", uvrange="", timerange="", correlation="", scan="", intent="", array="", observation="", feed="",
clipminmax=[0, 0.3], datacolumn="CORRECTED", clipoutside=True, channelavg=False, timeavg=False, timebin="0s",
clipzeros=False, quackinterval=1.0, quackmode="beg", quackincrement=False, tolerance=0.0, addantenna="",
lowerlimit=0.0, upperlimit=90.0, ntime="scan", combinescans=False, timecutoff=4.0, freqcutoff=3.0, timefit=
"line", freqfit="poly", maxnpieces=7, flagdimension="freqtime", usewindowstats="none", halfwin=1, extendflags
=True, winsize=3, timedev="", freqdev="", timedevscale=5.0, freqdevscale=5.0, spectralmax=1000000.0,
spectralmin=0.0, extendpols=True, growtime=50.0, growfreq=50.0, growaround=False, flagneartime=False,
flagnearfreq=False, minrel=0.0, maxrel=1.0, minabs=0, maxabs=-1, spwchan=False, spwcorr=False, basecnt=False,
fieldcnt=None, name="Summary", action="apply", display="", flagbackup=True, savepars=False, cmdreason="",
outfile="", writeflags=None)

```

```
# step: Split target
```

```
mystep = 10
```

```
if(mystep in thesteps):
```

```
casalog.post('Step_' + str(mystep) + '_' + step_title[mystep], 'INFO')
```

```
print 'Step_', mystep, step_title[mystep]
```

```

split(vis=msfile, outputvis='1331+305.A.ms', datacolumn="corrected", field="0", spw="", width=1, antenna="",
timebin="", timerange="", scan="", intent="", array="", uvrange="", correlation="", observation="", combine="",
keepflags=True, keepmms=False)

```

```

split(vis=msfile, outputvis='1635+381.A.ms', datacolumn="corrected", field="1", spw="", width=1, antenna="",
timebin="", timerange="", scan="", intent="", array="", uvrange="", correlation="", observation="", combine="",
keepflags=True, keepmms=False)

```

```

split(vis=msfile, outputvis='CL1604+432.A.ms', datacolumn="corrected", field="2", spw="", width=1, antenna="",
timebin="", timerange="", scan="", intent="", array="", uvrange="", correlation="", observation="", combine="",
keepflags=True, keepmms=False)

```

```
split(vis=msfile, outputvis='0137+331.A.ms', datacolumn="corrected", field="3", spw="", width=1, antenna="",
timebin="", timerange="", scan="", intent="", array="", uvrange="", correlation="", observation="", combine="",
keepflags=True, keepmms=False)
```

```
# step: Fourier Transform
```

```
mystep = 11
```

```
if(mystep in thesteps):
```

```
casalog.post('Step_' + str(mystep) + '_' + step_title[mystep], 'INFO')
```

```
print 'Step_', mystep, step_title[mystep]
```

```
ft(vis=mytarget, field="0", spw="", model=mymodel1, nterms=1, reffreq="", complist="", incremental=False,
usescratch=False)
```

```
# step: Clean and self-calibrate (phase) full dataset for z = 3.200
```

```
mystep = 12
```

```
if(mystep in thesteps):
```

```
casalog.post('Step_' + str(mystep) + '_' + step_title[mystep], 'INFO')
```

```
print 'Step_', mystep, step_title[mystep]
```

```
gaincal(vis=mytarget, caltable="selfphase.1200s.cal", field="0", spw="", intent="", selectdata=True, timerange=
"", uvrange="", antenna="", scan="", observation="", msselect="", solint="1200s", combine="spw", preavg=-1.0,
refant="14", minblperant=4, minsnr=3.0, solnorm=False, gaintype="G", smodel=[], calmode="p", append=False,
splinetime=3600.0, npointaver=3, phasewrap=180.0, docallib=False, callib="", gaintable="", gainfield=[],
interp=[], spwmap=[0,0], parang=False)
```

```
applycal(vis=mytarget, field="0", spw="", intent="", selectdata=True, timerange="", uvrange="", antenna="", scan=
"", observation="", msselect="", docallib=False, callib="", gaintable=['selfphase.1200s.cal'], gainfield=[],
interp=['linear'], spwmap=[[0],[0]], calwt=False, parang=False, applymode="", flagbackup=True)
```

```
clean(vis=mytarget, imagename=myimage1, outlierfile="", field="", spw="", selectdata=True, timerange="",
uvrange="", antenna="", scan="", observation="", intent="", mode="mfs", resmooth=False, gridmode="widefield",
wprojplanes=-1, facets=1, cfcache="cfcache.dir", rotpainc=5.0, painc=360.0, aterm=True, psterm=False, mterm=
True, wbawp=False, conjbeams=True, epjtable="", interpolation="linear", niter=100000, gain=0.01, threshold=
"0.00006Jy", psfmode="clark", imagermode="csclean", ftmachine="mosaic", mosweight=False, scaletype="SAULT",
multiscale=[], negcomponent=-1, smallscalebias=0.6, interactive=False, mask=mymask1, nchan=-1, start=0, width=
1, outframe="", veltype="radio", imsize=[4096,4096], cell=['0.5 arcsec'], phasecenter="", restfreq="", stokes=
```

```

" I", weighting="briggs", robust=0.0, uvtaper=False, outertaper=[''], innertaper=['1.0'], modelimage="",
restoringbeam=[''], pbcor=False, minpb=0.2, usescratch=True, noise="1.0Jy", npixels=0, npercycle=100,
cyclefactor=1.5, cyclespeedup=-1, nterms=1, reffreq="", chaniter=False, flatnoise=True, allowchunk=False)

# step: Clean and self-calibrate (phase) full dataset for z = 3.200
mystep = 13
if(mystep in thesteps):
    casalog.post('Step_' + str(mystep) + '_' + step_title[mystep], 'INFO')
    print 'Step_', mystep, step_title[mystep]

    gaincal(vis=mytarget, caltable="selfphase.600s.cal", field="0", spw="", intent="", selectdata=True, timerange=
    "", uvrange="", antenna="", scan="", observation="", msselect="", solint="600s", combine="spw", preavg=-1.0,
    refant="14", minblperant=4, minsnr=3.0, solnorm=False, gaintype="G", smodel=[], calmode="p", append=False,
    splinetime=3600.0, npointaver=3, phasewrap=180.0, docallib=False, callib="", gaintable="", gainfield=[], interp
    =[], spwmap=[0,0], parang=False)

    applycal(vis=mytarget, field="0", spw="", intent="", selectdata=True, timerange="", uvrange="", antenna="", scan
    = "", observation="", msselect="", docallib=False, callib="", gaintable=['selfphase.600s.cal'], gainfield=[],
    interp=['linear'], spwmap=[[0], [0]], calwt=False, parang=False, applymode="", flagbackup=True)

    clean(vis=mytarget, imagename=myimage2, outlierfile="", field="", spw="", selectdata=True, timerange="",
    uvrange="", antenna="", scan="", observation="", intent="", mode="mfs", resmooth=False, gridmode="widefield",
    wprojplanes=-1, facets=1, cfcache="cfcache.dir", rotpinc=5.0, pinc=360.0, aterm=True, psterm=False, mterm=
True, wbawp=False, conjbeams=True, epjtable="", interpolation="linear", niter=100000, gain=0.01, threshold=
    "0.00006Jy", psfmode="clark", imagermode="csclean", ftmachine="mosaic", mosweight=False, scaletype="SAULT",
    multiscale=[], negcomponent=-1, smallscalebias=0.6, interactive=False, mask=mymask1, nchan=-1, start=0, width=1,
    outframe="", veltype="radio", imsize=[4096,4096], cell=['0.5 arcsec'], phasecenter="", restfreq="", stokes="I",
    weighting="briggs", robust=0.0, uvtaper=False, outertaper=[''], innertaper=['1.0'], modelimage="",
    restoringbeam=[''], pbcor=False, minpb=0.2, usescratch=True, noise="1.0Jy", npixels=0, npercycle=100,
    cyclefactor=1.5, cyclespeedup=-1, nterms=1, reffreq="", chaniter=False, flatnoise=True, allowchunk=False)

# step: Clean and self-calibrate (phase) full dataset for z = 3.200
mystep = 14
if(mystep in thesteps):
    casalog.post('Step_' + str(mystep) + '_' + step_title[mystep], 'INFO')
    print 'Step_', mystep, step_title[mystep]

```

```
gaincal(vis=mytarget, caltable="selfphase.300s.cal", field="0", spw="", intent="", selectdata=True, timerange="" ,
uvrange="" , antenna="" , scan="" , observation="" , msselect="" , solint="300s" , combine="spw" , preavg=-1.0,
refant="14" , minblperant=4 , minsnr=3.0 , solnorm=False , gaintype="G" , smodel=[] , calmode="p" , append=False ,
splinetime=3600.0 , npointaver=3 , phasewrap=180.0 , docallib=False , callib="" , gaintable="" , gainfield=[] , interp
=[] , spwmap=[0,0] , parang=False)
```

```
applycal(vis=mytarget, field="0", spw="", intent="", selectdata=True, timerange="" , uvrange="" , antenna="" , scan
="" , observation="" , msselect="" , docallib=False , callib="" , gaintable=['selfphase.300s.cal'] , gainfield=[] ,
interp=['linear'] , spwmap=[[0], [0]] , calwt=False , parang=False , applymode="" , flagbackup=True)
```

```
clean(vis=mytarget, imagename=myimage3, outlierfile="" , field="" , spw="" , selectdata=True, timerange="" ,
uvrange="" , antenna="" , scan="" , observation="" , intent="" , mode="mfs" , resmooth=False , gridmode="widefield" ,
wprojplanes=-1 , facets=1 , cfcache="cfcache.dir" , rotpainc=5.0 , painc=360.0 , aterm=True , psterm=False , mterm=
True , wbawp=False , conjbeams=True , epjtable="" , interpolation="linear" , niter=100000 , gain=0.01 , threshold=
"0.00006Jy" , psfmode="clark" , imagermode="csclean" , ftmachine="mosaic" , mosweight=False , scaletype="SAULT" ,
multiscale=[] , negcomponent=-1 , smallscalebias=0.6 , interactive=False , mask=mymask1 , nchan=-1 , start=0 , width=1 ,
outframe="" , veltype="radio" , imsize=[4096,4096] , cell=['0.5 arcsec'] , phasecenter="" , restfreq="" , stokes="I" ,
weighting="briggs" , robust=0.0 , uvtaper=False , outertaper=[''] , innertaper=['1.0'] , modelimage="" ,
restoringbeam=[''] , pbcor=False , minpb=0.2 , usescratch=True , noise="1.0Jy" , npixels=0 , npercycle=100 ,
cyclefactor=1.5 , cyclespeedup=-1 , nterms=1 , reffreq="" , chaniter=False , flatnoise=True , allowchunk=False)
```

```
# step: Clean and self-calibrate (phase) full dataset for z = 3.200
```

```
mystep = 15
```

```
if(mystep in thesteps):
```

```
casalog.post('Step_' + str(mystep) + '_' + step_title[mystep], 'INFO')
```

```
print 'Step_' , mystep , step_title[mystep]
```

```
gaincal(vis=mytarget, caltable="selfphase.120s.cal", field="0", spw="", intent="", selectdata=True, timerange="" ,
uvrange="" , antenna="" , scan="" , observation="" , msselect="" , solint="120s" , combine="spw" , preavg=-1.0,
refant="14" , minblperant=4 , minsnr=3.0 , solnorm=False , gaintype="G" , smodel=[] , calmode="p" , append=False ,
splinetime=3600.0 , npointaver=3 , phasewrap=180.0 , docallib=False , callib="" , gaintable="" , gainfield=[] , interp
=[] , spwmap=[0,0] , parang=False)
```

```
applycal(vis=mytarget, field="0", spw="", intent="", selectdata=True, timerange="" , uvrange="" , antenna="" , scan
="" , observation="" , msselect="" , docallib=False , callib="" , gaintable=['selfphase.120s.cal'] , gainfield=[] ,
interp=['linear'] , spwmap=[[0], [0]] , calwt=False , parang=False , applymode="" , flagbackup=True)
```

```

clean(vis=mytarget, imagename=myimage4, outlierfile="", field="", spw="", selectdata=True, timerange="",
uvrange="", antenna="", scan="", observation="", intent="", mode="mfs", resmooth=False, gridmode="widefield",
wprojplanes=-1, facets=1, cfcache="cfcache.dir", rotpainc=5.0, painc=360.0, aterm=True, psterm=False, mterm=
True, wbawp=False, conjbeams=True, epjtable="", interpolation="linear", niter=100000, gain=0.01, threshold=
"0.00006Jy", psfmode="clark", imagermode="csclean", ftmachine="mosaic", mosweight=False, scaletype="SAULT",
multiscale=[], negcomponent=-1, smallscalebias=0.6, interactive=False, mask=mymask1, nchan=-1, start=0, width=1,
outframe="", veltype="radio", imsize=[4096,4096], cell=['0.5 arcsec'], phasecenter="", restfreq="", stokes="I",
weighting="briggs", robust=0.0, uvtaper=False, outertaper=[''], innertaper=['1.0'], modelimage="",
restoringbeam=[''], pbcor=False, minpb=0.2, usescratch=True, noise="1.0Jy", npixels=0, npercycle=100,
cyclefactor=1.5, cyclespeedup=-1, nterms=1, reffreq="", chaniter=False, flatnoise=True, allowchunk=False)

```

```
# step: Clean and self-calibrate (phase) full dataset for z = 3.200
```

```
mystep = 16
```

```
if(mystep in thesteps):
```

```
    casalog.post('Step_' + str(mystep) + '_' + step_title[mystep], 'INFO')
```

```
    print 'Step_', mystep, step_title[mystep]
```

```

gaincal(vis=mytarget, caltable="selfphase.120s.2.cal", field="0", spw="", intent="", selectdata=True, timerange=
"", uvrange="", antenna="", scan="", observation="", msselect="", solint="120s", combine="spw", preavg=-1.0,
refant="14", minblperant=4, minsnr=3.0, solnorm=False, gaintype="G", smodel=[], calmode="p", append=False,
splintime=3600.0, npointaver=3, phasewrap=180.0, docallib=False, callib="", gaintable="", gainfield=[], interp
=[], spwmap=[0,0], parang=False)

```

```

applycal(vis=mytarget, field="0", spw="", intent="", selectdata=True, timerange="", uvrange="", antenna="", scan
="", observation="", msselect="", docallib=False, callib="", gaintable=['selfphase.120s.2.cal'], gainfield=[],
interp=['linear'], spwmap=[[0], [0]], calwt=False, parang=False, applymode="", flagbackup=True)

```

```

clean(vis=mytarget, imagename=myimage5, outlierfile="", field="", spw="", selectdata=True, timerange="",
uvrange="", antenna="", scan="", observation="", intent="", mode="mfs", resmooth=False, gridmode="widefield",
wprojplanes=-1, facets=1, cfcache="cfcache.dir", rotpainc=5.0, painc=360.0, aterm=True, psterm=False, mterm=
True, wbawp=False, conjbeams=True, epjtable="", interpolation="linear", niter=100000, gain=0.01, threshold=
"0.00006Jy", psfmode="clark", imagermode="csclean", ftmachine="mosaic", mosweight=False, scaletype="SAULT",
multiscale=[], negcomponent=-1, smallscalebias=0.6, interactive=False, mask=mymask1, nchan=-1, start=0, width=1,
outframe="", veltype="radio", imsize=[4096,4096], cell=['0.5 arcsec'], phasecenter="", restfreq="", stokes="I",
weighting="briggs", robust=0.0, uvtaper=False, outertaper=[''], innertaper=['1.0'], modelimage="",
restoringbeam=[''], pbcor=False, minpb=0.2, usescratch=True, noise="1.0Jy", npixels=0, npercycle=100,

```

```
cyclefactor=1.5,cyclespeedup=-1,nterms=1,reffreq="",chaniter=False,flatnoise=True,allowchunk=False)
```

```
# step: Clean and self-calibrate (phase) full dataset for z = 3.200
```

```
mystep = 17
```

```
if(mystep in thesteps):
```

```
casalog.post('Step_' + str(mystep) + '_' + step_title[mystep], 'INFO')
```

```
print 'Step_', mystep, step_title[mystep]
```

```
clean(vis=mytarget,imagenname=myimage6,outlierfile="",field="",spw="",selectdata=True,timerange="",  
uvrange="",antenna="",scan="",observation="",intent="",mode="mfs",resmooth=False,gridmode="widefield",  
wprojplanes=-1,facets=1,cfcache="cfcache.dir",rotpainc=5.0,painc=360.0,aterm=True,psterm=False,mterm=  
True,wbawp=False,conjbeams=True,epjtable="",interpolation="linear",niter=1000000,gain=0.01,threshold=  
"0.00006Jy",psfmode="clark",imagermode="csclean",ftmachine="mosaic",mosweight=False,scaletype="SAULT",  
multiscale=[],negcomponent=-1,smallscalebias=0.6,interactive=False,mask=mymask1,nchan=-1,start=0,width=1,  
outframe="",veltype="radio",imsize=[7200,7200],cell=['0.5 arcsec'],phasecenter="",restfreq="",stokes="I",  
weighting="briggs",robust=0.0,uvtaper=False,outertaper=[''],innertaper=['1.0'],modelimage="",  
restoringbeam=[''],pbcor=False,minpb=0.2,uscratch=True,noise="1.0Jy",npixels=0,npercycle=100,  
cyclefactor=1.5,cyclespeedup=-1,nterms=1,reffreq="",chaniter=False,flatnoise=True,allowchunk=False)
```

```
print 'Calibration_and_imaging_completed'
```